Strategic Design of Cyclic Acetals for Living Cationic Copolymerization with Vinyl Monomers and Sequence-Controlled Polymer Synthesis

A Doctoral Thesis

by

Kazuya Maruyama

Submitted to

the Graduate School of Science,

Osaka University

February 2022

Acknowledgments

This thesis research was conducted at the Department of Macromolecular Science, Graduate School of Science, Osaka University under the direction of Professor Sadahito Aoshima from 2016 to 2022.

First of all, the author would like to express his deepest and sincere gratitude to Professor Sadahito Aoshima for his numerous advices, enthusiastic discussion and for always being supportive throughout the author's laboratory life. The author has been impressed by his insightful suggestions, great ideas, and enthusiasm on science. The author is also deeply grateful to Associate Professor Arihiro Kanazawa for his stimulating discussion, deep knowledge, and enormous help.

The author would like to express his deep appreciation to Professor Akihito Hashidzume and Professor Hiroyasu Yamaguchi for kindly reviewing this thesis and fruitful comments.

The author thanks Dr. Yasuto Todokoro and Dr. Naoya Inazumi for NMR spectroscopic measurements, and Dr. Akihito Ito for mass spectroscopy. The author also appreciates Associate Professor Nathaniel A. Lynd, Dr. Jennifer Imbrogno, and his group (The University of Texas at Austin) for collaboration on the research regarding polymer electrolyte mixtures using poly (vinyl ether)s.

The author is deeply indebted to Professor Yoshio Okamoto (Nagoya University; Harbin Engineering University), Professor Mitsuo Sawamoto (Kyoto University; Chubu University), Professor Eiji Yashima (Nagoya University), Professor Masami Kamigaito (Nagoya University), Professor Shokyoku Kanaoka (The Univesity of Shiga Prefecture), Professor Kotaro Satoh (Tokyo Institute of Technology), Professor Makoto Ouchi (Kyoto University), and all "ORION" members for active discussions.

The author thanks to all the members who supported and shared productive time with him in the Aoshima group. Specifically, the author is grateful to Dr. Kira B. Landenberger (Junior Associate Professor, Kyoto University), Dr. Norifumi Yokoyama, Dr. Suzuka Matsumoto, Dr. Sensho Kigoshi, Dr. Daichi Yokota, Dr. Motoki Higuchi, Dr. Hironobu Watanabe, Mr. Hiroshi Oda, Ms. Chihiro Suemitsu, Ms. Fumina Koga, Mr. Tadashi Naito, Mr. Tsuyoshi Nishikawa, Mr. Yoshiki Tatsuno, Ms. Yurika Miyamae, Mr. Shintaro Araoka, Ms. Haruka Nishimura, Mr. Daisuke Hotta, Mr. Kazutoshi Mishima, Mr. Ryusei Kato, Mr. Keisuke Hayashi, Ms. Maki Mimura, Ms. Haruna Kagosaki, Mr. Tomohito Asakawa, Ms. Rui Haraguchi, Ms. Kano Hyoi, Mr. Takuya Yamamoto, Ms. Tomo Yoshiki, Mr. Masamichi Inoue, Ms. Yui Kawamura, Ms. Sae Taniguchi, Mr. Syunya Hasegawa. Mr, Yuya Asada, Mr. Yuya Kinoshita, Mr. Jun-ichi Azuma, Mr. Mikiya Umemoto, Mr. Tomoki Nara, Mr. Ryosuke Hada, Ms. Yuka Takahashi, Ms. Kana Takebayashi, Mr. Naoki Matsuo, Mr. Yuji

Mishima, Mr. Masahiro Ueda, Mr. Yuto Eguchi, Ms. Aya Katto, Mr. Akihisa Numao, and Ms. Yuyu Furuki for sharing his memorable student life. The author is also obliged to Ms. Misato Nishiuchi, Ms. Mariko Okamoto, Ms. Naomi Imai, and Ms. Izumi Ichimura for their warm assistance in laboratory life.

The author is grateful to the Japan Society for the Promotion of Sciences (JSPS) for JSPS Research Fellowship for Young Scientists (DC2) and a Grant-in-Aid for JSPS Fellow (21J11361) from April 2021 to March 2022.

Finally, the author would like to express a great appreciation to his parents Yoko and Toshikazu Maruyama, and all his relatives for their constant care and considerable encouragement.

February 2022

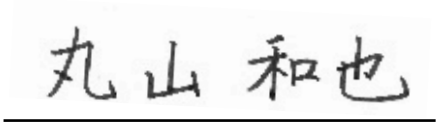

Kazuya Maruyama
Department of Macromolecular Science
Graduate School of Science
Osaka University

Contents

Chapter 1.

General Introduction

1. Background

1.1 Development of Polymerization Techniques

Since the establishment of the concept of macromolecules by Staudinger in 1920s, synthetic polymers have been widely used for household items and industrial products, becoming an essential part of our lives today. Various properties of polymers depend on the number of monomers, monomer structure, monomer sequence, molecular weight (MW), molecular weight distribution (MWD), chain end structure, and tacticity (Figure 1). These elements are perfectly controlled in natural macromolecules, such as proteins and DNA consisting of amino acids or nucleotides, respectively, with various side chains, through biological synthesis in a cell, which dictates higher-order structures with characteristic functions.[1] In synthetic polymers, fundamental investigations into polymerization reactions have been demonstrated to control the basic components of polymers such as molecular weight, sequences, or a combination of these factors, establishing a wide range of synthetic approaches with various monomers.[2–21] These methods include novel polymerization mechanisms based on the combination of the existing reactions or the design of specific primary structures with unprecedented monomers inspired by the progress of organic chemistry. The development of simple and sophisticated methods for polymer structures utilizing various monomers based on insights into polymerization reactions has led to a dramatical improvement of material designs.

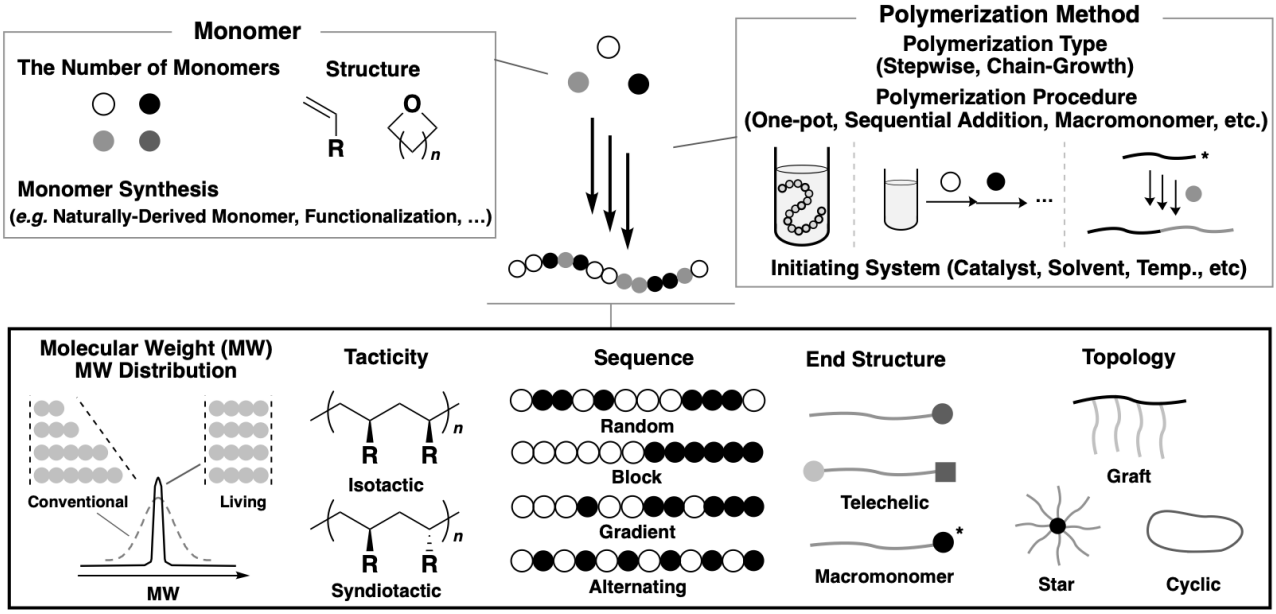

Figure 1. Primary structures of polymers and methodologies for polymer design.

1.2 Polymerization Mechanisms

In polymer synthesis, difference of monomer structures greatly affects their polymerization mechanisms. Polymerization reactions are roughly classified into step-growth or chain-growth mechanisms. In the step-growth mechanism, all the molecules including monomers, oligomers, and polymers, in a reaction system can react with each other. In contrast, propagation reactions selectively occur at active chain ends in the chain-growth mechanism. Chain-growth polymerization is further categorized into radical, cationic, anionic, and coordination polymerization according to the types of active species.[2] The electronic and/or steric effects of substituents around a polymerizable group significantly affect the polymerizability of monomers. For example, in the case of vinyl monomers, the relationships between the electronic or resonance contribution of substituents to the vinyl group and the polymerization mechanism are systematically investigated via the polymerizability evaluation summarized as the Q-e plot.[22] For example, the electron-donating or electron-withdrawing group-substituted styrene derivatives are effective for cationic or anionic polymerization, respectively.[5,7]

Another important category of monomers for the chain-growth mechanism is cyclic monomers, which are polymerized by ring-opening polymerization (ROP).[23,24] ROP of cyclic monomers generally introduces functional groups into the main chains of the resulting polymers because polymerizable functional groups, such as ether and ester moieties, in the monomer are maintained after the propagating reaction. In many cases, the major driving force of propagating reaction is the release of ring strain, which leads to a smaller change in the Gibbs free energy in ROP than vinyl-addition polymerization.[24] These differences are often responsible for nonnegligible occurrences of depolymerization in ROP. Another feature of ROP is the significant influence of heteroatoms in cyclic monomers on the reactivity and stability of the active species. In cationic or anionic polymerization of cyclic ethers, active species with a positive or negative charge on the oxygen atom possess properties unlike those with a carbocation or a carbanion.[16] These features in propagating reactions are also important factors to be considered for the design of polymerization reactions (Figure 2).

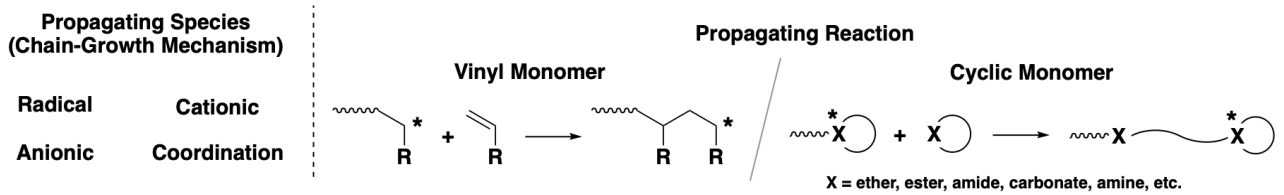

Figure 2. Propagating reactions via the chain-growth mechanism.

Copolymerization between different polymerization mechanisms has a potential to generate novel functional polymers with special primary structures that cannot be achieved by homopolymerization. However, such copolymerization is generally difficult because the differences in the reactivity of different propagating species adversely affect crossover reactions between the different types of monomers. To overcome this restriction, the following strategies have been devised for the copolymerization via different types of propagating mechanisms: (A) orthogonal polymerization through independently occurring propagation reactions in a single chain,[26–28] (B) polymerization via an intermediate between the different types of active species,[29,30] and (C) generation of active species with similar reactivity via modulation of the property of active species (Figure 3).[31,32] Orthogonal copolymerization affords block copolymers composed of different types of

monomers (Figure 3A). For example, Trollsas and coworkers[26] demonstrated the concurrent nitroxide-mediated radical polymerization of styrene and living coordination ROP of ε-caprolactone using a bifunctional initiator with an alkoxyamine and a primary alcohol. Nonorthogonal copolymerization is an attractive method for polymers with various monomer sequences because the kinetics of each polymerization and the frequency of crossover reactions can be tuned by controlling reaction conditions. Kamigaito and coworkers[29] developed the interconvertible radical and cationic copolymerization of acrylates and vinyl ethers (VEs) via reversible activation of common dormant species (Figure 3B). Trithiocarbonate and dithiocarbamate worked as effective chain transfer agents for reversible addition-fragmentation chain transfer radical polymerization, while the thioester ends were also activated by Lewis acids to generate carbocationic species inducing the cationic polymerization of VEs. Aoshima and coworkers[32] reported the concurrent vinyl-addition and ring-opening cationic copolymerization of VEs and oxiranes by focusing on the reactivity of the propagating cationic species, generating copolymers with a variety of sequences (Figure 3C). The carbocations derived from oxirane monomers generated by ring-opening reaction of the oxonium ion species led to the crossover reactions between vinyl monomers and cyclic monomers. These developments have demonstrated the potential of simultaneous copolymerization based on different mechanisms to construct polymers with structural and compositional diversities via chain-growth polymerization.

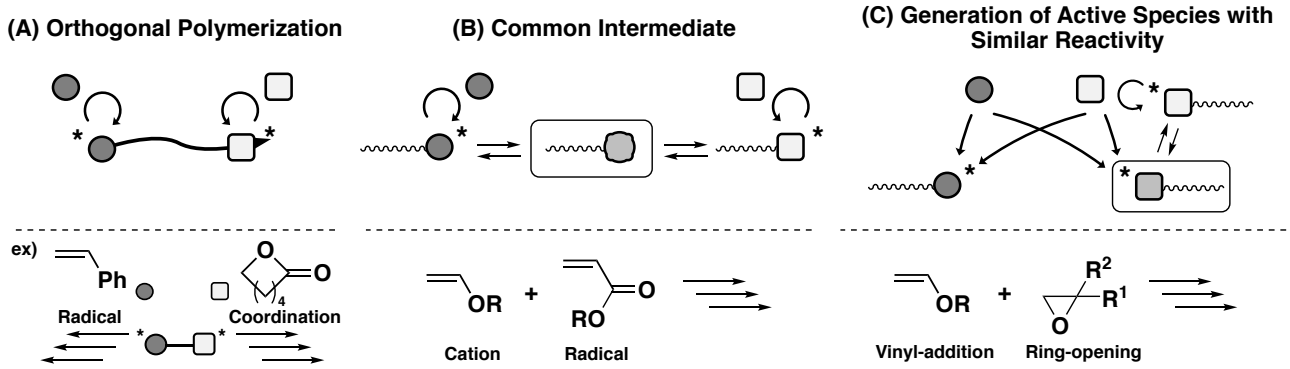

Figure 3. Concurrent copolymerization via (A) orthogonal mechanism, (B) common intermediate-mediated mechanism, or (C) generation of propagating species with similar reactivity.

1.3 Living Cationic Polymerization

In conventional polymerization, the active chain end leads to not only propagation but also the irreversible termination and chain transfer reaction. In general, living polymerization consists of only initiation and propagation reactions, which enables the precise control of the polymer structures in terms of molecular weight, molecular weight distribution, composition of monomers, and chain end structures. Living polymerization was first reported by Szwarc in 1956 for the anionic polymerization of styrene.[33] After this discovery, controlled/living polymerizations have been reported via relatively stable propagating species including cationic ROP,[34] ring-opening metathesis polymerization,[35,36] and coordination polymerization.[37]

Living/cocntrolled polymerization via unstable propagating species, such as carbocation or radical, was achieved by introduction of a fast and reversible deactivation process into the active chain ends. The first living cationic polymerization was achieved in the polymerization of isobutyl VE with the HI/I_2 initiating system in 1984 and the polymerization of isobutene with the tertiary ester/BCl_3 system in 1986.[38,39] In the HI/I_2 initiating system, the fast initiation with HI and the reversible activation of the carbon–iodide propagating ends

by I_2 were responsible for the construction of an appropriate dormant–active equilibrium. Based on these concepts, various kinds of living cationic[40–49] and radical[50–54] polymerization systems have been developed.

Aoshima and Higashimura[41–45] reported the living cationic polymerization of VEs or styrene derivatives using metal catalysts in conjunction with a weak Lewis base (Figure 4). Lewis bases contribute to establishing a suitable dormant–active equilibrium via the interaction with the Lewis acid catalysts and propagating cationic species. The effects of various weak Lewis bases, such as ester,[41–43] ether,[44] and cyclic acetal[45,55] on the rate of the living cationic polymerization of VEs were also investigated. Moreover, Aoshima and coworkers[56,57] demonstrated the systematic investigation using a series of metal halides in living cationic polymerization of isobutyl VE or *p*-methoxystyrene. A comprehensive study revealed that the nature of the central metals, such as the oxo- and chlorophilicities, and the structures of counteranions largely affect the polymerization controllability. For example, the use of $TiCl_4$, which has a strong oxophilicity, in conjunction with ester or ether resulted in much slower polymerization than that without additives, while the use of $FeCl_3$ or $SnCl_4$ resulted in very fast living cationic polymerization of isobutyl VE even in the presence of ester or ether.[56] These results suggest that understanding the properties of various metal chlorides and additives in cationic polymerization has great potential to access the versatile design of initiating systems, and consequently, the development of controlled/living cationic polymerization of monomers with various structures.

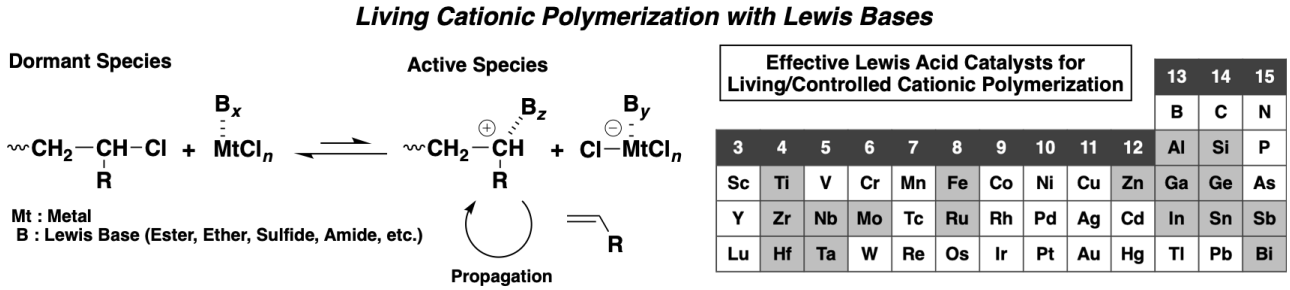

Figure 4. The base-assisting living cationic polymerization of vinyl monomers with various initiating systems.

1.4 Sequence-Controlled Polymerization

Sophisticated designs of the structures of monomers and polymerization conditions have spurred the development of the synthetic strategies for the sequence-controlled polymers consisting of more than two types of monomers. Such methods are mainly categorized into the three groups shown in Figure 5.[58,59] The most reliable strategy for sequence control is the step-by-step monomer addition, such as the polypeptide synthesis with a Merrifield resin (Figure 5i).[60–63] The iterative method affords well-defined polymers with desired monomer sequences, although considerable amounts of time and efforts are required to prepare high molecular weight polymers. Another method involves polymerization of a monomer containing specific sequences prepared by multistep single unit monomer addition and functionalization (Figure 5ii).[64–76] For example, the radical polyaddition of a series of sequence-incorporated monomers produced the polymers with ABC-, ABCD-, or ABBAC-type sequences.[68–70] However, the preparation of these monomers generally requires a multistep reaction and purification steps, and these drawbacks often results in low polymer yield from the starting materials. The most practical approach is direct polymerization of several types of monomers, whereas successful reports are very limited because the extremely high selectivity in the crossover reactions among monomers is indispensable for sequence regulation (Figure 5iii).[77–80]

A successive process consisting of the synthesis of sequence-incorporated monomers and subsequent copolymerization with other monomers is an attractive approach for sequence control in terms of practicality and controllability. Yokozawa and coworkers[81,82] demonstrated the synthesis of sequence-incorporated monomers by cycloaddition reaction of electron-deficient olefin and VE and subsequent alternating copolymerization of the obtained cyclic monomer with an oxirane (Figure 5iv). This method requires purification and isolation of the cycloaddition product before the copolymerization with an oxirane; however, exclusive crossover reactions occurred, which showed the significant potential of this two-step strategy for sequence-controlled polymers.

Step-growth polymerization based on the multicomponent organic reactions, such as Passerini or Ugi reactions, has also been reported for sequence-controlled polymers.[83] Moreover, a stepwise process of two or more consecutive multicomponent reactions affords sequence-controlled polymers consisting of four or more monomers.[84,85] An elaborate incorporation of the features of each method into a single reaction system can enable the development of a simple and sophisticated strategy for synthesis of polymers with well-defined sequences.

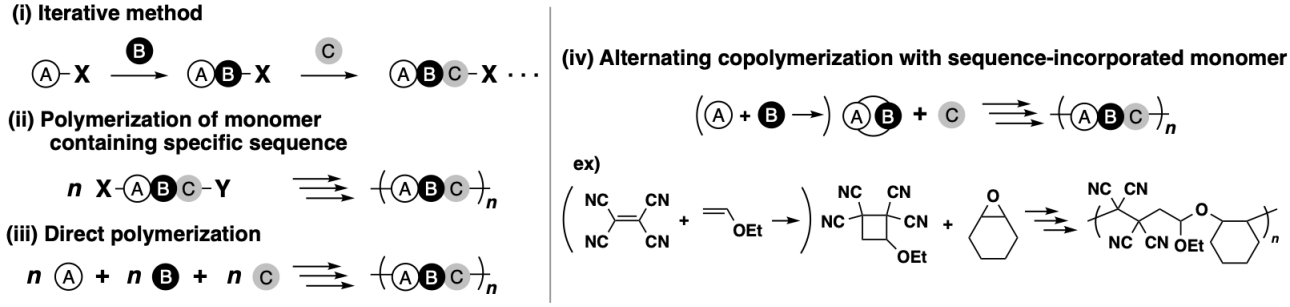

Figure 5. Various approaches for synthesis of sequence-controlled polymers.

1.5 Acetal Structure in Polymer Synthesis

Acetal is one of the major structural skeletons in organic synthesis, as found in a variety of compounds, such as natural saccharides and their derivatives, pharmaceutical synthesis, organic solvents, fragrances, and thermoplastic resins in materials engineering. Acetal is stable to base, nucleophile, and reducing conditions, while it is completely decomposed under acid conditions. Owing to high selectivity and the simple procedures for introduction and elimination, acetal is widely applied as a protecting group of carbonyl and hydroxy groups in organic synthesis.[86] Among the various synthetic methods for acetal structures,[87,88] the most typical procedure involves the condensation reaction between carbonyl compounds and alcohols in the presence of a Brønsted or Lewis acid catalyst (Figure 6). Transacetalization between acetals and alcohols is a useful approach under mild and solvent-free conditions.[89–92] For the case of diols, dioxolanes and dioxanes, which are five- and six-membered cyclic acetals, respectively, are often utilized as the protective groups. The addition of alcohol to VE is also a promising method for asymmetrical acetals.[93–96] In particular, tetrahydropyranyl ethers, which are synthesized by addition of alcohol to 3,4-dihydro-2H-pyran (DHP), are common and widely used due to inexpensive and easy procedures. Oxirane, which is an attractive building block in synthetic chemistry and is a basic component of epoxy resin, is transformed into a cyclic acetal via cycloaddition reaction with carbonyl compounds (mainly acetone) in the presence of Lewis acid catalysts.[97–

[102] Other methods including oxidative method,[103] Prins cyclization,[104,105] and Wacker-type catalysts,[106] also synthesize various acetal structures.

One of the notable advantages of acetal structures in organic synthesis is the selective protection/deprotection and the tuning of the reactivities depending on the structural factors around acetals. For example, an increase in the number of substituents on the central carbon atom of an acetal group improved the rate of the hydrolysis reaction.[107–109] Steric differences, such as the ring-member of cyclic acetals and acyclic or cyclic structures, affect the stability of acetal structures.[110] Moreover, the electron-donating or withdrawing effects of the substituents on the aromatic ring adjacent to the central carbon of acetal are related to the rate of hydrolysis.[111,112] These structure–reactivity relationships for acetal structures are useful for the design of organic compounds in synthetic strategies.

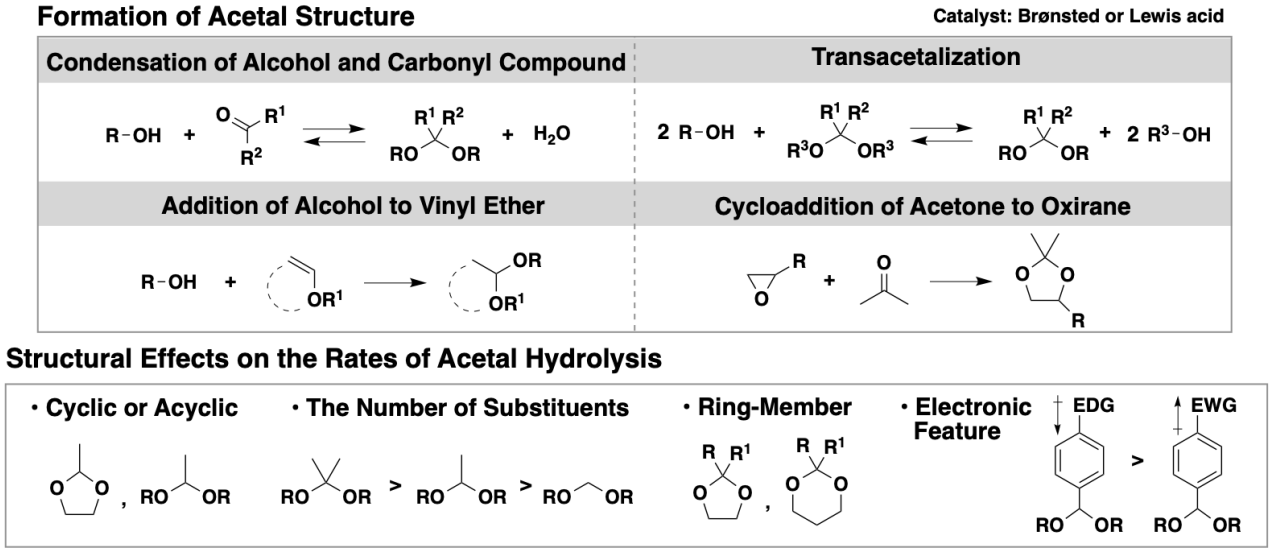

Figure 6. Methods for the synthesis of acetal structures and the structural factors affecting the rate of acid hydrolysis.

In polymer chemistry, polymerization of acetal compounds provides various properties with synthetic polymers, such as acid degradability, introduction of reactive sites for further polymerization, or protection of functional groups. Specifically, acetal compounds are generally applied as monomers, initiators, additives, or crosslinkers (Figure 7). Among the various aspects of acetals in polymer synthesis, the most fundamental usage is a monomer for polyacetals.

Cyclic acetals, such as 1,3-dioxolane, 1,3-dioxepane, and trioxane are employed to produce polyacetals via cationic ring-opening polymerization with Brønsted or Lewis acid catalysts.[23] Copolymerization of cyclic acetals with cyclic ethers or cyclic esters also generates various types of main chain structures with acid degradable properties.[113–117] Structural studies revealed the homopolymerizability of non-substituted cyclic acetals and the very low homopolymerizability (low ceiling temperature) of 2-substituted cyclic acetals,[118] which showed a similar trend to the case of cyclic ethers, such as the high reactivity of tetrahydrofuran and the inertness of 2-methyltetrahydrofuran in cationic ring-opening polymerization.[119] The use of appropriate initiators enabled controlled ring-opening polymerization.[113,120]

Acetal compounds are effective for precise synthesis of polymers with specific structures when used as initiators, additives, and crosslinkers. Cationic species derived from acetals through activation by a suitable

Lewis acid catalyst can initiate the cationic polymerization.[121–125] For example, living cationic polymerization of vinyl monomers initiated by a cationogen derived from 1,3-dioxolane led to polymers with a hydroxy chain end.[121] In addition, appropriate Lewis acid catalysts with the oxophilic nature selectively activate acetal groups on the side chains of polymers to initiate the polymerization from prepolymers, yielding graft copolymers with well-defined structures.[124,125] The polymerization of acetal-containing vinyl monomers via anionic[126–134] or radical mechanisms[135–138] also produced vinyl polymers with protected hydroxy groups. As an additive, cyclic acetals stabilize propagating cationic species to adjust the acidity of Lewis acid catalysts in the living cationic polymerization of VEs.[45] Moreover, divinyl monomers containing acetal moieties are used as acid-labile crosslinkers of nanocapsules and cross-linked micelles.[139,140] The substituent effects of acetals and ketals on acid hydrolysis properties were also investigated for a variety of applications including drug delivery and tissue engineering.[141]

Copolymerization through different polymerization mechanisms, such as vinyl-addition and ring-opening mechanisms, potentially allows for synthesis of polymers with various primary structures depending on the reaction conditions. Indeed, the conventional copolymerization of vinyl monomers and cyclic acetals was reported several decades ago.[142,143] More recently, Aoshima and coworkers[144] reported the controlled cationic copolymerization of 2-chloroethyl VE and 1,3-dioxepane using a carefully designed initiating system based on the living cationic polymerization of VEs. The properties and reactivities of cyclic acetals described above can be a key to developing synthetic strategies of copolymers and material designs from different types of monomers.

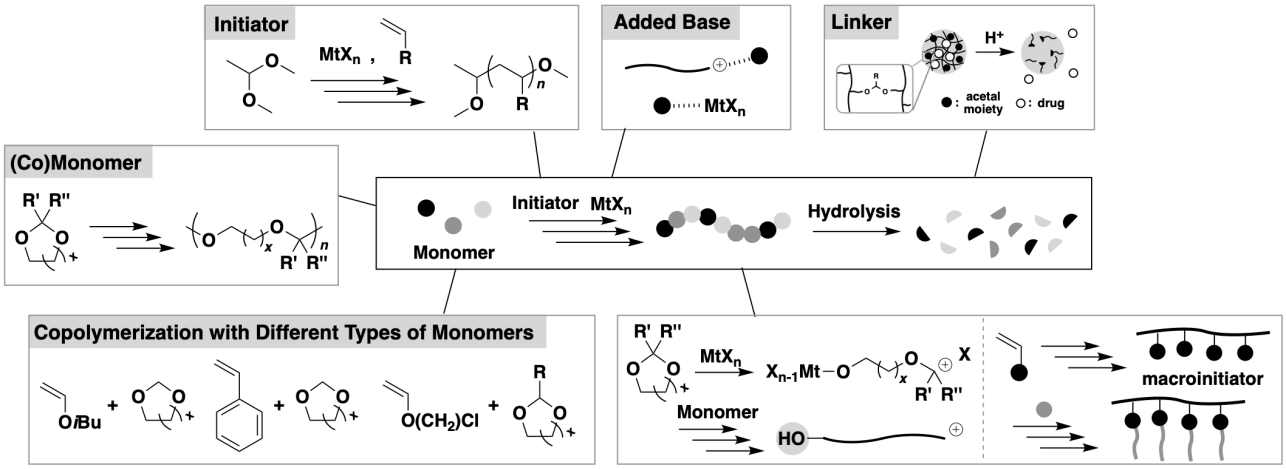

Figure 7. Versatility of acetal structures for polymer synthesis.

2. Objective and Outline of This Thesis

The objective of this thesis is to comprehensively study the relationship between the structures of active species and copolymerization behavior in vinyl-addition and ring-opening copolymerization and to construct novel strategies for the sequence-controlled polymers using different types of monomers (Figure 8). For successful crossover reactions between different types of monomers, suitable mediation using common intermediates or active species is required. As a promising candidate to meet this requirement, the author focuses on cyclic acetals because the carbocations generated by the ring-opening reaction of the oxonium ion species derived from cyclic acetals are structurally similar to those derived from VEs. In addition, the differences in electronic and steric features around the active species probably influence the crossover reactions between vinyl monomers and cyclic monomers. Therefore, the author designs a series of cyclic acetals with various substituents and ring-members from aldehydes and ketones to investigate the correlation between the structural difference and the copolymerizability in the concurrent vinyl-addition and ring-opening copolymerization of cyclic acetals and vinyl monomers. The author develops facile approaches for sequence-controlled polymers based on a rationally designed process consisting of selective cyclic acetal formation from oxirane/carbonyl compound or cyclic enol ether/alcohol pairs and subsequent alternating cationic copolymerization with a vinyl monomer.

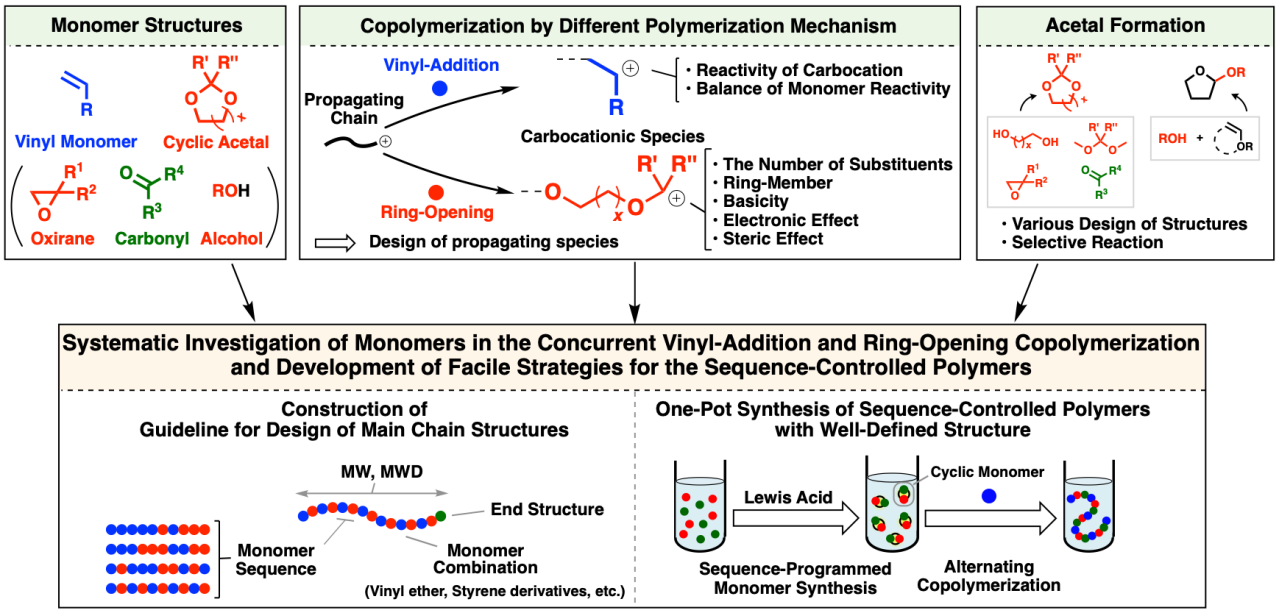

Figure 8. Objective and outline of this thesis.

This thesis consists of two parts. Part I (Chapters 2 and 3) describes the development of guidelines for the control of copolymer primary structures such as molecular weight and sequence in the concurrent vinyl-addition and ring-opening copolymerization. In Part II (Chapters 4 and 5), the author presents novel strategies for the synthesis of sequence-controlled polymers with different types of monomers via a one-pot approach consisting of selective generation of sequence-incorporated cyclic monomers and subsequent living copolymerization with vinyl monomers.

Chapter 2 describes the effects of the substituents and ring members of cyclic acetals on the copolymerization behavior with VEs (Figure 9). The controlled cationic copolymerization of 2-chloroethyl VE (CEVE) and various cyclic acetals successfully proceeds in a living manner, while the rate of the copolymerization and the sequences of the copolymers are significantly related with the number of methyl substituents at the 2-position of cyclic acetals and the ring member of cyclic acetals. The systematic study based on the reaction mechanism of vinyl monomers and cyclic acetals in the propagating step reveals that several factors, including the stability of the generated carbocation in the crossover reactions, the ring strain of the oxonium ion species, and the Lewis basicity of cyclic acetals, influence the polymerization rate and the sequences of the copolymers.

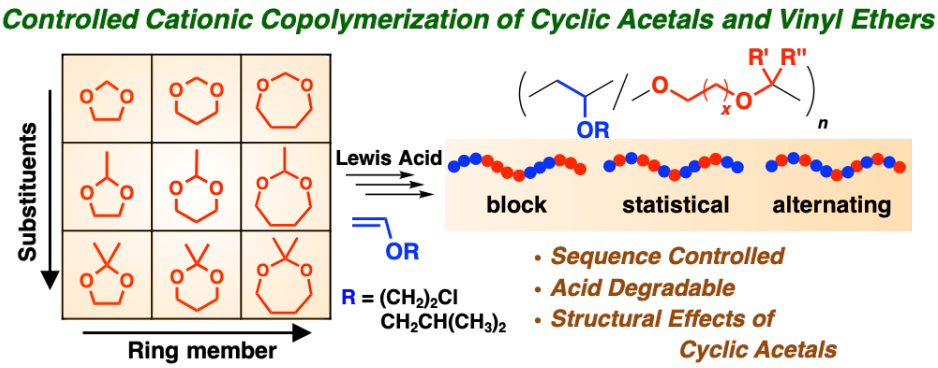

Figure 9. The effects of the number of substituents and ring-member of cyclic acetals on the copolymerization behavior in the controlled cationic copolymerization with VEs.

Chapter 3 presents a structural investigation of cyclic acetals in the concurrent vinyl-addition and ring-opening copolymerization and the improvement of copolymerizability with various vinyl monomers (Figure 10). The electronic and steric features around the active species have a great influence on the polymerizability and controllability in polymer synthesis. The author designs 2-aryl-substituted cyclic acetals, which introduce a resonance effect at the propagating chain ends, and various bulky cyclic acetals. As a result of systematic studies, substituent-derived stabilization effects on the propagating cationic species dramatically increase the frequency of the crossover reactions in the copolymerization with various vinyl monomers.

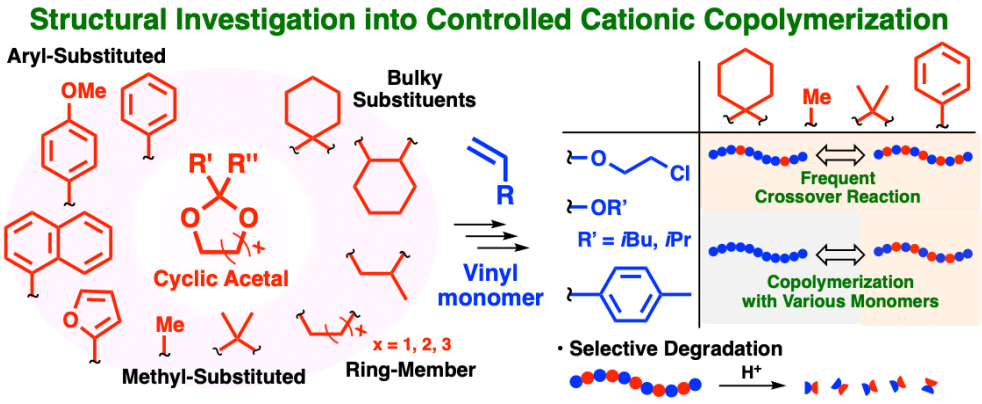

Figure 10. The structural investigation of cyclic acetals on the sequence of copolymers and the copolymerizability of cyclic acetals with various vinyl monomers.

In Chapter 4, the author develops the one-pot synthesis of ABC-type periodic terpolymers via a successive process consisting of the selective generation of sequence-programmed cyclic acetals and subsequent living alternating copolymerization with vinyl monomers (Figure 11). In this method, a cyclic acetal generated by a selective cyclodimerization reaction of an oxirane and a carbonyl compound is subjected to subsequent copolymerization without any isolation or purification. Alternating cationic copolymerization of the cyclic acetal and VE proceeds smoothly under suitable conditions, which allows for simultaneous control of the molecular weight, molecular weight distribution, and chain ends in addition to ABC-type periodic sequence. In addition, the sequential addition of vinyl monomers during the living copolymerization afforded ABC-*b*-ABD-type periodic block quaterpolymers.

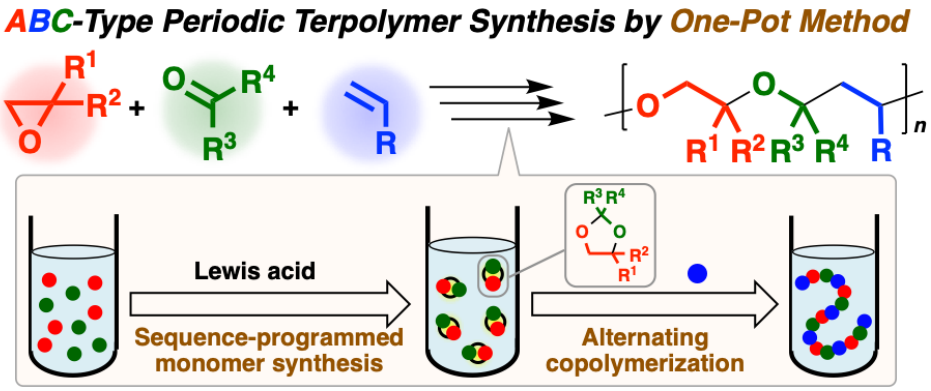

Figure 11. One-pot synthesis of ABC-type periodic sequence terpolymers via the selective synthesis of sequence-programmed cyclic acetals and subsequent alternating copolymerization with vinyl monomers.

Chapter 5 addresses the construction of a simple and versatile approach for copolymers with well-defined sequences based on the methodology developed in Chapter 4 (Figure 12). As a conventional and rational resource for diverse polymer structures, the author focuses on alcohol, which is an inhibitor in cationic polymerization, for the one-pot synthesis of cyclic monomers and subsequent copolymerization with a VE. Specifically, 2-alkoxy cyclic ether monomers, which are cyclic acetals with an exocyclic alkoxy group, are selectively synthesized via the addition reaction of alcohol to a cyclic enol ether. The obtained cyclic acetals are copolymerized with CEVE without isolation, yielding alternating copolymers. Highly frequent crossover reactions between CEVE and a series of alcohol-derived cyclic acetals including natural-occurring alcohol-derived monomers successfully proceed.

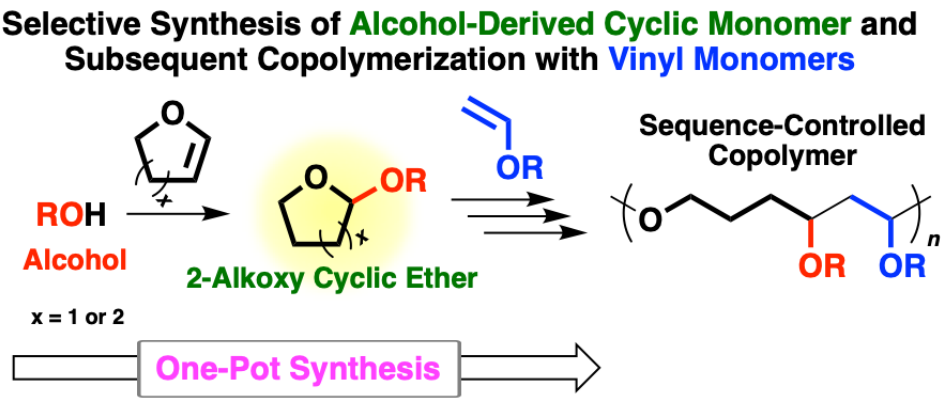

Figure 12. Synthesis of sequence-controlled copolymers via the selective generation of alcohol-derived cyclic monomers and subsequent copolymerization with VEs in one-pot process.

References

1. Anfinsen, C. B. *Science* **1973**, *181*, 223–230.
2. Grubbs, R. B.; Grubbs, R. H. *Macromolecules* **2017**, *50*, 6979–6997.
3. Hadjichristidis, N.; Pitsikalis, M.; Pispas, S.; Iatrou, H. *Chem. Rev.* **2001**, *101*, 3747–3792.
4. Polymeropoulos, G.; Zapsas, G.; Ntetsikas, K.; Bilalis, P.; Gnanou, Y.; Hadjichristidis, N. *Macromolecules* **2017**, *50*, 1253–1290.
5. Hirao, A.; Goseki, R.; Ishizone, T. *Macromolecules* **2014**, *47*, 1883–1905.
6. Kennedy, J. P. *J. Polym. Sci. Part A: Polym. Chem.* **1999**, *37*, 2285–2293.
7. Aoshima, S.; Kanaoka, S. *Chem. Rev.* **2009**, *109*, 5245–5287.
8. Ouchi, M.; Terashima, T.; Sawamoto, M. *Chem. Rev.* **2009**, *109*, 4963–5050.
9. Matyjaszewski, K. *Macromolecules* **2012**, *45*, 4015–4039.
10. Hawker, C. J.; Bosman, A. W.; Harth, E. *Chem. Rev.* **2001**, *101*, 3661–3688.
11. Moad, G.; Rizzardo, E.; Thang, S. H. *Polymer* **2008**, *49*, 1079–1131.
12. Yamago, S. *Chem. Rev.* **2009**, *109*, 5051–5068.
13. Goto, A.; Ohtsuki, A.; Ohfuji, H.; Tanishima, M.; Kaji, H. *J. Am. Chem. Soc.* **2013**, *135*, 11131–11139.
14. Rosen, B. M.; Percec, V. *Chem. Rev.* **2009**, *109*, 5069–5119.
15. Yokozawa, T.; Yokoyama, A. *Chem. Rev.* **2009**, *109*, 5595–5619
16. Penczek, S.; Cypryk, M.; Duda, A.; Kubisa, P.; Slomkowski, S. *Prog. Polym. Sci.* **2007**, *32*, 247–282.
17. Domski, G. J.; Rose, J. M.; Coates, G. W.; Bolig, A. D.; Brookhart, M. *Prog. Polym. Sci.* **2007**, *32*, 30–92.
18. Coates, G. W.; Hustad, P. D.; Reinartz, S. *Angew. Chem. Int. Ed.* **2002**, *41*, 2236–2257.
19. Nakamura, A.; Ito, S.; Nozaki, K. *Chem. Rev.* **2009**, *109*, 5215–5244.
20. Schrock, R. R. *Acc. Chem. Res.* **1990**, *23*, 158–165.
21. Webster, O. W. *Science* **1991**, *251*, 887–893.
22. Leonard, J. In *Polymer Handbook 4th Edition*; Brandrup, J.; Immergut, E. H.; Grulke, E. A. Eds., Wiley, New York, **1999**.
23. Nuyken, O.; Pask, S. *Polymers* **2013**, *5*, 361–403.
24. Duda, A.; Kowalski, A. In *Handbook of Ring-Opening Polymerization*; Dubois, P., Coulembier, O., Raquez, J.-M., Eds.; Wiley-VCH Verlag GmbH & Co. KGaA: Weinheim, Germany, **2009**; pp 1–51.
25. Penczek, S.; Cypryk, M.; Duda, A.; Kubisa, P.; Slomkowski, S. *Prog. Polym. Sci.* **2007**, *32*, 247–282.
26. Mecerreyes, D.; Moineau, G.; Dubois, P.; Jérôme, R.; Hedrick, J. L.; Hawker, C. J.; Malmström, E. E.; Trollsas, M. *Angew. Chem. Int. Ed.* **1998**, *37*, 1274–1276.
27. Bielawski, C. W.; Louie, J.; Grubbs, R. H. *J. Am. Chem. Soc.* **2000**, *122*, 12872–12873.
28. de Freitas, A. G. O.; Trindade, S. G.; Muraro, P. I. R.; Schmidt, V.; Satti, A. J.; Villar, M. A.; Ciolino, A. E.; Giacomelli, C. *Macromol. Chem. Phys.* **2013**, *214*, 2336–2344
29. Aoshima, H.; Uchiyama, M.; Satoh, K.; Kamigaito, M. *Angew. Chem. Int. Ed.* **2014**, *53*, 10932–10936.
30. Zhang, Z.; Xia, L.; Zeng, T.-Y.; Wu, D.-C.; Zhang, W.-J.; Hong, C.-Y.; You, Y.-Z. *Polym. Chem.* **2019**, *10*, 2117–2125.
31. Yang, H.; Xu, J.; Pispas, S.; Zhang, G. *Macromolecules* **2012**, *45*, 3312–3317.
32. Kanazawa, A.; Kanaoka, S.; Aoshima, S. *J. Am. Chem. Soc.* **2013**, *135*, 9330–9333.
33. Szwarc, M. *Nature* **1956**, *178*, 1168–1169.
34. Dreyfuss, M. P.; Dreyfuss, P. *Polymer* **1965**, *6*, 93–95.
35. Gilliom, L. R.; Grubbs, R. H. *J. Am. Chem. Soc.* **1986**, *108*, 733–742.
36. Wallace, K. C.; Schrock, R. R. *Macromolecules* **1987**, *20*, 448–450.

37. Doi, Y.; Ueki, S.; Keii, T. *Macromolecules* **1979**, *12*, 814–819.
38. Miyamoto, M.; Sawamoto, M.; Higashimura, T. *Macromolecules* **1984**, *17*, 265–268.
39. Faust, R.; Kennedy, J. P. *Polym. Bull.* **1986**, *15*, 317–323.
40. Sawamoto, M.; Okamoto, C.; Higashimura, T. *Macromolecules* **1987**, *20*, 2693–2697.
41. Aoshima, S.; Higashimura, T. *Polym. Bull.* **1986**, *15,* 417–423.
42. Aoshima, S.; Higashimura, T. *Macromolecules* **1989**, *22*, 1009–1013.
43. Aoshima, S.; Shachi, K.; Kobayashi, E.; Higashimura, T. *Makromol. Chem.* **1991**, *192*, 1749–1757.
44. Kishimoto, Y.; Aoshima, S.; Higashimura, T. *Macromolecules* **1989**, *22*, 3877–3882.
45. Aoshima, S.; Fujisawa, T.; Kobayashi, E. *J. Polym. Sci., Part A: Polym. Chem.* **1994**, *32*, 1719–1728.
46. Kamigaito, M.; Maeda, Y.; Sawamoto, M.; Higashimura, T. *Macromolecules* **1993**, *26*, 1643–1649.
47. Nuyken, O.; Kröner, H. *Makromol. Chem.* **1990**, *191*, 1–16.
48. Cramail, H.; Deffieux, A.; Nuyken, O. *Makromol. Chem. Rapid Commun.* **1993**, *14*, 17–27.
49. Cho, C. G.; Feit, B. A.; Webster, O. W. *Macromolecules* **1990**, *23*, 1918–1923.
50. Georges, M. K.; Veregin, R. P. N.; Kazmaier, P. M.; Hamer, G. K. *Macromolecules* **1993**, *26*, 2987–2988.
51. Hawker, C. J. *J. Am. Chem. Soc.* **1994**, *116*, 11185–11186.
52. Wang, J.-S.; Matyjaszewski, K. *J. Am. Chem. Soc.* **1995**, *117*, 5614–5615.
53. Kato, M.; Kamigaito, M.; Sawamoto, M.; Higashimura, T. *Macromolecules* **1995**, *28*, 1721–1723.
54. Chiefari, J.; Chong, Y. K.; Ercole, F.; Krstina, J.; Jeffery, J.; Le, T. P. T.; Mayadunne, R. T. A.; Meijs, G. F.; Moad, C. L.; Moad, G.; Rizzardo, E.; Thang, S. H. *Macromolecules*, **1998**, *31*, 5559–5562.
55. Yamashita, Y.; Tsuda, T.; Okada, M.; Iwatsuki, S. *J. Polym. Sci. Part A1* **1966**, *4*, 2121–2135.
56. Kanazawa, A.; Kanaoka, S.; Aoshima, S. *Macromolecules* **2009**, *42*, 3965–3972.
57. Kanazawa, A.; Shibutani, S.; Yoshinari, N.; Konno, T.; Kanaoka, S.; Aoshima, S. *Macromolecules* **2012**, *45*, 7749–7757.
58. Lutz, J.-F.; Ouchi, M.; Liu, D. R.; Sawamoto, M. *Science* **2013**, *341*, No. 1238149.
59. Lutz, J.-F. *Macromol. Rapid Commun.* **2017**, *38*, No. 1700582.
60. Merrifield, R. B. *J. Am. Chem. Soc.* **1963**, *85*, 2149–2154.
61. Trinh, T. T.; Laure, C.; Lutz, J.-F. *Macromol. Chem. Phys.* **2015**, *216*, 1498–1506.
62. Solleder, S. C.; Schneider, R. V.; Wetzel, K. S.; Boukis, A. C.; Meier, M. A. R. *Macromol. Rapid Commun.* **2017**, *38*, No. 1600711.
63. Hill, S. A.; Gerke, C.; Hartmann, L. *Chem. Asian J.* **2018**, *13*, 3611–3622.
64. Cho, I.; Hwang, K. M. *J. Polym. Sci., Part A: Polym. Chem.* **1993**, *31*, 1079–1081.
65. Cho, I. *Prog. Polym. Sci.* **2000**, *25*, 1043−1087.
66. Zhang, J.; Matta, M. E.; Hillmyer, M. A. *ACS Macro Lett.* **2012**, *1*, 1383–1387.
67. Yokota, K. Periodic Copolymers. *Prog. Polym. Sci.* **1999**, *24*, 517−563.
68. Satoh, K.; Ozawa, S.; Mizutani, M.; Nagai, K.; Kamigaito, M. *Nat. Commun.* **2010**, *1*, 6.
69. Miyajima, M.; Satoh, K.; Horibe, T.; Ishihara, K.; Kamigaito, M. *J. Am. Chem. Soc.* **2020**, *142*, 18955–18962.
70. Satoh, K.; Ishihara, K.; Hamada, T.; Handa, M.; Abe, T.; Ozawa, S.; Mizutani, M.; Kamigaito, M. *Macromolecules* **2019**, *52*, 3327–3341.
71. Zhang, C.; Ling, J.; Wang, Q. *Macromolecules* **2011**, *44*, 8739–8743.
72. Schulz, M. D.; Wagener, K. B. *Macromol. Chem. Phys.* **2014**, *215*, 1936–1945.
73. Gutekunst, W. R.; Hawker, C. J. *J. Am. Chem. Soc.* **2015**, *137*, 8038–8041.
74. Yang, C.; Flynn, J. P.; Niu, J. *Angew. Chem. Int. Ed.* **2018**, *57*, 16194–16199.
75. Kreye, O.; Tóth, T.; Meier, M. A. R. *J. Am. Chem. Soc.* **2011**, *133*, 1790–1792.

76. Yu, Z.; Wang, M.; Chen, X.; Huang, S.; Yang, H. *Angew. Chem. Int. Ed.* **2021**, *60*, 1–5.
77. Saegusa, T.; Kobayashi, S.; Kimura, Y. *Macromolecules* **1977**, *10*, 68–72.
78. Hsieh, H. L. *J. Macromol. Sci., Part A: Chem.* **1973**, *7*, 1525−1535.
79. Kanazawa, A.; Aoshima, S. *ACS Macro Lett.* **2015**, *4*, 783–787.
80. Mimura, M.; Kanazawa, A.; Aoshima, S. *Macromolecules* **2019**, *52*, 7572–7583.
81. Yokozawa, T.; Suzuki, T. *Macromolecules* **1996**, *29*, 22–25.
82. Yokozawa, T.; Tagami, M.; Takehana, T.; Suzuki, T. *Tetrahedron* **1997**, *53*, 15603–15616.
83. Zhang, Z.; You, Y.; Hong, C. *Macromol. Rapid Commun.* **2018**, *39*, 1800362.
84. Zhang, Z.; You, Y.-Z.; Wu, D.-C.; Hong, C.-Y. *Macromolecules* **2015**, *48*, 3414–3421.
85. Yan, J.-J.; Wang, D.; Wu, D.-C.; You, Y.-Z. *Chem. Commun.* **2013**, *49*, 6057.
86. Wuts, P. G. M.; Greene, T. W. *Protective Groups in Organic Synthesis, 4th ed.*, John Wiley & Sons, New York, **2007**.
87. Krompiec, S.; Penkala, M.; Szczubiałka, K.; Kowalska, E. *Coord. Chem. Rev.* **2012**, *256*, 2057–2095.
88. Meskens, F. A. J. *Synthesis* **1981**, *7*, 501-522.
89. Firouzabadi, H.; Iranpoor, N.; Karimi, B. *Synlett* **1999**, *3*, 321–323.
90. Lin, C.-H.; Lin, S. D.; Yang, Y.-H.; Lin, T.-P. *Catal. Lett.* **2001**, *73*, 121–125.
91. Sülü, M.; Venanzi, L. M. *Helv. Chim. Acta* **2001**, *84*, 898–907.
92. Smith, B. M.; Kubczyk, T. M.; Graham, A. E. *Tetrahedron* **2012**, *68*, 7775–7781.
93. Kumar, B.; Aga, M. A.; Rouf, A.; Shah, B. A.; Taneja, S. C. *RSC Adv* **2014**, *4*, 21121–21130.
94. Rezai, N.; Meybodi, F. A.; Salehi, P. *Synth. Commun.* **2000**, *30*, 1799–1805.
95. Gogoi, D.; Baruah, N.; Bez, G. *Synth. Commun.* **2007**, *37*, 593–597.
96. Moneno, T. *Tetrahedron Lett.* **2002**, *43*, 7975–7978.
97. Bogert, M. T.; Roblin, R. O. *J. Am. Chem. Soc.* **1933**, *55*, 3741–3745.
98. Hanzlik, R. P.; Leinwetter, M. *J. Org. Chem.* **1978**, *43*, 438–440.
99. Iranpoor, N.; Zeynizadeh, B. *J. Chem. Res.* **1998**, No. 8, 466–467.
100. Vyvyan, J. R.; Meyer, J. A.; Meyer, K. D. *J. Org. Chem.* **2003**, *68*, 9144–9147.
101. Saha, S.; Mandal, S. K.; Roy, S. C. *Tetrahedron Lett.* **2008**, *49*, 5928–5930.
102. Nagata, T.; Takai, T.; Yamada, T.; Imagawa, K.; Mukaiyama, T. *Bull. Chem. Soc. Jpn.,* **1994**, *67*, 2614–2616.
103. Kato, K.; Yamamoto, Y.; Akita, H. *Tetrahedron Lett.* **2002**, *43*, 4915–4917.
104. Prins, H. *J. Chem. Weekbl.* **1919**, *16*, 1072.
105. Arundale, E.; Mikeska, L. A. *Chem. Rev.* **1952**, *51*, 505–555.
106. Alonso, F.; Rodriguez-Fernandez, M.; Sanchez, D.; Yus, M. *Synthesis* **2010**, *17*, 3013–3020.
107. Deslongchamps, P.; Dory, Y. L.; Li, S. *Tetrahedron* **2000**, *56*, 3533–3537.
108. Satchell, D. P. N.; Satchell, R. S. *Chem. Soc. Rev.* **1990**, *19*, 55–81.
109. Salomaa, P.; Kankaanperä, A. *Acta Chem. Scand.*, **1961**, *15*, 871–878.
110. Newman, M. S.; Harper, R. J. *J. Am. Chem. Soc.* **1958**, *80*, 6350–6355.
111. Fife, T. H.; Jao, L. K. *J. Org. Chem.* **1965**, *30*, 1492–1495.
112. Vitullo, V. P.; Pollack, R. M.; Faith, W. C.; Keiser, M. L. *J. Am. Chem. Soc.* **1974**, *96*, 6682–6685.
113. Chwialkowska, W.; Kubisa, P.; Penczek, S. *Makromol. Chem.* **1982**, *183*, 753–769.
114. Okada, M.; Takikawa, N.; Iwatsuki, S.; Yamashita, Y.; Ishii, Y. *Makromol. Chem.* **1965**, *82*, 16–24.
115. Yamashita, Y.; Asakura, T.; Okada, M.; Ito, K. *Makromol. Chem.* **1969**, *129*, 1–11
116. Yamashita, Y.; Kozawa, S.; Chiba, K.; Okada, M. *Makromol. Chem.* **1970**, *135*, 75–86.
117. Yokoyama, Y.; Okada, M.; Sumitomo, H. *Polym. J.* **1979**, *11*, 629–639.

118. Okada, M. Polymerization of 1, 3-Dioxolane. *J. Soc. Chem. Ind. Jpn.* **1962**, *65*, 691–695.
119. Ishigaki, A.; Shono, T.; Hachihama, Y. *Makromol. Chem.* **1964**, *79*, 170–179.
120. Kubisa, P.; Penczek, S. *Makromol. Chem.* **1978**, *179*, 445–454.
121. Van Meirvenne, D.; Haucourt, N.; Goethals, E. J. *Polym. Bull.* **1990**, *23*, 185–190.
122. Haucourt, N. H.; Goethals, E. J.; Schappacher, M.; Deffieux, A. *Makromol. Chem. Rapid Commun.* **1992**, *13*, 329–336.
123. Satoh, K.; Kamigaito, M.; Sawamoto, M. *Macromolecules* **2000**, *33*, 748–753.
124. Shimomoto, H.; Yoshida, H.; Kanaoka, S.; Aoshima, S. *J. Polym. Sci., Part A: Polym. Chem.* **2012**, *50*, 3703–3709.
125. Yokoyama, N.; Kanazawa, A.; Kanaoka, S.; Aoshima, S. *Macromolecules* **2018**, *51*, 884–894.
126. Ishizone, T.; Mochizuki, A.; Hirao, A.; Nakahama, S. *Macromolecules* **1995**, *28*, 3787–3793.
127. Loykulnant, S.; Hayashi, M.; Hirao, A. *Macromolecules* **1998**, *31*, 9121–9126.
128. Leibig, D.; Lange, A.-K.; Birke, A.; Frey, H. *Macromol. Chem. Phys.* **2017**, *218*, 1600553.
129. Ishizone, T.; Tominaga, T.; Kitamura, K.; Hirao, A.; Nakahama, S. *Macromolecules* **1995**, *28*, 4829–4836.
130. Leibig, D.; Müller, A. H. E.; Frey, H. *Macromolecules* **2016**, *49*, 4792–4801.
131. Zhen, Y.; Wan, S.; Liu, Y.; Yan, H.; Shi, R.; Wang, C. *Macromol. Chem. Phys.* **2005**, *206*, 607–612.
132. Sweat, D. P.; Yu, X.; Kim, M.; Gopalan, P. *J. Polym. Sci. Part A: Polym. Chem.* **2014**, *52*, 1458–1468.
133. Sweat, D. P.; Kim, M.; Schmitt, A. K.; Perroni, D. V.; Fry, C. G.; Mahanthappa, M. K.; Gopalan, P. *Macromolecules* **2014**, *47*, 6302–6310.
134. Wang, K.; Liu, Q.; Lu, G.; Zhang, Y.; Zhou, Y.; Chen, S.; Ma, Q.; Liu, G.; Zeng, Y. *Macromolecules* **2021**, *54*, 3725–3734.
135. Zhang, Z.; Liu, G.; Bell, S. *Macromolecules* **2000**, *33*, 7877–7883.
136. Feng, X.-S.; Pan, C.-Y.; Wang, J. *Macromol. Chem. Phys.* **2001**, *202*, 3403–3409.
137. Van Camp, W.; Du Prez, F. E.; Bon, S. A. F. *Macromolecules* **2004**, *37*, 6673–6675.
138. Li, R. C.; Broyer, R. M.; Maynard, H. D. *J. Polym. Sci. Part A: Polym. Chem.* **2006**, *44* (17), 5004–5013.
139. Murthy, N.; Thng, Y. X.; Schuck, S.; Xu, M. C.; Fréchet, J. M. J. *J. Am. Chem. Soc.* **2002**, *124*, 12398–12399.
140. Binauld, S.; Stenzel, M. H. *Chem. Commun.* **2013**, *49*, 2082–2102.
141. Liu, B.; Thayumanavan, S. *J. Am. Chem. Soc.* **2017**, *139*, 2306–2317.
142. Okada, M.; Yamashita, Y.; Ishii, Y. *Makromol. Chem.* **1966**, *94*, 181–193.
143. Okada, M.; Yamashita, Y. *Makromol. Chem.* **1969**, *126*, 266−275.
144. Shirouchi, T.; Kanazawa, A.; Aoshima, S. *Macromolecules* **2016**, *49*, 7184–7195.

Part I

Structural Investigation of Cyclic Acetals in the Concurrent Cationic Vinyl-Addition and Ring-Opening Copolymerization with Vinyl Monomers

Chapter 2.

Controlled Cationic Copolymerization of Vinyl Monomers and Cyclic Acetals via Concurrent Vinyl-Addition and Ring-Opening Mechanisms: the Systematic Study of Structural Effects on the Copolymerization Behavior

Introduction

The structures of polymerizable monomers have a considerable influence on their polymerizability and the properties of the resulting polymers. The rational design of the propagating species based on the monomer structures is also of great importance for controlling the primary structure, including the molecular weight, chain end, and tacticity, of the resulting polymer. In addition, the polymerization of more than one monomer enables the precise synthesis of polymers with various structures, such as block, gradient, graft, and star-shaped polymers.[1–6] The copolymerization of different types of monomers, such as vinyl and cyclic monomers,[7–14] is an attractive method for synthesizing materials with novel functions that cannot be achieved in homopolymers or copolymers from similar types of monomers. However, the copolymerization of different types of monomers is inherently challenging because of the differences in the active species generated during the polymerization. Understanding the copolymerization mechanism based on systematic studies is expected to provide guidelines for designing propagating species derived from different types of monomers.

In the concurrent cationic vinyl-addition and ring-opening copolymerization, the generation of the carbocation through the ring-opening of the oxonium ion is critical because the oxonium ion species derived from the oxirane does not react with the vinyl monomer.[14] In previous work, oxiranes, such as isobutylene oxide and isoprene monoxide, which generate tertiary and resonance-stabilized carbocations, respectively, by the ring-opening reactions of the oxonium ion, were demonstrated to efficiently copolymerize with isopropyl vinyl ether (VE) using $B(C_6F_5)_3$ as a Lewis acid catalyst. Moreover, the copolymerization of IPVE with alkoxyoxirane, which is a cyclic monomer that generates an alkoxy group-adjacent, VE-type carbocation via ring-opening, proceeded efficiently despite the fact that the copolymerization involved an intramolecular alkoxy group transfer.[15] Long-lived propagating species were also generated in the latter case, which is partly due to the structural similarities between the active species derived from the alkoxyoxirane and VE.

Cyclic acetals also generate an alkoxy group-adjacent carbocation through ring-opening reactions. Indeed, conventional cationic copolymerizations of VEs or styrene with cyclic acetals were reported several decades ago.[7,8] Recently, we have achieved a controlled cationic copolymerization of 2-chloroethyl VE (CEVE) with 1,3-dioxepane (DOP) or 2-methyl-1,3-dioxolane (MDOL) using a carefully selected initiating system based on the living cationic polymerization of vinyl monomers.[16] The reversible activation–deactivation reaction of the carbon–chlorine bond at the propagating chain end was most likely required for achieving the appropriate dormant–active equilibrium (Scheme 1).

In this chapter, the author aims to synthesize various controlled copolymers and systematically investigate the effects of the structures of cyclic acetals on their polymerization behaviours. Cyclic acetals are prepared by the acetalization or the acetal exchange from the corresponding diols with carbonyl compounds or acetals, respectively;[17] hence, the author first synthesized five-, six-, and seven-membered cyclic acetalswith

no substituents or one or two methyl substituents at the 2-position; the five- and unsubstituted six-membered cyclic acetals were obtained commercially (Scheme 2). The as-prepared cyclic acetals were used for the cationic copolymerization with CEVE. The copolymerizations of vinyl monomers and various cyclic acetals proceeded in a controlled manner using a suitably designed initiating system. Based on the results of the systematic copolymerizations, we discuss the effects of the number of substituents at the 2-position and the ring member, which are related to the stabilities of the generated carbocation and the ring strain, respectively, of the cyclic acetals on the polymerization rates and the frequencies of the crossover reactions.

Scheme 1. Possible Mechanisms of Controlled Cationic Copolymerization of Vinyl Monomers and Cyclic Acetals

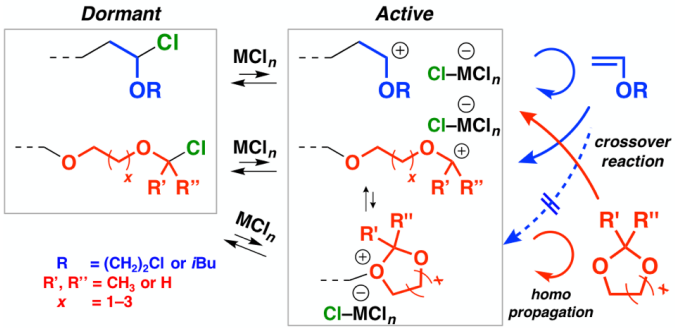

Scheme 2. Concurrent Cationic Vinyl-Addition and Ring-Opening Copolymerization of Vinyl Monomers and Cyclic Acetals.

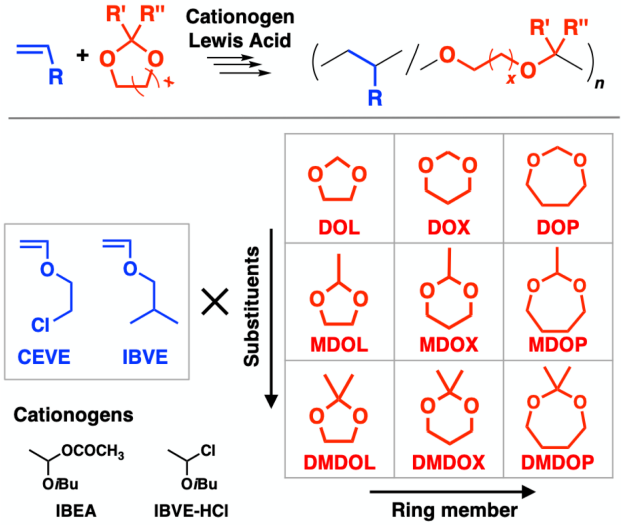

Experimental Section

Materials

2-Chloroethyl VE (CEVE; TCI; >97.0%) and isobutyl VE (IBVE; TCI; >99.0%) were washed with a sodium hydroxide solution and then water, and distilled twice over calcium hydride under reduced (CEVE) or at atmospheric (IBVE) pressure. 1,3-Dioxolane (DOL; TCI; >98.0%), 2,2-dimethyl-1,3-dioxolane (DMDOL; TCI; >98.0%), 1,3-dioxane (DOX; TCI; >98.0%), ethyl acetate (Wako; >99.5%), and heptane (Nacalai Tesque; >99.0%) were distilled twice over calcium hydride. 1,3-Dioxepane (DOP) was synthesized

via the reaction of 1,4-butanediol (TCI; >99.0%) and paraformaldehyde (Sigma-Aldrich; 95%) according to the previously reported procedure.[18] 2-Methyl-1,3-dioxolane (MDOL; TCI; >98.0%) was distilled over calcium hydride and then lithium aluminum hydride. 2,6-Di-*tert*-butylpyridine (DTBP; Wako; 97%) was distilled twice over calcium hydride under reduced pressure. The adducts of IBVE with HCl (IBVE–HCl) or acetic acid (IBEA) were prepared by addition reactions of IBVE with HCl or acetic acid, respectively.[19,20] $TiCl_4$ (Sigma-Aldrich; 1.0 M solution in toluene), $SnCl_4$ (Sigma-Aldrich; 1.0 M solution in heptane), and 3-buten-1-ol (TCI; >98.0%) were used without further purification. Toluene (Wako; 99.5%), dichloromethane (Wako; 99.0%), and hexane (Wako; >96.0%) were dried by passage through solvent purification columns (Glass Contour). All chemicals except for toluene, dichloromethane, hexane, and 3-buten-1-ol were stored in brown ampules under dry nitrogen.

Synthesis of 2-Methyl-1,3-dioxane (MDOX), 2,2-Dimethyl-1,3-dioxane (DMDOX), 2-Methyl-1,3-dioxepane (MDOP), and 2,2-Dimethyl-1,3-dioxepane (DMDOP)

The six- and seven-membered methyl and dimethyl cyclic acetals were synthesized by acetal exchange between the corresponding acetal and diol using indium (III) trifluoromethanesulfonate as a catalyst at room temperature.[17] After the acetal exchange, the reaction mixture was concentrated to remove ethanol or methanol, which was generated as a byproduct. The product was purified by distillation under reduced pressure.

2-Methyl-1,3-dioxane (MDOX)

Synthesized from diethylacetal (60 g) and 1,3-propanediol (40 g). Colorless liquid. Isolated yield: 28%. ^{1}H NMR ($CDCl_3$; 500 MHz): δ 4.68 (1H, q), 4.11-4.07 (2H, m), 3.80-3.75 (2H, m), 2.12-2.02 (1H, m), 1.35-1.31 (1H, m), 1.30 (3H, d). ^{13}C NMR ($CDCl_3$; 125 MHz): δ 99.4, 67.0, 25.7, 21.4. MS (ESI) *m*/*z* $[M+Na]^+$, calcd: 125.0537, found: 125.0537.

2,2-Dimethyl-1,3-dioxane (DMDOX)

Synthesized from 2,2-dimethoxypropane (54 g) and 1,3-propanediol (42 g). Colorless liquid. Isolated yield: 29%. ^{1}H NMR ($CDCl_3$; 500 MHz): δ 3.91 (4H, dd), 1.70 (2H, m), 1.43 (6H, s). ^{13}C NMR ($CDCl_3$; 125 MHz): δ 98.2, 60.3, 25.9, 24.6. MS (ESI) *m*/*z* $[M+Na]^+$, calcd: 139.0730, found: 139.0729.

2-Methyl-1,3-dioxepane (MDOP)

Synthesized from diethylacetal (126 g) and 1,4-butanediol (99 g). Colorless liquid. Isolated yield: 48%. ^{1}H NMR ($CDCl_3$; 500 MHz): δ 4.90 (1H, q), 3.90-3.60 (4H, m), 1.76-1.65 (4H, m), 1.28 (3H, d). ^{13}C NMR ($CDCl_3$; 125 MHz): δ 99.5, 65.4, 29.3, 20.8. MS (ESI) *m*/*z* $[M+Na]^+$, calcd: 139.0730, found: 139.0729.

2,2-Dimethyl-1,3-dioxepane (DMDOP)

Synthesized from 2,2-dimethoxypropane (107 g) and 1,4-butanediol (102 g). Colorless liquid. Isolated yield: 49%. ^{1}H NMR ($CDCl_3$; 500 MHz): δ 3.68 (4H, m), 1.60 (4H, m), 1.33 (6H, s). ^{13}C NMR ($CDCl_3$; 125 MHz): δ 101, 62.3, 29.8, 25.2. MS (ESI) *m*/*z* $[M+Na]^+$, calcd: 153.0886, found: 153.0885.

Polymerization Procedure

The following is a typical polymerization procedure with the IBEA/$TiCl_4$/$SnCl_4$ initiating system. A glass tube equipped with a three-way stopcock was dried using a heat gun (Ishizaki; PJ-206A; at 450 °C) under

dry nitrogen. Dichloromethane, toluene, heptane or hexane (as an internal standard for gas chromatography), ethyl acetate, a solution of DTBP in dichloromethane, and a solution of IBEA in hexane were added into the tube using dry medical syringes. After cooling the solution to 0 °C for 10 min, a solution of $TiCl_4$ in toluene was added to the tube. After 15 min, the solution was cooled to −78 °C. The polymerization was started by sequentially adding a solution of $SnCl_4$ in toluene and a mixture of CEVE and cyclic acetals to the tube. After a predetermined interval, the reaction was terminated with methanol or 3-buten-1-ol containing a small amount of aqueous ammonia or triethylamine, respectively. The quenched mixture was diluted with dichloromethane and washed with water. The volatiles were then removed under reduced pressure at 50 °C to yield the polymer. The monomer conversion was determined by gas chromatography (or by gravimetry and ^{1}H NMR spectroscopy for some reactions).

Acid Hydrolysis

The acid hydrolysis of the copolymers was conducted using 1.0 M HCl(aq) in 1,2-dimethoxyethane at room temperature over 3 h (sample: 0.5 wt%). The quenched mixture was diluted with dichloromethane and washed with aqueous sodium hydroxide and then water. The volatiles were removed at ordinary temperature and normal pressure.

Characterization

The molecular weight distributions (MWDs) of the obtained polymers were determined by gel permeation chromatography (GPC) in chloroform at 40 °C on polystyrene gel columns (TSKgel GMH_{HR}-M × 2 with an exclusion limit molecular weight = 4×10^6; bead size = 5 μm; column size = 7.8 mm i.d. × 300 mm; flow rate = 1.0 mL min^{-1}) connected to a Tosoh DP-8020 pump, a CO-8020 column oven, a UV-8020 ultraviolet detector, and an RI-8020 refractive-index detector. The number-average molecular weight (M_n) and the polydispersity ratio (weight-average molecular weight/number-average molecular weight [M_w/M_n]) were calculated from the chromatographs based on 16 polystyrenes standards (Tosoh; M_n = 577—1.09×10^6, $M_w/M_n \leq 1.1$). NMR spectra were recorded using a JEOL JNM-ECA 500 (500.16 MHz for ^{1}H and 125.77 MHz for ^{13}C) spectrometer. Matrix-assisted laser desorption/ionization time-of-flight mass spectrometry (MALDI-TOF-MS) analyses were performed on a Shimadzu/Kratos AXIMA-Performance spectrometer (linear mode) using dithranol as a matrix and sodium trifluoroacetate as an ion source. Electrospray ionization mass spectra (ESI-MS) were recorded using a LTQ Orbitrap XL (Thermo Scientific) spectrometer.

Results and Discussion

Controlled Cationic Copolymerization of CEVE and Various Cyclic Acetals

Initially, the cationic copolymerization of DMDOL, which has two methyl substituents at the 2-position, with CEVE was conducted using an IBEA/$TiCl_4$/$SnCl_4$ initiating system in the presence of ethyl acetate and DTBP at –78 °C. Ethyl acetate was used as a Lewis basic additive to both suppress side reactions by stabilizing the growing carbocation and adjust the dormant–active equilibrium through the interaction with Lewis acid catalysts.[21] DTBP was employed as a proton trap reagent to suppress chain transfer reactions caused by adventitious water.[22,23] This initiating system was designed based on the living cationic polymerization of

CEVE (entry 20 in Table 1).[24] In previous study, DOL, which is unsubstituted at the 2-position, did not copolymerize with CEVE, while the copolymerization of CEVE and MDOL, which has one methyl substituent, proceeded in a highly controlled manner.[16] DMDOL also copolymerized with CEVE very efficiently to yield copolymers with unimodal MWDs (Figure 1C). Interestingly, the copolymerization of DMDOL proceeded approximately 10^3-times faster than the reaction of MDOL, suggesting that the substituents at the 2-position significantly affected the polymerization behavior. The sharp MWD peaks (M_w/M_n = 1.2—1.3) of the obtained copolymers shifted to the high-molecular-weight region as the polymerization proceeded, indicating the generation of the long-lived propagating species. Moreover, the M_n values measured by GPC analysis were consistent with the values calculated from the conversions of the two monomers (Figure 1B). These results suggest that the cationic copolymerization of CEVE and DMDOL proceeded in a highly controlled manner.

^{1}H NMR analysis of the copolymer of CEVE and DMDOL revealed the occurrence of frequent crossover reactions (Figure 2., see Figure S1 for ^{13}C NMR spectra). The peak at 4.9 ppm (peak 6) was assigned

Table 1. Cationic Copolymerization of CEVE and Various Cyclic Acetals[a]

				conv[b] (%)				crossover per chain[d]		units per block[d]	
entry	vinyl	cyclic	time	vinyl	cyclic	$M_n \times 10^{-3}$ [c]	M_w/M_n[c]	V to A[e]	A to V[e]	vinyl	cyclic
1	CEVE	DOL	27 h	100	18(0[f])	11.5	1.10	—	—	—	—
2	—	DOL	48 h	—	22	1.5	3.68	—	—	—	—
3	CEVE	MDOL	70 h	60	31	5.2	1.37	30	25	2.7	0.98
4	—	MDOL	24 h	—	7	—	—	—	—	—	—
5	CEVE	DMDOL	30 s	36	11	3.2	1.33	11	11	2.1	0.96
6			13 min	75	34	9.9	1.19	59	59	2.5	0.96
7	—	DMDOL	10 min	—	0	—	—	—	—	—	—
8	CEVE	DOX	2 h	32	18(0[f])	3.1	1.10	—	—	—	—
9	—	DOX	96 h	—	15	—	—	—	—	—	—
10	CEVE	MDOX	2 h	68	24	7.2	1.19	21	21	5.1	1.0
11	—	MDOX	5 h	—	19	—	—	—	—	—	—
12	CEVE	DMDOX	30 s	84[f]	65[f]	16.5	1.85	74	74	1.3	1.0
13	—	DMDOX	49 h	—	37	—	—	—	—	—	—
14	CEVE	DOP	44 h	71	92	11.2	1.84	9.0	13	8.3	12
15	—	DOP	24 h	—	23	4.2	1.69	—	—	—	—
16	CEVE	MDOP	4 h	61	62	6.8	1.65	33	37	1.5	1.7
17	—	MDOP	4 h	—	29	0.3	1.58	—	—	—	—
18	CEVE	DMDOP	30 s	91[f]	72	15.6	1.41	66	66	1.7	0.92
19	—	DMDOP	24 h	—	22	—	—	—	—	—	—
20	CEVE	—	30 s	94	—	11.5	1.15	—	—	—	—

[a] $[CEVE]_0$ = 0 or 0.40 M, [cyclic acetal]$_0$ = 0 or 0.40 M, $[IBEA]_0$ = 4.0 mM, $[TiCl_4]_0$ = 5.0 mM, $[SnCl_4]_0$ = 20 mM, $[DTBP]_0$ = 10 mM, [ethyl acetate] = 20 mM in toluene/dichloromethane (9/1 v/v) at –78 °C. [b] Determined by gas chromatography. [c] Determined by GPC (polystyrene standards). [d] Estimated by ^{1}H NMR analysis. [e] V: vinyl monomer; A: cyclic acetal. [f] Determined by gravimetry and ^{1}H NMR analysis of products.

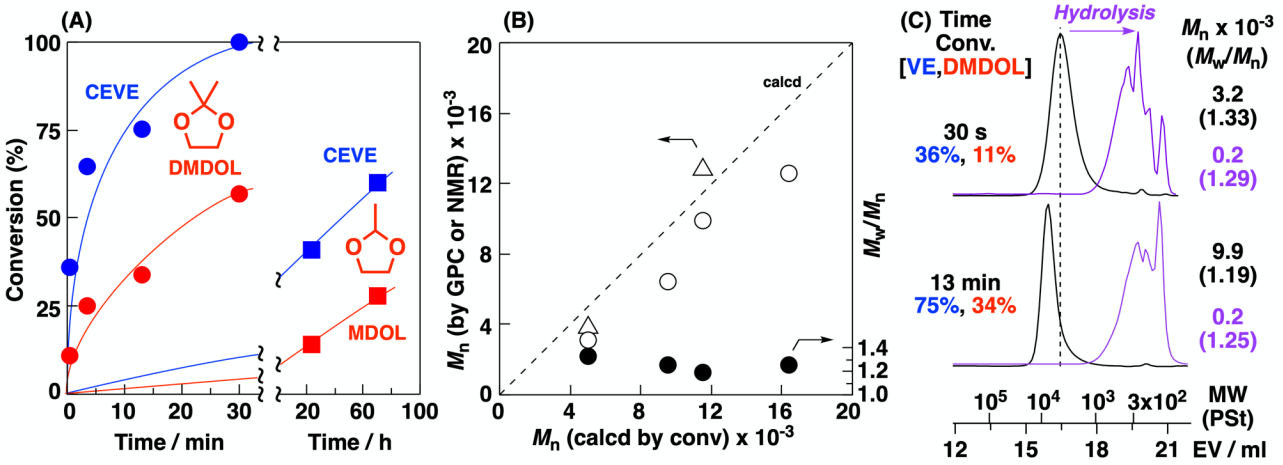

Figure 1. (A) Time–conversion curves for the copolymerization of CEVE and DMDOL (circle) or MDOL (square), (B) the M_n determined by GPC (circle) or NMR (triangle; calculated from the integral ratios of the peaks of the main chain and the ω-ends) and M_w/M_n (filled) values of poly(CEVE-*co*-DMDOL)s, and (C) MWD curves of poly(CEVE-*co*-DMDOL)s (black) and acid hydrolysis products (purple). Hydrolysis conditions: 1.0 M HCl in 1,2-dimethoxyethane (0.5 wt% polymer) at room temperature for 3 h. The data correspond to entries 3, 5 and 6 in Table 1 and entry 3 in Table S1.

to the acetal proton derived from the crossover reaction from CEVE to DMDOL. However, the peaks assigned to the structure derived from the crossover from DMDOL to CEVE (peaks 9 and 10) overlapped with peaks of the CEVE units at 3.4 ppm. The integral of the methyl peak at 1.2 ppm (peak 11) derived from DMDOL was almost six times that of the acetal peak (peak 6), indicating that the homopropagation of DMDOL was negligible. This fact was also supported by the inefficient homopolymerization of DMDOL (entry 7 in Table 1). The numbers of crossover reactions from CEVE to DMDOL per chain were calculated to be 11 and 59 for the copolymers obtained after 30 s and 13 min, respectively (entries 5 and 6 in Table 1). The average numbers of CEVE/DMDOL monomer units per block were calculated to be 2.1/0.96 (30 s) and 2.5/0.96 (13 min) (the numbers of DMDOL units per block were less than one due to acceptable error), which suggests that the crossover reactions occurred at similar frequency regardless of monomer conversion.

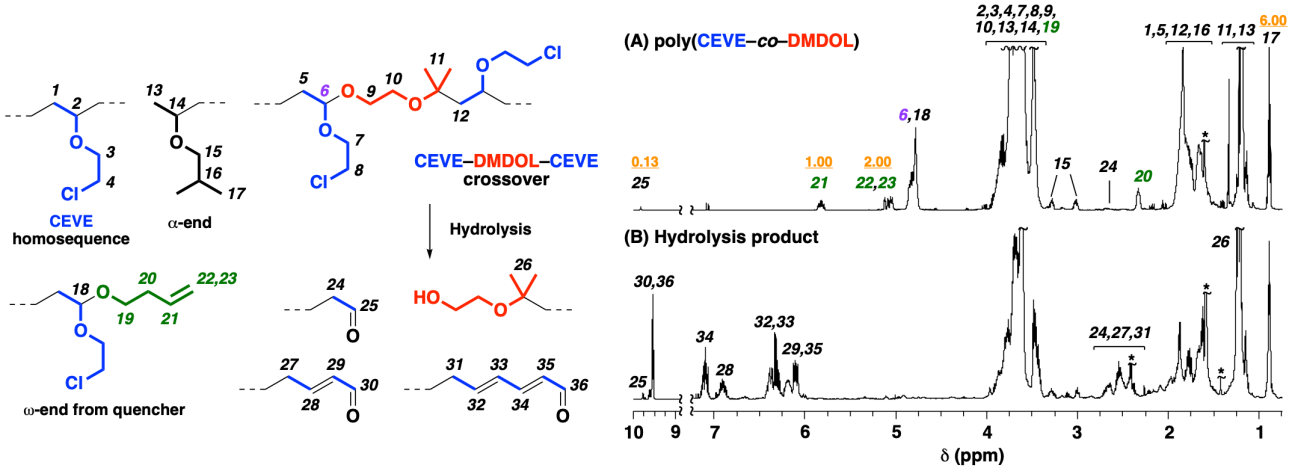

Figure 2. ^{1}H NMR spectra of (A) poly(CEVE-*co*-DMDOL) (entry 5 in Table 1) and (B) the hydrolysis product (in $CDCl_3$ at 30 °C; * water, grease, etc; number written in orange: integral ratio).

The copolymerization via crossover reactions was corroborated by acid hydrolysis (by HCl in 1,2-dimethoxyethane; see the experimental part) of the obtained copolymer. In the ^{1}H NMR spectrum of the acid hydrolysis product (Figure 2B), the signals from the acid-labile acetal structures generated via the crossover reaction from CEVE to DMDOL (peak 6) had disappeared, and instead, aldehyde peaks at 9.5 and 9.8 ppm (peaks 25, 30, and 36) emerged.[16,25–27] Moreover, the hydrolysis products had much lower M_n values (0.2×10^3) than the original copolymers regardless of the monomer conversion, which supports the frequent occurrence of crossover reactions (Figure 1C).

The introduction of the structures derived from the quencher was confirmed by chain-end analysis, indicating the generation of long-lived species in the copolymerization. 3-Buten-1-ol was used as a quencher because the olefin moiety is easily distinguishable from the other peaks by ^{1}H NMR analysis. The peaks at 2.3, 5.1, and 5.8 ppm (peaks 20, 22, 23 and 21) were assigned to the fragment derived from 3-buten-1-ol. A very small peak assigned to an aldehyde moiety (peak 25), which was generated from the reaction of the CEVE-derived propagating carbocation with adventitious water, was also detected (Scheme S1). Based on the ratios of the integrals of these peaks, approximately 90% of the ω-ends stemmed from the quencher, indicating the copolymerization was highly controlled via an appropriate dormant-active equilibrium of the propagating chain ends. In addition, the sum of the integrals from 3-buten-1-ol (peak 21) and aldehyde (peak 25) agreed with that of the α-end structures derived from IBEA (peak 17). Moreover, the M_n value calculated from the ratios of the integrals of the peaks from the detectable ω-ends and the main chain (3.6×10^3) was comparable to the value obtained by GPC analysis (3.2×10^3; Figure 1B). These facts suggest that most of the dormant species were derived from CEVE instead of DMDOL because the DMDOL-derived ω-ends are difficult to detect due to the instability of the structure formed after the reaction with the quencher.[28] In addition, most of the ω-ends stemmed from the quencher at higher monomer conversions, indicating that side reactions negligibly occurred even at the late stage of the copolymerization. MALDI-TOF-MS analysis also supported the generation of copolymers with the fragments derived from the cationogen and the quencher (Figure S2).

The livingness of the copolymerization of CEVE and DMDOL was also confirmed by a monomer addition experiment (Figure 3). The unimodal and sharp MWD curves shifted to the high-molecular-weight region after addition of a second portion of CEVE late in the copolymerization reaction, indicating that the occurrence of side reactions such as chain transfer reactions was negligible.

Other cyclic acetals, except for DOL and DOX, were also successfully copolymerized with CEVE in a controlled manner (entries 10, 12, 14, 16, and 18 in Table 1 and entries 7, 9, 11, 13, and 15 Table S1; Fig. 4). MDOX, DMDOX, DOP, MDOP, and DMDOP were synthesized by acetalization or acetal exchange from 1,3-propandiol or 1,4-butandiol with paraformaldehyde, diethyl acetal, or 2,2-dimethoxypropane using an acid catalyst. In the copolymerizations of these cyclic acetals with CEVE, polymers with unimodal MWDs were produced under conditions similar to those used for MDOL and DMDOL. The peaks of the MWD curves shifted to higher molecular weights as the reactions progressed (Figure 4). The molecular weights obtained by GPC analysis were consistent with the theoretical values. In addition, these M_n values increased linearly with increasing monomer conversion. The generation of low-MW compounds from the hydrolysis of the obtained copolymers indicated that acetal structures were introduced into the main chain by the crossover reaction from CEVE to the cyclic acetal.

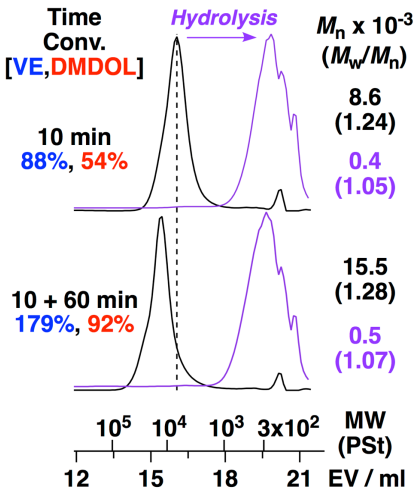

Figure 3. MWD curves of poly(CEVE-*co*-DMDOL)s (black) and acid hydrolysis products (purple) obtained in the monomer-addition experiment. Polymerization conditions: $[CEVE]_0 = [CEVE]_{add} = 0.40$ M, $[DMDOL]_0 = 0.40$ M, $[IBEA]_0 = 4.0$ mM, $[TiCl_4]_0 = 5.0$ mM, $[SnCl_4]_0 = 20$ mM, [ethyl acetate] = 20 mM, $[DTBP]_0 = 10$ mM, in toluene/dichloromethane (9/1 v/v) at –78 °C. Hydrolysis conditions: 1.0 M HCl in 1,2-dimethoxyethane (0.5 wt% polymer) at room temperature for 3 h.

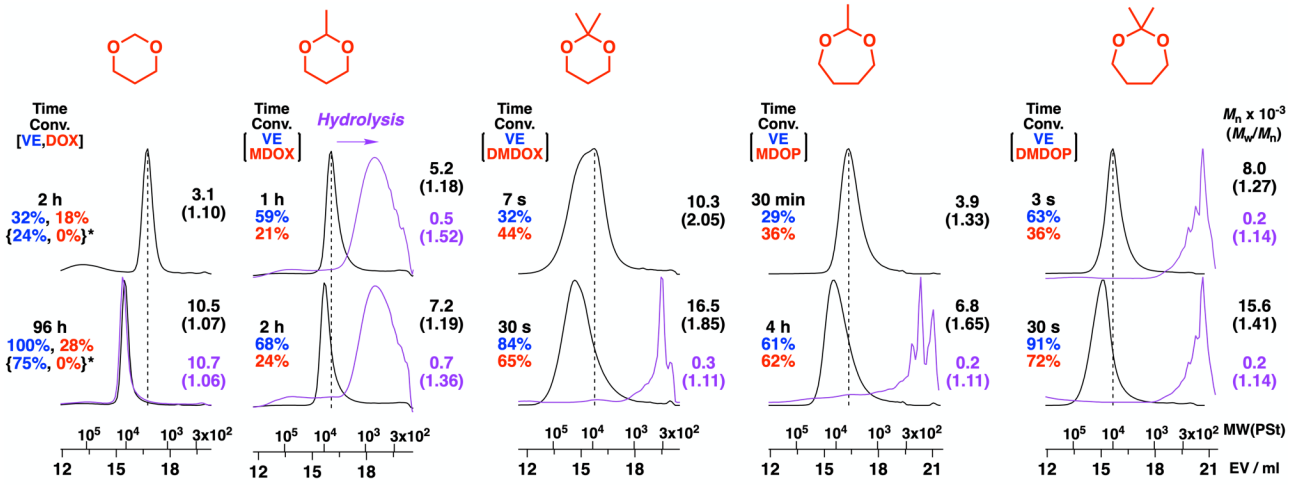

Figure 4. MWD curves of poly(CEVE-*co*-cyclic acetal)s (black) and acid hydrolysis products (purple). * monomer conversion values calculated from ^{1}H NMR and gravimetry. The data correspond to entries 8, 10, 12, 16, 18 in Table 1 and entries 6, 7, 9, 13, and 15 in Table S1

The difference in the number of substituents at the 2-position and the ring member of the cyclic acetal had a remarkable influence on the polymerization rate and the frequencies of the crossover reactions in the copolymerization with CEVE (Figure 5, left). Increasing the number of methyl groups at the 2-position resulted in an increase in the frequency of crossover reactions (e.g., CEVE/DOL: no copolymerization, CEVE/MDOL: 2.7/0.98 units per block, and CEVE/DMDOL: 2.1/0.96 units per block) and an acceleration of the copolymerization (e.g., MDOL: 40 h and DMDOL: 2 min, for 50% conversion of CEVE). The ring member also influenced the polymerization rate (e.g., MDOL: 40 h, MDOX: 1 h, and MDOP: 2 h, for 50% conversion of CEVE). The controlled copolymerization of six- (DMDOX) and seven-membered (DMDOP) analogues of DMDOL with CEVE also involved frequent crossover reactions (CEVE/DMDOX: 1.3/1.0 units per block and

CEVE/DMDOP: 1.7/0.92 units per block) at very high rates (DMDOX: 7 s and DMDOP: 3 s, for 50% conversion of CEVE). Crossover reactions were also frequent in the copolymerizations of CEVE and cyclic acetals with one methyl group at the 2-position, although unlike MDOL and MDOX, homosequences were observed in the case of MDOP (CEVE/MDOL: 2.7/0.98 units per block, CEVE/MDOX = 5.1/1.0 units per block, CEVE/MDOP = 1.5/1.7 units per block).

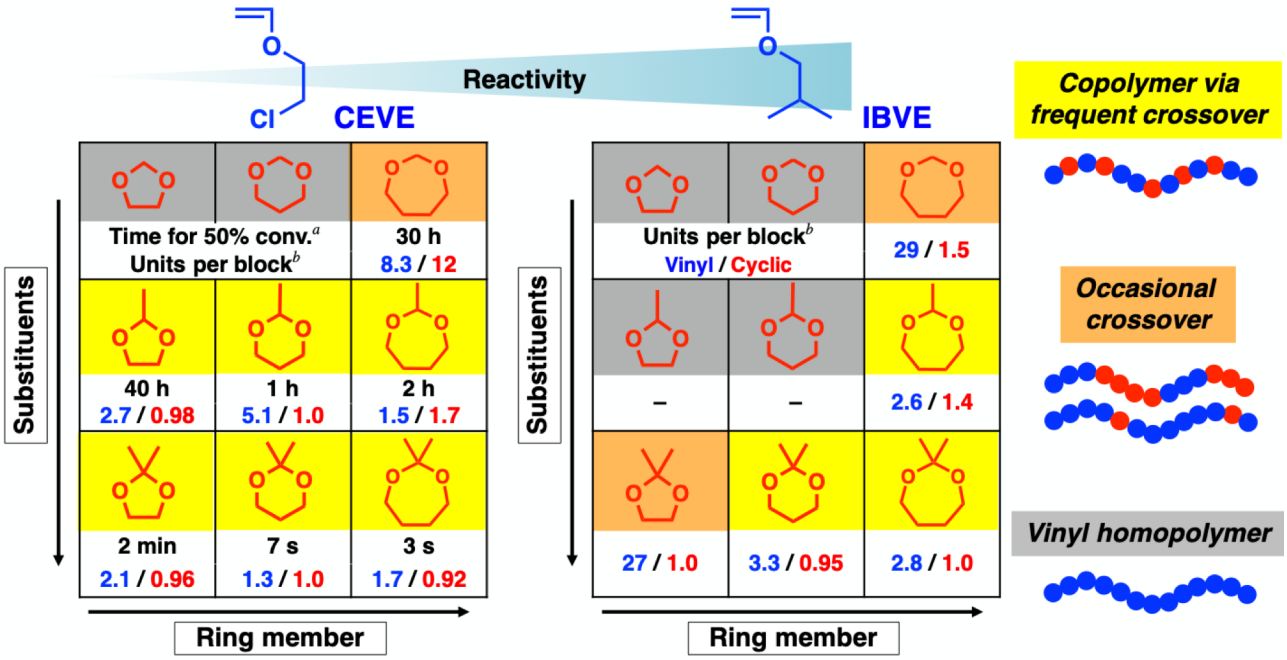

Figure 5. Summary of the products obtained in the copolymerization of VEs and cyclic acetals ([a] Time for 50% conversion of CEVE. [b] Average numbers of VE (blue) and cyclic acetal (red) units per block).

The monomer reactivity ratios determined by the Kelen−Tüdõs method[29,30] (Table 2 and Figure 6) were consistent with the frequencies of the crossover reactions. The decrease in the r_1 values was in agreement with the increase in the number of methyl substituents and indicates the crossover reaction is favored over homopropagation at the CEVE-derived propagating ends. The r_2 values of approximately zero in the cases of MDOL, DMDOL, MDOX, DMDOX, and DMDOP are consistent with the nonhomopolymerizability of these cyclic acetals (Table 2).

Among the examined cyclic acetals, DOL, DOP, and MDOP underwent homopolymerization under the conditions used in the copolymerizations (entries 2, 15, and 17 in Table 1). In the cases of DOL and DOP, long-lived species were generated, although the M_w/M_n values were relatively large (M_w/M_n = 1.7—3.7). The homopolymerization of MDOP gave oligomers ($M_n = 0.3 \times 10^3$). The homopolymerizabilities of the other cyclic acetals were negligible (entries 4, 7, 9, 11, 13, and 19 in Table 1).

Table 2 Monomer Reactivity Ratios[a]

M_1	M_2	r_1	r_2
CEVE	DOL	—	—
	MDOL	2.6[b]	0.06[b]
	DMDOL	1.4	0.01
	DOX	—	—
	MDOX	1.7	0.02
	DMDOX	0.32	0.09
	DOP	4.8[b]	18[b]
	MDOP	1.6	1.3
	DMDOP	0.58	0.01
IBVE	DMDOX	1.2	0.02
	MDOP	2.8	0.24
	DMDOP	2.0	0.07

[a] Determined by the Kelen−Tüdõs method. The values were calculated from the data shown in Figure 6 and S5. [b] Values reported in reference 16.

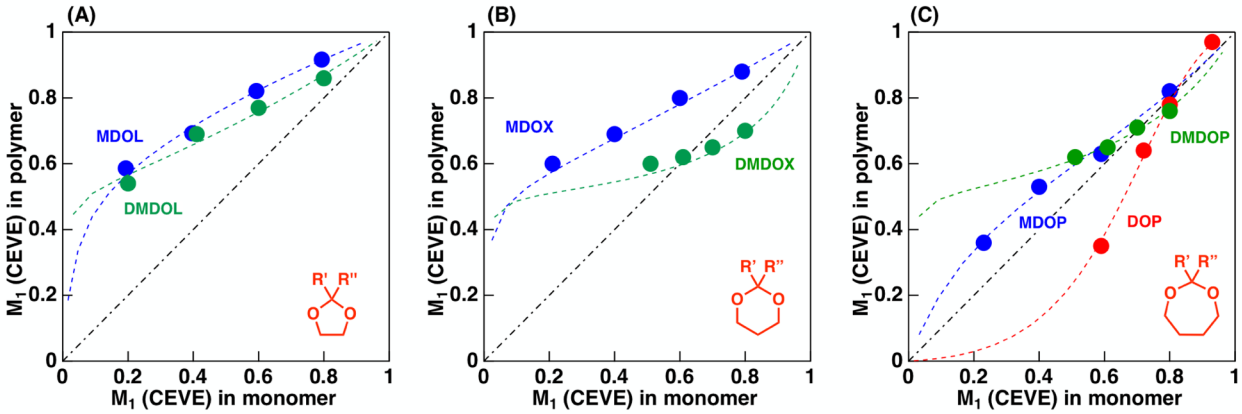

Figure 6. Copolymer compositions for the cationic copolymerizations of CEVE and (A) five-, (B) six-, or (C) seven-membered cyclic acetals (broken curves: curves that were drawn using the *r* values obtained by the Kelen–Tüdõs method; dashed-dotted lines: azeotropic lines). Polymerization conditions: $[CEVE]_0$ + [cyclic acetal]$_0$ = 1.0 M, $[IBEA]_0$ = 4.0 mM, $[TiCl_4]_0$ = 5.0 mM, $[SnCl_4]_0$ = 20 mM, [ethyl acetate] = 20 mM, $[DTBP]_0$ = 10 mM, in toluene/dichloromethane (9/1 v/v) at –78 °C. The data for DOP and MDOL are the same to those shown in reference 16.

Discussion of the Effects of Substituents at the 2-Position and the Ring Member on the Copolymerization Behavior

The differences in the copolymerization behaviors, such as the polymerization rate and the frequency of the crossover reactions, most likely stemmed from several factors based on the structure of the cyclic acetals. The ring-opening reaction of cyclic acetals at the propagation step proceeds in the manner shown in Figure 7. A cyclic acetal adds to the propagating species and subsequently forms an oxonium ion, which is then converted to a carbocation via a ring-opening reaction. In this reaction, the nucleophilicities of the cyclic acetals toward the propagating cationic species are primarily responsible for the addition of the cyclic acetal

to the cation. Increasing the ring strain in the oxonium ion and the stability of the generated carbocation facilitate the ring-opening of the oxonium ion. Therefore, the number of substituents at the 2-position and the ring member of the cyclic acetal most likely affect the propagation reaction. The effects of these factors are discussed in the following sections.

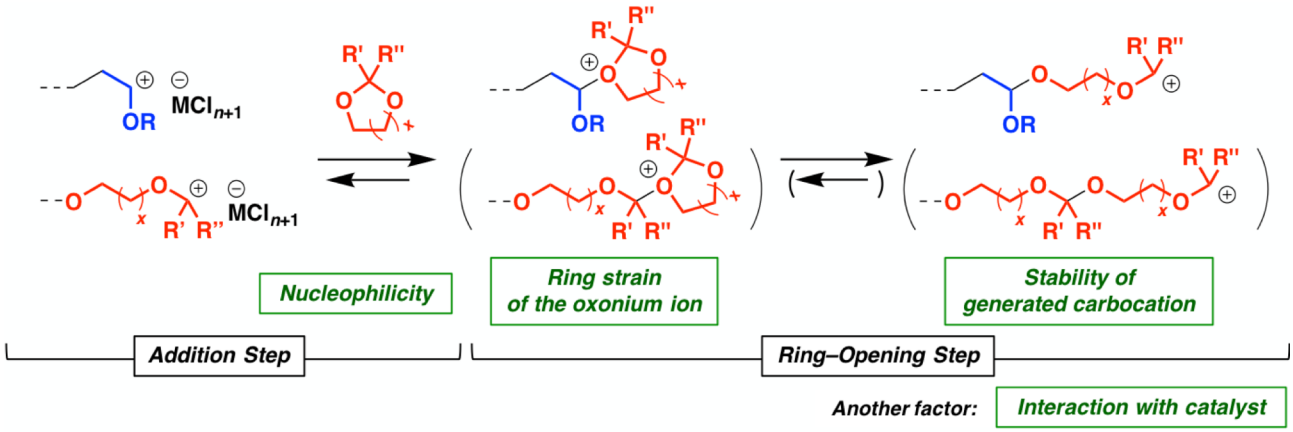

Figure 7. Factors affecting the copolymerization behavior

Effects of the number of methyl groups at the 2-position.

The number of methyl groups at the 2-position of the cyclic acetal mainly influences the stability of the carbocation generated by the ring-opening reaction of the oxonium ion. Cyclic acetals with zero, one, or two substituents generate primary, secondary, or tertiary carbocations, respectively. The ring-opening of the oxonium ion occurs more efficiently when the generated carbocation is more stable (primary < secondary < tertiary), resulting in an acceleration of the copolymerization due to the facilitation of the crossover reaction to CEVE. This trend is consistent with the high reaction rates of the acid hydrolysis reactions of cyclic acetals with larger numbers of substituents at 2-position.[31]

Crossover reactions were more frequent in the copolymerizations of cyclic acetals with larger numbers of methyl groups (Figure 8) likely because the addition-ring elimination equilibrium of a cyclic acetal monomer forms at the propagating end derived from CEVE (Figure 7). An inefficient ring-opening reaction, related to the instability of the carbocation generated via the ring-opening, causes frequent elimination of the

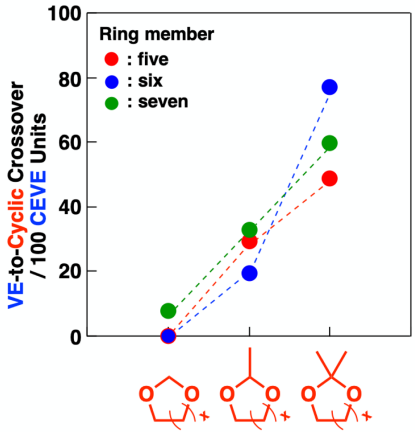

Figure 8. Frequencies of crossover reactions per chain: By ^{1}H NMR analysis. The values were calculated from the data shown in entries 1, 3, 6, 8, 10, 12, 14, 16, and 18 in Table 1.

cyclic acetal from the propagating end, leading to an increase in the homopropagation of CEVE and decreasing the frequency of the crossover reaction to the cyclic acetal. The improvement in the stability of the carbocation generated by the ring-opening of the oxonium ion contributes to the decrease in the rate of the reverse reaction from the oxonium ion to the CEVE-derived carbocation, which enhances the efficiency of the crossover reaction. This discussion is based on the assumption that cyclic acetals with the same ring member have comparable nucleophilicities and ring strain regardless of the number of methyl groups at the 2-position.

Effects of the ring member.

The ring member of the cyclic acetal is related to its ring strain. In the reaction mechanism shown in Figure 7, the ring-opening of the oxonium ion is most likely facilitated by higher ring strain (six- < five- ~ seven-membered ring).[32–39] However, the copolymerization of MDOX, a six-membered cyclic acetal, was the fastest among the three cyclic acetals with one methyl substituent (MDOL: 40 h, MDOX: 1 h, and MDOP: 2 h, for 50% conversion of CEVE). These results suggest that factors other than ring strain also affect the copolymerization behavior.

The difference in the Lewis basicities of the five- and six-membered cyclic acetals, which interact with a Lewis acid catalyst, had a noticeable effect on the polymerization rates. Cyclic acetals are used as an additive to moderate the Lewis acidity of the catalyst in controlled cationic polymerizations of VEs. In previous report, cyclic acetals were an efficient additive in a manner similar to weak Lewis bases such as ethyl acetate, 1,4-dioxane, and tetrahydrofuran.[40] To examine the abilities of cyclic acetals to serve as Lewis basic additives, the polymerization of IBVE was conducted in the presence of DOL, MDOL, DMDOL, or MDOX (Table 3). In all cases, the incorporation of the cyclic acetal into the polymer chains under the examined conditions was negligible. Notably, the polymerization of IBVE in the presence of MDOX proceeded much faster than that in the presence of MDOL (entries 2 and 3 in Table 3), suggesting that MDOL is more Lewis basic than MDOX. This tendency is consistent with the polymerization rates of the copolymerizations with CEVE. In addition, the order of the basicity (six < five-membered [DOX < DOL]) is consistent with the previous report.[40,41] Moreover, the polymerization rates of IBVE were comparable regardless of the number of substituents (entries 1, 2, and 4; DOL, MDOL, and DMDOL). These results indicate that not only the ring strain but also the Lewis basicity of the cyclic acetal affects the copolymerization rate.

Table 3. Homopolymerization of IBVE in the Presence of Cyclic Acetals as an Additive[a]

			conv. (%)	
entry	cyclic	time	vinyl[b]	cyclic[c]
1	DOL	60 s	12	0
2	MDOL	60 s	24	0
3	MDOX	60 s	75	0
4	DMDOL	60 s	18	1

[a] Polymerization conditions: $[IBVE]_0$ = 0.76 M, $[cyclic\ acetal]_0$ = 1.0 M, $[IBVE\text{-}HCl]_0$ = 4.0 mM, $[SnCl_4]_0$ = 5.0 mM, in toluene at –78 °C. [b] Determined by gas chromatography. [c] By gravimetry and ^1H NMR analysis of products.

Copolymerization of Cyclic Acetals with IBVE

The reactivity of the VE also affected the copolymerization via the concurrent vinyl-addition and ring-opening mechanism. The copolymerization of cyclic acetals with IBVE, a more reactive VE than CEVE, using the same initiating system as that used in the controlled copolymerization with CEVE yielded ill-defined copolymers (Figure S3); hence, an initiating system was designed based on the living cationic polymerization of IBVE.[42] As a result, the controlled copolymerization was achieved using $SnCl_4$ as a Lewis acid catalyst in conjunction with IBVE–HCl as a cationogen in the presence of ethyl acetate. The copolymerization results are listed in Table 4 and Table S2. In previous study, DOP and MDOL were shown to be inefficient comonomers for copolymerization with IBVE.[16] In sharp contrast, DMDOL, DMDOX, MDOP, and DMDOP were demonstrated to copolymerize with IBVE in a controlled manner (entries 3, 6, 8, and 9 in Table 4). For example, the narrow MWD peak ($M_w/M_n < 1.2$) of the DMDOP copolymer shifted to the high-molecular-weight region as the reaction progressed (Figure 9C). The M_n values obtained by GPC analysis linearly increased in accordance with the values calculated from the monomer conversion (Figure 9B), which indicates that the copolymerization was mediated by long-lived species. In all cases, the M_w/M_n values of the copolymers with IBVE were smaller than those with CEVE, suggesting an improvement in the controllability. The occurrences of the crossover reactions were confirmed by the detection of acetal protons derived from the crossover reactions in the ^{1}H NMR spectrum of the product (Figure S4). The acid hydrolysis products had much lower M_n values than the original copolymers (Figure 9C), which supports the frequent occurrence of crossover reactions. Accordingly, the selection of an appropriate initiating system allowed the controlled copolymerization of VEs with different reactivities and suitable cyclic acetals.

The reactivities of the vinyl monomers mainly affected the frequencies of the crossover reactions. The average numbers of IBVE units per block were larger than those in the case of CEVE (Figure 5), indicating that the crossover reactions from IBVE to the cyclic acetals were less favorable. For example, the

Table 4. Cationic Copolymerization of IBVE and Various Cyclic Acetals[a]

			conv (%)[b]				crossover per chain[d]		units per block[d]	
entry	cyclic	time	vinyl	cyclic	$M_n \times 10^{-3}$ [c]	M_w/M_n[c]	V to A[e]	A to V[e]	vinyl	cyclic
1	DOL	30 s	73	0[f]	7.1	1.10	—	—	—	—
2	MDOL	60 s	60	1[f]	6.7	1.09	—	—	—	—
3	DMDOL	3 min	84	3[f]	9.9	1.09	3	3	27	1.0
4	DOX	60 s	68	0[f]	6.4	1.18	—	—	—	—
5	MDOX	60 s	64	0[f]	6.8	1.09	—	—	—	—
6	DMDOX	30 s	98	24[f]	12.8	1.16	30	30	3.3	0.95
7	DOP	6 h	83	8	4.5	1.34	1.5	~0	29	1.5
8	MDOP	90 s	92	58	8.6	1.36	20	21	2.6	1.4
9	DMDOP	30 s	82	28[f]	13.0	1.16	28	28	2.8	1.0

[a] $[IBVE]_0 = 0.50$ M, $[\text{cyclic acetal}]_0 = 0.50$ M, $[IBVE\text{-}HCl]_0 = 5.0$ mM, $[SnCl_4]_0 = 5.0$ mM, [ethyl acetate] = 1.0 M in dichloromethane at –78 °C. [b] Determined by gas chromatography. [c] Determined by GPC (polystyrene standards). [d] Estimated by ^{1}H NMR analysis. [e] V: vinyl monomer; A: cyclic acetal. [f] Determined by gravimetry and ^{1}H NMR analysis of products.

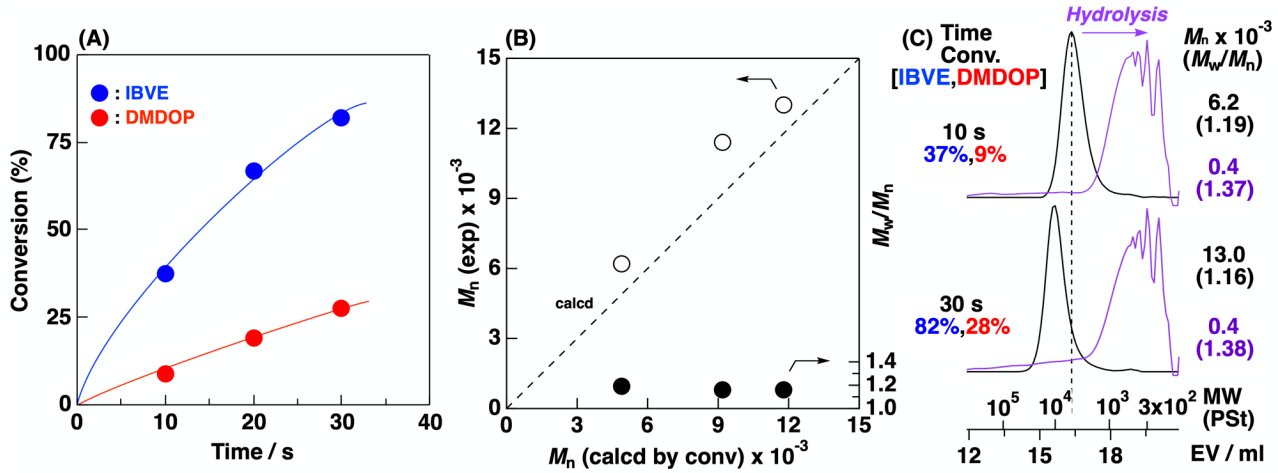

Figure 9. (A) Time–conversion curves for the copolymerization of IBVE and DMDOP, (B) the M_n (open) and M_w/M_n (filled) values of the copolymers obtained, and (C) MWD curves of poly(IBVE-co-DMDOP)s (black) and acid hydrolysis products (purple). Polymerization conditions: $[IBVE]_0$ = 0.50 M, $[DMDOP]_0$ = 0.50 M, $[IBVE\text{-}HCl]_0$ = 5.0 mM, $[SnCl_4]_0$ = 5.0 mM, [ethyl acetate] = 1.0 M, in dichloromethane at –78 °C. Hydrolysis conditions: 1.0 M HCl in 1,2-dimethoxyethane (0.5 wt% polymer) at room temperature for 3 h. The data correspond to entry 9 in Table 4 and entry 17 in Table S3.

CEVE/DMDOL units per block were calculated to be 2.1/0.96, while for IBVE this value was 27/1.0. Moreover, MDOL and MDOX, which produced copolymers with CEVE, did not copolymerize with IBVE (entries 2 and 5 in Table 4). In the case of IBVE, the homopropagation of the vinyl monomer is favored due to the high reactivity of IBVE, which disturbs the crossover reaction to the cyclic acetals. The larger r_1 values of the copolymerizations with IBVE relative to those with CEVE are consistent with the smaller ratios of the crossover reactions to the homopropagation (Table 2; Figure S5). Suitable combinations of both vinyl and cyclic monomers based on their reactivities are crucial for copolymerizations via efficient crossover reactions.

Conclusion

In conclusion, the systematic study of the controlled cationic copolymerizations of VEs and cyclic acetals demonstrated the significant effects of both the numbers of substituents and the ring member of the cyclic acetal on the copolymerization behavior. In most cases, the copolymerizations of CEVE and cyclic acetals proceeded in a living manner, resulting in the generation of well-defined acid-degradable copolymers with acetal moieties in the main chain. The differences in the structures of the cyclic acetals significantly affected the propagation reactions. Specifically, an increase in the number of substituents at the 2-position of the cyclic acetal improved the stability of the carbocation generated from the ring-opening reaction. In addition, the ring member was responsible for the ring strain and the Lewis basicity. These factors affected both the frequency of the crossover reactions and the polymerization rates. The balance between the reactivities of the vinyl and cyclic monomers also influenced the sequence of the copolymer. The results of this study help elucidate the correlation between the structure and the copolymerization behaviors of different types of monomers. The synthesis of well-defined, acid-degradable copolymers from a variety of cyclic acetals, which are easily synthesized from commercially available aldehyde or ketone, will enable the design of unique copolymer chains.

References and Notes

1. Polymeropoulos, G.; Zapsas, G.; Ntetsikas, K.; Bilalis, P.; Gnanou, Y.; Hadjichristidis, N. *Macromolecules* **2017**, *50*, 1253–1290.
2. Matyjaszewski, K. *Prog. Polym. Sci.* **2005**, *30*, 858–875.
3. Guo, X.; Choi, B.; Feng, A.; Thang, H. S. *Macromol. Rapid Commun.* **2018**, *39*, 1800479
4. Hadjichristidis, N.; Iatrou, H.; Pitsikalisa, M.; Mays, J. *Prog. Polym. Sci.* **2006**, *31*, 1068–1132.
5. Sumerlin, S. B.; Vogt, P. A. *Macromolecules* **2010**, *43*, 1–13.
6. Herzberger, J.; Niederer, K. Pohlit, H.; Seiwert, J.; Worm, M.; Wurm, R. F.; Frey, H. *Chem. Rev.* **2016**, *116*, 2170−2243.
7. Okada, M.; Yamashita, Y.; Ishii, Y. *Makromol. Chem.* **1966**, *94*, 181–193.
8. Okada, M.; Yamashita, Y. *Makromol. Chem.* **1969**, *126*, 266−275.
9. Saegusa, T. *Angew. Chem., Int. Ed. Engl.* **1977**, *16*, 826−835.
10. Saegusa, T. *Makromol. Chem.* **1981**, *4*, 73−84.
11. Simionescu, C. I.; Grigoras, M.; Bicu, E.; Onofrei, G. *Polym. Bull.* **1985**, *14*, 79−83.
12. Rivas, B. L.; Pizarro, C.; Canessa, G. S. *Polym. Bull.* **1988**, *19*, 123−128.
13. Yang, H.; Xu, J.; Pispas, S.; Zhang, G. *Macromolecules* **2012**, *45*, 3312−3317.
14. Kanazawa, A.; Kanaoka, S.; Aoshima, S. *Macromolecules* **2014**, *47*, 6635–6644.
15. Kanazawa, A; Kanda, S.; Kanaoka, S.; Aoshima, S. *Macromolecules* **2014**, *47*, 8531–8540.
16. Shirouchi, T.; Kanazawa, A.; Aoshima, S. *Macromolecules* **2016**, *49*, 7184–7195.
17. Smith, M. B.; Kubczyk, M. T.; Graham, E. A. *Tetrahedron* **2012**, *68*, 7775-7781.
18. Pattinson, D. B. *J. Org. Chem.* **1957**, *22*, 662–664.
19. Higashimura, T.; Kamigaito, M.; Kato, M.; Hasebe, T.; Sawamoto, M. *Macromolecules* **1993**, *26*, 2670–2673.
20. Aoshima, S.; Higashimura, T. *Macromolecules* **1989**, *22*, 1009−1013.
21. Aoshima, S.; Yoshida, T.; Kanazawa, A; Kanaoka, S. *J. Polym. Sci., Part A: Polym. Chem.* **2007**, *45*, 1801–1813.
22. Kennedy, J. P.; Chou, R. T. *J. Macromol. Sci., Chem.* **1982**, *18*, 11–16.
23. Bae, Y. C.; Faust, R *Macromol. Symp.* **1998**, *132*, 11–23
24. Kimura, R.; Yamada, M.; Kanazawa, A.; Kanaoka, S.; Aoshima, S. *Polym. Prepr., Jpn.* **2013**, *62*, 2412.
25. Peaks assignable to olefin structures adjacent to the aldehyde moiety were also observed (peaks 28, 29, and 32–35). These alkenal structures were likely derived from dealcohoization reactions (ref. 16, 26 and 27).
26. Yonezumi, M.; Takaku, R.; Kanaoka, S; Aoshima, S. *J. Polym. Sci., Part A: Polym. Chem.* **2008,** *46*, 2202–2211.
27. Aoshima, S.; Higashimura, T. *Polym. J.* **1984**, *16*, 249–258.
28. The reaction of the DMDOL-derived propagating carbocation with 3-buten-1-ol likely resulted in the formation of an alcohol structure at the ω-end because of the spontaneous degradation of the unstable ketal structure after the quench. The quantitative analysis of the alcohol structure was difficult because the peak overlaps with other peaks.
29. Kelen, T.; Tüdõs, F. *Kinet. Catal. Lett.* **1974**, *1*, 487−492.
30. Kennedy, J. P.; Kelen, T.; Tüdõs, F. *J. Polym. Sci., Polym. Chem. Ed.* **1975**, *13*, 2277−2289.
31. Deslongchamps, P.; Dory, L. Y.; Li, S. *Tetrahedron* **2000**, *56*, 3533–3537.

32. The order of ring strain of cyclic acetals is based on several previous reports (references 33–39).
33. Yamashita, Y.; Okada, M.; Suyama, K.; Kasahara, H. *Makromol. Chem.* **1968**, *114*, 146–154.
34. Plesch, P. H.; Westermann, P. H. *Polymer* **1969**, *10*, 105–111.
35. Pihlaja, K. *Acta Chem. Scand.* **1971**, *25*, 451–464.
36. Dainton, F. S.; Ivin, K. J. *Q. Rev., Chem. Soc.* **1958**, *12*, 61–92.
37. Wiberg, K. B. *Angew. Chem., Int. Ed. Engl.* **1986**, *25*, 312–322.
38. Dudev, T.; Lim, C. *J. Am. Chem. Soc.* **1998**, *120*, 4450–4458.
39. Leonard, J. In *Polymer Handbook*, 4nd ed.; Brandrup, J.; Immergut, E. H.; Grulke, E., Eds.; A. Wiley-Interscience, New York, **1999**; p 363–414.
40. Aoshima, S.; Fujisawa, T.; Kobayashi, E. *J. Polym. Sci., Part A: Polym. Chem.* **1994**, *32*, 1719–1728.
41. Yamashita, Y. Tsuda, T.; Okada, M; Iwatsuki, S. *J. Polym. Sci., Part A: Polym. Chem.* **1966**, *4*, 2121-2135.
42. Kanazawa, A.; Kanaoka, S.; Aoshima, S. *Macromolecules* **2009** *42*, 3965–3972.

Supporting Information

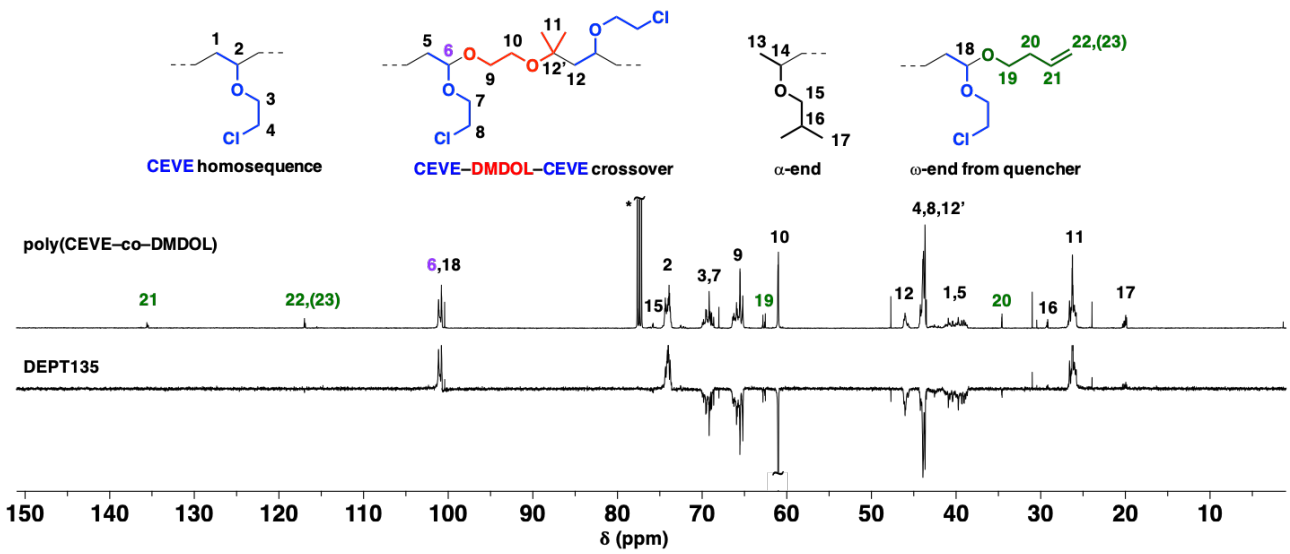

Figure S1. ^{13}C and DEPT 135 NMR spectra of poly(CEVE-*co*-DMDOL) (entry 5 in Table 1) (in $CDCl_3$ at 30 °C; * $CDCl_3$, etc.

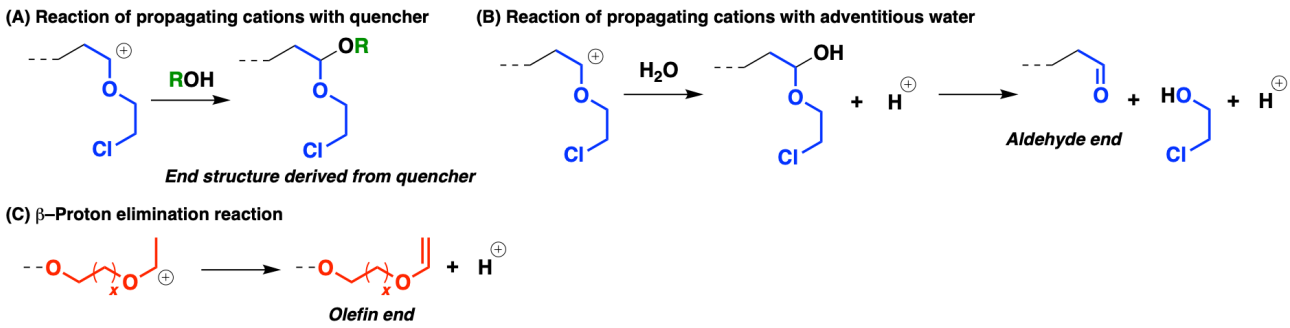

Scheme S1. Possible chain end structures.

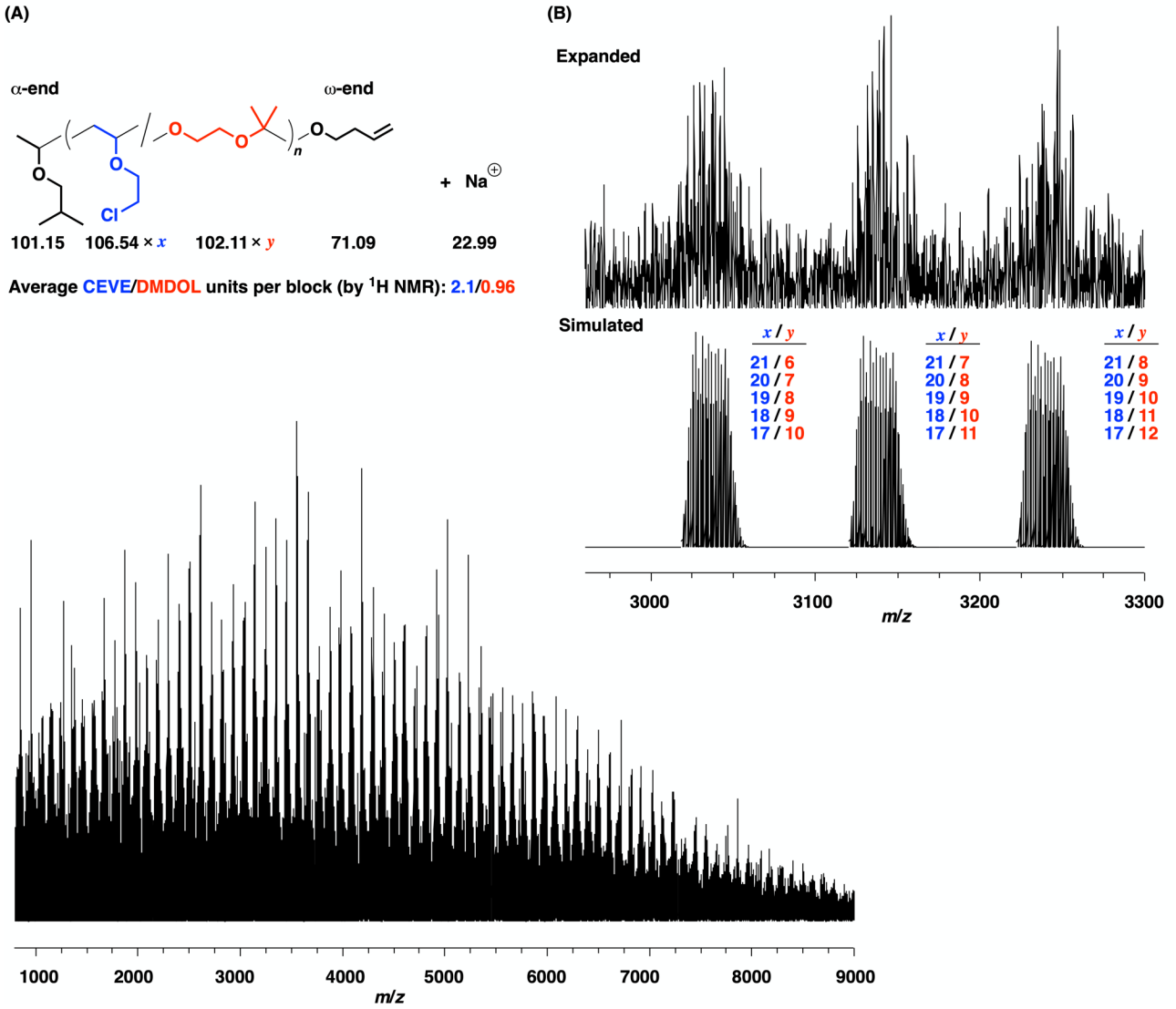

Figure S2. MALDI-TOF-MS spectrum of the copolymer of CEVE and DMDOL (entry 5 in Table 1): (A) the whole spectrum and (B) the expanded spectrum and the simulated patterns.

Note for Figure S2

The spectrum had a series of peak groups at intervals of an *m*/*z* value of approximately 100. Notably, each peak group had a relatively wide *m*/*z* range. Isotopes of chlorine atoms derived from CEVE and slight differences of the molecular weights of both monomer units (CEVE: 106.55, DMDOL: 102.13) are responsible for the wide *m*/*z* range of each peak group. To analyze the spectrum, peak simulation was conducted. The simulation is based on the structures consisting of an α-end derived from the cationogen, CEVE and DMDOL units, and an ω-end derived from the quencher. The ratio of CEVE and DMDOL units (2.1/0.96), which was determined by ^{1}H NMR, was used for the simulation. For example, simulated peaks at the *m*/*z* range of 3100 to 3200 correspond to a mixture of equal amounts of copolymer chains consisting of 21/7 ($C_{129}H_{237}O_{37}Cl_{21}Na$), 20/8 ($C_{130}H_{240}O_{38}Cl_{20}Na$), 19/9 ($C_{131}H_{243}O_{39}Cl_{19}Na$), 18/10 ($C_{132}H_{246}O_{40}Cl_{18}Na$), and 17/10 ($C_{133}H_{249}O_{41}Cl_{17}Na$) of CEVE/DMDOL units. The observed peak groups had similar patters to the simulated peak groups, which suggests the generation of copolymers with the fragments derived from the cationogen and the quencher.

Table S1. Cationic Copolymerization of CEVE and Various Cyclic Acetals[a]

			conv[b] (%)		units per block[d]	
entry	cyclic	time	vinyl	cyclic	vinyl	cyclic
1	DOL	2 h	82	11(0[c])	—	—
2		27 h	100	18(0[c])	—	—
3	MDOL	2 h	19	9[c]	2.2	0.97
4		70 h	60	31	2.7	0.98
5	DOX	2 h	32	18(0[c])	—	—
6		96 h	100	28(0[c])	—	—
7	MDOX	1 h	59	21	5.6	1.0
8		2 h	68	24	5.1	1.0
9	DMDOX	7 s	44[c]	32[c]	1.4	1.0
10		30 s	84[c]	65[c]	1.3	1.0
11	DOP	23 h	36	75	2.7	2.5
12		44 h	71	92	8.3	12
13	MDOP	0.5 h	29	36	1.5	1.8
14		4 h	61	62	1.5	1.7
15	DMDOP	3 s	63	36	1.7	1.0
16		30 s	91[c]	72	1.7	0.92

[a] $[CEVE]_0$ = 0.40 M, [cyclic acetal]$_0$ = 0.40 M, $[IBEA]_0$ = 4.0 mM, $[TiCl_4]_0$ = 5.0 mM, $[SnCl_4]_0$ = 20 mM, $[DTBP]_0$ = 10 mM, [ethyl acetate] = 20 mM in toluene/dichloromethane (9/1 v/v) at –78 °C. Entries 2, 4, 5, 8, 10, 12, 14 and 16 correspond to entries 1, 3, 8, 10, 12, 14, 16 and 18 in Table 1, respectively [b] Determined by gas chromatography. [c] Determined by gravimetry and ^{1}H NMR analysis of products. [d] Calculated by ^{1}H NMR analysis.

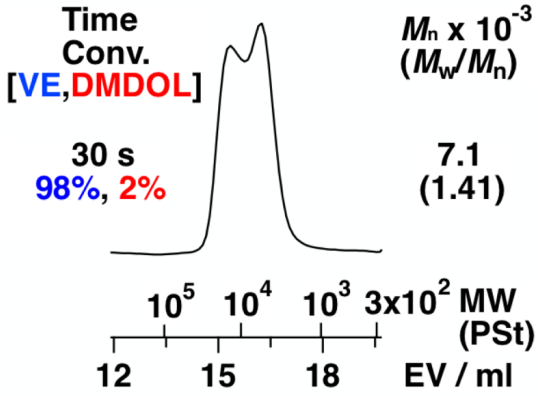

Figure S3. MWD curves of products obtained via the copolymerization of IBVE and DMDOL. Polymerization conditions: $[IBVE]_0$ = 0.40 M, $[DMDOL]_0$ = 0.40 M, $[IBEA]_0$ = 4.0 mM, $[TiCl_4]_0$ = 5.0 mM, $[SnCl_4]_0$ = 20 mM, [ethyl acetate] = 20 mM, $[DTBP]_0$ = 10 mM, in toluene/dichloromethane (9/1 v/v) at –78 °C.

Table S2. Cationic Copolymerization of IBVE and Various Cyclic Acetals[a]

				conv (%)[b]				crossover per chain[d]		units per block[d]	
entry	vinyl	cyclic	time	vinyl	cyclic	$M_n \times 10^{-3}$ [c]	M_w/M_n[c]	V to A[e]	A to V[e]	vinyl	cyclic
1	IBVE	DOL	15 s	48	11(0[f])	5.0	1.13	—	—	—	—
2			30 s	73	14(0[f])	7.1	1.10	—	—	—	—
3	IBVE	MDOL	30 s	46	9(1[f])	5.0	1.15	—	—	—	—
4			60 s	60	4(1[f])	6.7	1.09	—	—	—	—
5	IBVE	DMDOL	30 s	38	0(1[f])	4.4	1.12	1	1	35	1.0
6			3 min	84	0(3[f])	9.9	1.09	3	3	27	1.0
7	IBVE	DOX	30 s	55	0	5.3	1.17	—	—	—	—
8			60 s	68	0	6.4	1.18	—	—	—	—
9	IBVE	MDOX	30 s	43	13(0[f])	4.6	1.10	—	—	—	—
10			60 s	64	3(0[f])	6.8	1.09	—	—	—	—
11	IBVE	DMDOX	10 s	48	11[f]	7.3	1.20	12	12	3.5	0.93
12			30 s	98	24[f]	12.8	1.16	30	30	3.3	0.95
13	IBVE	DOP	6 h	83	8	4.5	1.49	1.5	~0	29	1.5
14			24 h	100	46	5.1	1.34	1.0	~0	40	11
15	IBVE	MDOP	30 s	60	35	7.5	1.22	16	17	3.0	1.4
16			90 s	92	58	8.6	1.36	20	21	2.6	1.4
17	IBVE	DMDOP	10 s	37	9[f]	6.2	1.19	9	9	3.4	1.0
18			30 s	82	28[f]	13.0	1.16	28	28	2.8	1.0

[a] $[IBVE]_0$ = 0.50 M, [cyclic acetal]$_0$ = 0.50 M, $[IBVE\text{-}HCl]_0$ = 5.0 mM, $[SnCl_4]_0$ = 5.0 mM, [ethyl acetate] = 1.0 M in dichloromethane at –78 °C. Entries 2, 4, 6, 8, 10, 12, 13, 16 and 18 correspond to entries 1, 2, 3, 4, 5, 6, 7, 8 and 9 in Table 4, respectively. [b] Determined by gas chromatography. [c] Determined by GPC (polystyrene standards). [d] Estimated by ^{1}H NMR analysis. [e] V: vinyl monomer; A: cyclic acetal. [f] Determined by gravimetry and ^{1}H NMR analysis of products.

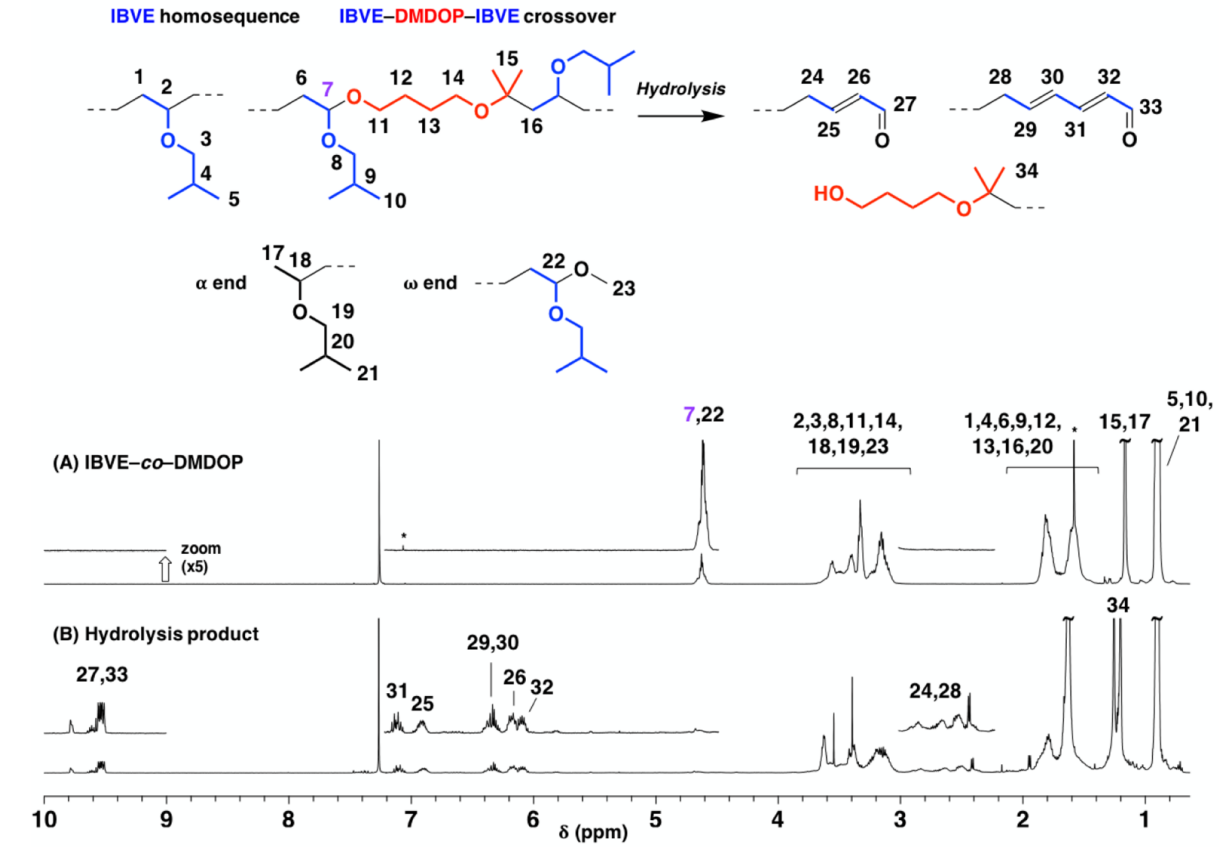

Figure S4. ^{1}H NMR spectra of (A) poly(IBVE-*co*-DMDOP) (entry 17 in Table S3) and (B) the hydrolysis product (in $CDCl_3$ at 30 °C; * water, satellite, etc).

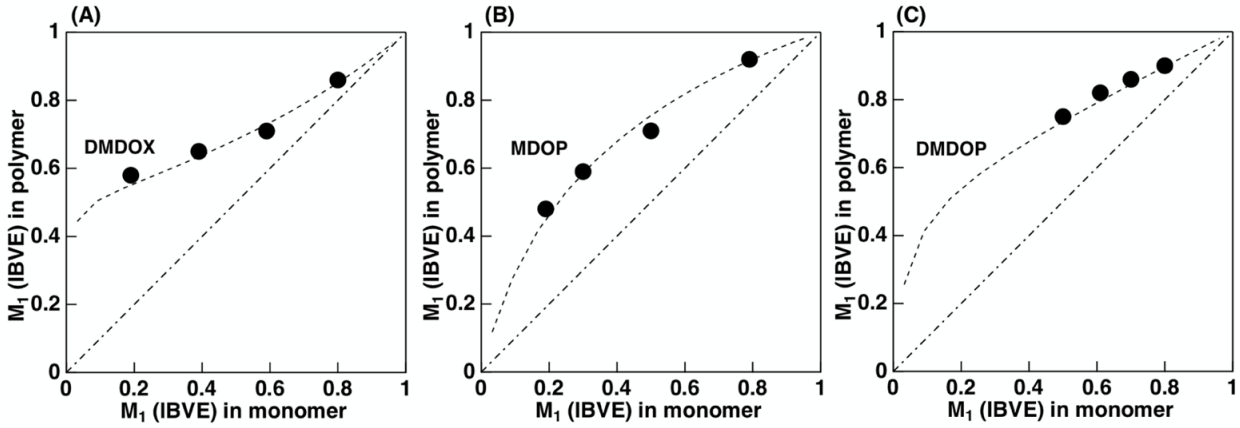

Figure S5. Copolymer compositions for the cationic copolymerizations of IBVE with (A) DMDOX, (B) MDOP, and (C) DMDOP (broken curves: curves that were drawn using the *r* values obtained by the Kelen–Tüdõs method; dashed-dotted lines: azeotropic lines). Polymerization conditions: $[IBVE]_0 + [cyclic\ acetal]_0$ = 1.0 M, $[IBVE–HCl]_0$ = 5.0 mM, $[SnCl_4]_0$ = 5.0 mM, [ethyl acetate] = 1.0 M, in dichloromethane at –78 °C.

Chapter 3.

Alternating Cationic Copolymerization of Vinyl Ethers and Cyclic Acetals with Resonance-Stabilized Substituents: Structural Investigation of Cyclic Acetals on the Copolymerizability

Introduction

The design of active chain ends is of great importance for controlling polymerization reactions.[1–3] In chain-growth polymerization of vinyl monomers, the electronic and resonance effects derived from substituents of the vinyl groups are systematically investigated for the evaluation of polymerizability.[4–7] The structure–reactivity relationships summarized as the Q-e scheme demonstrate an experimental principle that the vinyl monomers with an electron-donating, electron-withdrawing, or resonance group are effective for cationic, anionic, or radical polymerization, respectively. The suitable adjustment of the reactivity of active chain ends leads to the living/controlled polymerization, which enables the control of primary structure of synthetic polymers.[8–15] In addition, the bulky substituents, such as α,α- or α,β-disubstituents, generally decrease the polymerizability due to the steric hindrance around the active species. These facts suggest that the relationship between the structures of active species and the polymerization behavior is a fundamental information in polymer synthesis.

The structural differences of active species also affect the copolymerizations of different types of monomers. For example, the cationic polymerization of vinyl monomers and cyclic ethers proceeds via carbocation and oxonium ion species, respectively. The generation of carbocation via the ring-opening reaction of the cyclic ether-derived oxonium ion is of great importance in the occurrence of crossover reaction because the nucleophilic addition of vinyl monomers to the oxonium ion species is difficult due to the difference in reactivities of propagating species.[16] In terms of the reactivity of carbocation species, cyclic acetals, which generate an alkoxy group-adjacent carbocation species by the ring-opening reaction of the oxonium ion, are promising candidates for copolymerization with vinyl monomers. Indeed, conventional cationic copolymerization of cyclic acetals and vinyl monomers was reported several decades ago.[17,18] Recently, the controlled cationic copolymerization of vinyl ether and cyclic acetals was reported via a carefully designed initiating systems based on the living cationic polymerization of vinyl ethers (VEs).[19]

The copolymerization behavior in the cationic polymerization of VE and cyclic acetals is closely related to the structural difference of cyclic acetals (Scheme 1).[20] For example, the use of cyclic acetals with no, one, or two methyl substituents at the 2-position generated the copolymers with multiblock, random, or approximately alternating sequences, respectively. The ring member of cyclic acetals also affected the frequency of the crossover reactions and the polymerization rates depending on their degree of ring strain and Lewis basicity. The use of cyclic acetals with various other substituents in the cationic copolymerization is expected to afford systematic information of the copolymerization behavior between different types of monomers. However, copolymerization behavior of various cyclic acetals, such as aryl-substituted cyclic acetals, has been not reported.

Scheme 1. Effects of Substituents of Cyclic Acetals on the Copolymerization with Vinyl Monomers and the Aim of This Study (Counteranions are Omitted)

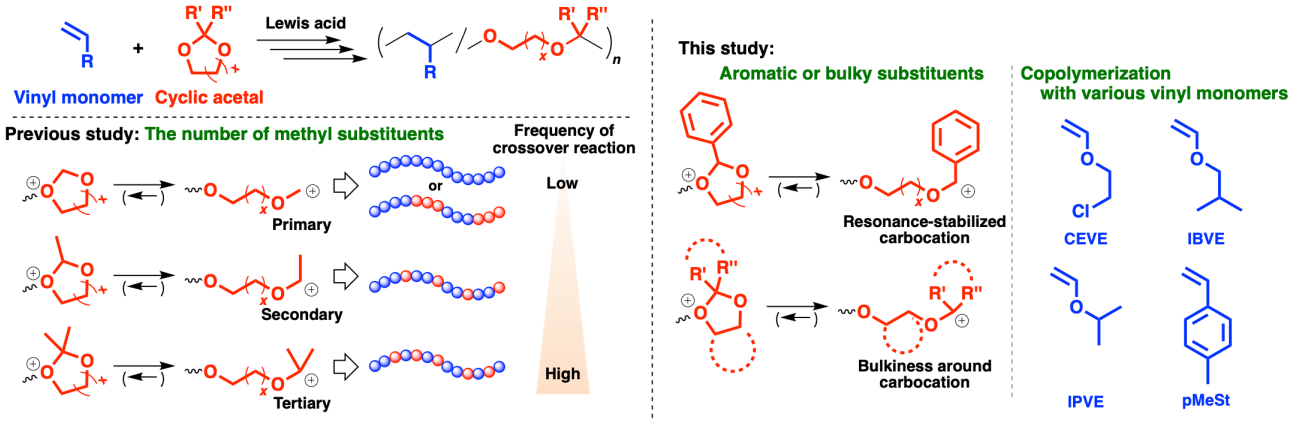

In this chapter, the author aims to investigate the resonance and steric effects on the copolymerization behavior and copolymerizability of cyclic acetals with various vinyl monomers. To investigate the stabilization effect derived from the substituents on cyclic acetals, the author designs the various alkyl- and/or aryl-substituted cyclic acetals, as shown in Scheme 2. These cyclic acetals were simply synthesized by either the acid-catalyzed condensation reaction of carbonyl compounds and diols or transacetalization of acetal and diols. The cationic copolymerization of various aryl- or alkyl-substituted cyclic acetals and VEs successfully proceeded in a controlled manner. In particular, the use of cyclic acetals with an aryl ring at the 2-position underwent exclusive crossover reactions over homopropagation of each monomer, resulting in the generation of alternating copolymers. The extremely high copolymerizabilities of these cyclic acetals enabled copolymerization with various vinyl monomers. The relationship between the structural difference of cyclic acetals and copolymerizability is comprehensively discussed.

Scheme 2. Cyclic Acetals Used in This Study

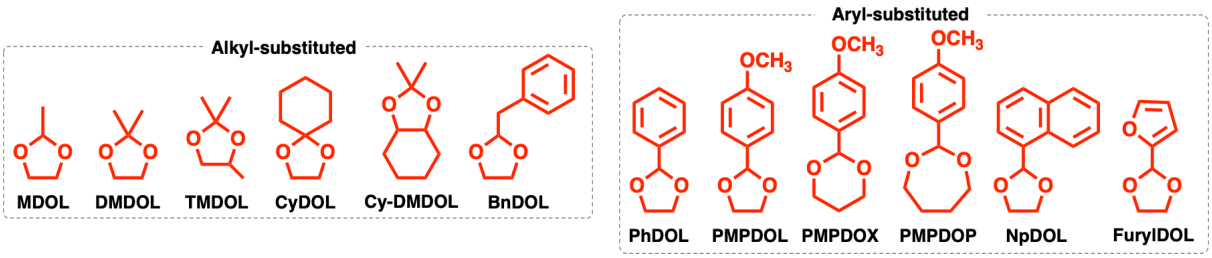

Experimental Section

Materials

p-Methylstyrene (pMeSt; Sigma-Aldrich; 96.0%) and isopropyl VE (IPVE; Wako; >97.0%) were washed with 10% sodium hydroxide solution and then water and distilled twice over calcium hydride under reduced (pMeSt) or atmospheric (IPVE) pressure, respectively. 2,2,4-Trimethyl-1,3-dioxolane (TMDOL; TCI; >98.0%) was distilled twice over calcium hydride. 2-Benzyl-1,3-dioxolane (BnDOL; TCI; >98.0%), 2-(2-furyl)-1,3-dioxolane (FurylDOL; TCI; >98.0%), and *p*-methoxybenzaldehyde (Nacalai Tesque; ≥99.0%) were

distilled over calcium hydride under reduced pressure. Ethanesulfonic acid ($EtSO_3H$; Sigma-Aldrich; 95%), tetrabutylammonium chloride (Fluka; ≥99.0%), methanol (Nacalai Tesque; ≥99.8%), 3-buten-1-ol (TCI; >98.0%), ammonia water (Nacalai Tesque), triethylamine (Wako; >99.0%), 1,2-dimethoxyethane (Nacalai Tesque; ≥99.0%), hydrochloric acid (Nacalai Tesque; 35–37%), trifluoroacetic acid (Nacalai Tesque; ≥99.0%), and sodium hydroxide (Nacalai Tesque; ≥97.0%) were used without further purification. Other materials were prepared and used as described in Chapter 2.

Synthesis of Cyclic Acetals

Cyclic acetals other than MDOL, DMDOL, TMDOL, BnDOL, and FurylDOL were synthesized by condensation reaction of the corresponding aldehyde and diol (method A) or acetal exchange between the corresponding acetal and diol using indium(III) trifluoromethanesulfonate (method B).[21] The following is a typical procedure for method A (PMPDOL synthesis as an example): 55 g (0.40 mol) of *p*-methoxybenzaldehyde (Nacalai Tesque; ≥99.0%; used as received), 62 g (1.0 mol) of ethylene glycol (Nacalai Tesque; ≥99.5%), 0.17 g (8.9×10^{-4} mol) of *p*-toluenesulfonic acid (monohydrate; TCI; >98.0%), and 70 g of toluene were added to a round-bottomed flask with a Dean-Stark trap. The mixture was stirred at approximately 150 ºC for 6 h. After the condensation reaction, the reaction mixture was added to 150 mL of aqueous $NaHCO_3$ and then washed with water and brine. A large part of toluene was removed by evaporation under reduced pressure. The crude product was purified by double or triple distillation over calcium hydride under reduced pressure to yield PMPDOL. The following is a typical procedure for method B[21] (PhDOL synthesis as an example): 26 g (0.17 mol) of benzaldehyde dimethyl acetal (TCI; >98.0%), 19 g (0.30 mol) of ethylene glycol, and 0.29 g (5.3×10^{-4} mol) of indium(III) trifluoromethanesulfonate (Sigma-Aldrich) was added to a round-bottomed flask and the mixture was stirred for 1 h at room temperature. After acetal exchange, the reaction mixture was evaporated under reduced pressure to remove methanol generated as a byproduct during exchange reaction. The crude product was purified by double or triple distillation over calcium hydride under reduced pressure to yield PhDOL.

2-(4-Methoxyphenyl)-1,3-dioxolane (PMPDOL)

Synthesized from 55 g (0.40 mol) of *p*-methoxybenzaldehyde and 62 g (1.0 mol) of ethylene glycol by method A. Final yield after distillation: 54%. ^{1}H NMR ($CDCl_3$; 500MHz): δ 7.40 (2H, d, J = 9.0 Hz), 6.90 (2H, d, J = 9.0 Hz), 5.76 (1H, s), 4.11–4.14 (2H, m), 4.00–4.03 (2H, m), 3.81 (3H, s). ^{13}C NMR ($CDCl_3$; 125 MHz): δ 160.5, 130.1, 128.0, 113.9, 103.8, 65.4, 55.4. MS (ESI) *m/z* $[M + Na]^+$, calcd: 203.0679, observed: 203.0682.

2-Phenyl-1,3-dioxolane (PhDOL)

Synthesized from 26 g (0.17 mol) of benzaldehyde dimethyl acetal and 19 g (0.30 mol) of ethylene glycol by method B. Final yield after distillation: 30%. ^{1}H NMR ($CDCl_3$; 500MHz): δ 7.36–7.50 (5H, m), 5.82 (1H, s), 4.11–4.15 (2H, m), 4.01–4.05 (2H, m). ^{13}C NMR ($CDCl_3$; 125MHz): δ 138.0, 129.3, 128.5, 126.6, 103.9, 65.4. MS (ESI) *m/z* $[M + Na]^+$, calcd: 173.0573, observed: 173.0575.

2-(4-Methoxyphenyl)-1,3-dioxane (PMPDOX)

Synthesized from 68 g (0.50 mol) of *p*-methoxybenzaldehyde and 93 g (1.2 mol) of 1,3-propanediol (TCI; >98.0 %) by method A. Final yield after distillation: 36%. ^{1}H NMR ($CDCl_3$; 400MHz): δ 7.40 (2H, d, J = 8.8 Hz), 6.88 (2H,

d, J = 8.8 Hz), 5.45 (1H, s), 4.24 (2H, ddd, J = 12.0, 5.2, 1.2 Hz), 3.97 (2H, m(probably ddd, J = 12.4, 12.0, 2.8 Hz)), 3.79 (3H, s), 2.21 (1H, dtt, J = 13.6, 12.4, 5.2 Hz), 1.42 (1H, dtt, J = 13.6, 2.8, 1.2 Hz). ^{13}C NMR ($CDCl_3$; 125MHz): δ 160.1, 131.5, 127.4, 113.7, 101.7, 67.5, 55.4, 25.9. MS (ESI) *m/z* $[M + Na]^+$, calcd: 217.0835, observed: 217.0835.

2-(4-Methoxyphenyl)-1,3-dioxepane (PMPDOP)

Synthesized from 68 g (0.50 mol) of *p*-methoxybenzaldehyde and 91 g (1.0 mol) of 1,4-butanediol (TCI; >99.0 %) by method A. Final yield after distillation: 16%. ^{1}H NMR ($CDCl_3$; 500MHz): δ 7.41 (2H, d, J = 9.0 Hz), 6.88 (2H, d, J = 9.0 Hz), 5.69 (1H, s), 3.89–3.94 (2H, m), 3.72–3.77 (2H, m), 3.80 (3H, s), 1.72–1.78 (4H, m). ^{13}C NMR ($CDCl_3$; 125MHz): δ 159.6, 132.6, 127.6, 113.6, 100.8, 65.4, 55.4, 29.4. MS (ESI) *m/z* $[M + Na]^+$, calcd: 231.0992, observed: 231.0998.

2-Naphtyl-1,3-dioxolane (NpDOL)

Synthesized from 16 g (0.10 mol) of 1-naphthaldehyde (Aldrich; 95 %) and 16 g (0.25 mol) of ethylene glycol by method A. Final yield after purification by column chromatography (silica gel, hexane/ethyl acetate = 5/1): 65%. ^{1}H NMR ($CDCl_3$; 400MHz): δ 8.22 (1H, d, J = 8.4 Hz), 7.85–7.887 (2H, m), 7.77 (1H, d, J = 7.2 Hz), 7.45–7.56 (3H, m), 6.48 (1H, s), 4.19–4.23 (2H, m), 4.13–4.18 (2H, m). ^{13}C NMR ($CDCl_3$; 125MHz): δ 134.0, 133.2, 131.1, 129.7, 128.7, 126.4, 125.9, 125.2, 124.1, 123.7, 102.4, 65.4. MS (ESI) *m/z* $[M + Na]^+$, calcd: 223.0730, observed: 223.0726.

1,3-Dioxolane-2-spirocyclohexane (CyDOL)

Synthesized from 34 g (0.35 mol) of cyclohexanone (TCI; >99.0 %) and 49 g (0.79 mol) of ethylene glycol by method A. Final yield after distillation: 44%. ^{1}H NMR ($CDCl_3$; 500MHz): δ 3.94 (4H, s), 1.60–1.65 (4H, m), 1.41 (2H, s). ^{13}C NMR ($CDCl_3$; 125MHz): δ 109.2, 64.3, 35.3, 25.3, 24.1. MS (ESI) *m/z* $[M + Na]^+$, calcd: 165.0886, observed: 165.0889.

2,2-Dimethyl-hexahydro-1,3-benzodioxole (Cy-DMDOL)

Synthesized from 26 g (0.25 mol) of 2,2-dimethoxypropane (Wako; >95.0%) and 25 g (0.22 mol) of 1,2-cyclohexanediol (TCI; >98.0%) by method B. Final yield after distillation: 49%. A mixture of diastereomers (93/7). ^{1}H NMR ($CDCl_3$; 500MHz): Major diastereomer: δ 4.08–4.12 (2H, m), 1.67–1.82 (4H, m), 1.53–1.61 (2H, m), 1.51 (3H, s), 1.35 (3H, s), 1.25–1.32 (2H, m), Minor diastereomer: δ 3.26–3.29 (2H, m), 2.09–2.12 (2H, m), 1.67–1.82 (2H, m), 1.42–1.48 (2H, m), 1.43 (6H, s), 1.25–1.32 (2H, m). ^{13}C NMR ($CDCl_3$; 125MHz): Major diastereomer: δ 107.8, 73.9, 28.6, 28.4, 26.5, 21.0, Minor diastereomer: δ 108.3, 80.3, 29.0, 27.1, 23.9. MS (ESI) *m/z* $[M + Na]^+$, calcd: 179.1043, observed: 179.1047.

Polymerization Procedure

Polymerization was conducted in a manner similar to that described in Chapter 2.

Acid Hydrolysis

Acid hydrolysis was conducted in a manner similar to that described in Chapter 2. Acidolysis of the obtained polymers was conducted with 0.50 M trifluoroacetic acid in dichloromethane at room temperature for 1 h (sample: 0.5 wt%). After the reaction, the mixture was diluted with dichloromethane and washed with an aqueous sodium hydroxide solution and then water. The volatiles were removed at room temperature at atmospheric pressure.

Characterization

The MWD, NMR spectra, and electrospray ionization mass spectra (ESI-MS) were measured in a manner similar to that described in Chapter 2.

Results and Discussion

Controlled Cationic Copolymerization of PMPDOL and Various Vinyl Monomers

To investigate the effects of substituents other than a methyl group on the copolymerizability of cyclic acetals, aromatic or bulky substituents-containing cyclic acetals were subjected to the cationic copolymerization with vinyl monomers in this study. The results of the copolymerizations of 2-(4-methoxyphenyl)-1,3-dioxolane (PMPDOL) with CEVE, IBVE, or pMeSt are listed in Table 1. The copolymerizations of MDOL,[20] which is a methyl-substituted counterpart, are also listed in the table for comparison. The copolymerizations were conducted using the initiating systems that are effective for the living cationic polymerization of vinyl monomers.[19,22–24] Ethyl acetate was used as a Lewis base additive to suppress side reactions such as chain transfer reactions by interacting with the propagating species and/or Lewis acid catalysts.[25] DTBP was employed as a proton trap reagent to suppress the undesired initiation or chain transfer reaction caused by adventitious water.[26,27] The cationic homopolymerization of PMPDOL under the adopted conditions did not proceed (Table S1).

Under these conditions, the cationic copolymerization of aryl-substituted PMPDOL and CEVE resulted in copolymers with narrow MWDs and a comparable incorporation of both monomers (Figure 1). Both monomers were consumed at similar rates, and the MWDs of the obtained copolymers shifted to a high-MW region as the reaction progressed (Figure 1C), indicating the generation of long-lived species. However,

Table 1. Cationic Copolymerization of Vinyl Monomers and Cyclic Acetals[a]

				conv (%)[b]				units per block[e]	
entry	vinyl	cyclic acetal	time	vinyl	cyclic	$M_n \times 10^{-3}$ [d]	M_w/M_n[d]	vinyl	cyclic
1	CEVE	PMPDOL	35 min	99	98	5.4	1.23	1.0_5	1.0
2[f]		MDOL	2 h	19[c]	9[c]	2.9	1.42	2.7	1.0
3	IBVE	PMPDOL	1 h	99	83	18.1	1.21	1.0_5	1.0
4[f]		MDOL	60 s	60[c]	1[c]	6.7	1.09	–	–
5	pMeSt	PMPDOL	49 h	66	25	3.1	1.11	2.5	1.0
6		MDOL	96 h	77[c]	9[c]	3.8	1.33	14	1.0

[a] Polymerization conditions for entries 1 and 2: $[CEVE]_0$ = 0.40 M, [cyclic acetal]$_0$ = 0.40 M, $[IBEA]_0$ = 4.0 mM, $[TiCl_4]_0$ = 5.0 mM, $[SnCl_4]_0$ = 20 mM, [ethyl acetate] = 20 mM, $[DTBP]_0$ = 10 mM, in dichloromethane (entry 1) or toluene/dichloromethane (9/1 v/v) (entry 2) at −78 °C. Polymerization conditions for entries 3 and 4: $[IBVE]_0$ = 0.50 M, [cyclic acetal]$_0$ = 0.50 M, $[IBVE–HCl]_0$ = 5.0 mM, $[SnCl_4]_0$ = 5.0 mM, [ethyl acetate] = 1.0 M, in dichloromethane at −78 °C. Polymerization conditions for entries 5 and 6: $[pMeSt]_0$ = 0.50 (entry 5) or 1.0 M (entry 6), [cyclic acetal]$_0$ = 0.50 (entry 5) or 1.0 M (entry 6), $[EtSO_3H]_0$ = 10 (entry 5) or 20 mM (entry 6), $[SnCl_4]_0$ = 20 mM, $[n\text{Bu}_4\text{NCl}]_0$ = 8.0 (entry 5) or 10 mM (entry 6) in dichloromethane at 0 °C. Hydrolysis conditions for entries 1–4: 0.50 M HCl in 1,2-dimethoxyethane (0.5 wt% polymer) at room temperature for 3 h. Acidolysis conditions for entries 5 and 6: 0.50 M trifluoroacetic acid in dichloromethane (0.5 wt% polymer) at room temperature for 1 h. [b] Determined by ^{1}H NMR analysis. [c] Determined by gas chromatography. [d] Determined by GPC (polystyrene standards). [e] Evaluated by ^{1}H NMR analysis. [f] Reported in reference 20.

the M_n values measured by GPC analysis were lower than the theoretical values calculated by the feed of the initiator (IBEA) and the monomer conversion (Figure 1B open circle; dushed line), suggesting the generation of additional cationogens in a similar manner to the acetal-initiated living cationic polymerization of vinyl monomers (Scheme S1).[28–31]

PMPDOL was also effectively copolymerized with IBVE and pMeSt (Figure 2), which is in sharp contrast to MDOL. MDOL was negligibly copolymerized with IBVE, which is more reactive than CEVE, or pMeSt (Figure 2), demonstrating the effects of the substituents of cyclic acetals on copolymerizability.

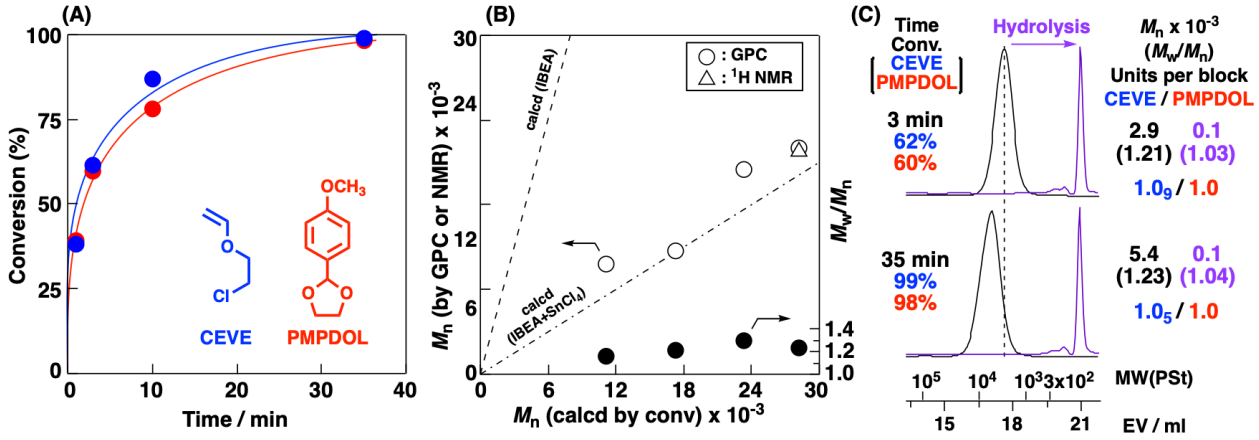

Figure 1. (A) Time–conversion curves for the copolymerization of CEVE and PMPDOL, (B) the M_n (open) determined by GPC (circle; polystyrene standards) or NMR (triangle; calculated from the integral ratios of peaks of the main chain and the ω-ends) and M_w/M_n (filled circle) values of poly (CEVE-*co*-PMPDOL)s (dashed line: theoretical line calculated by the ratio of the conversion of both monomers and IBEA feed; dashed-dotted line: theoretical line based on the sum of IBEA and $SnCl_4$ feed), and (C) MWD curves of poly(CEVE-*co*-PMPDOL)s (black) and acid hydrolysis products (purple). The data correspond to entry 1 in Table 1.

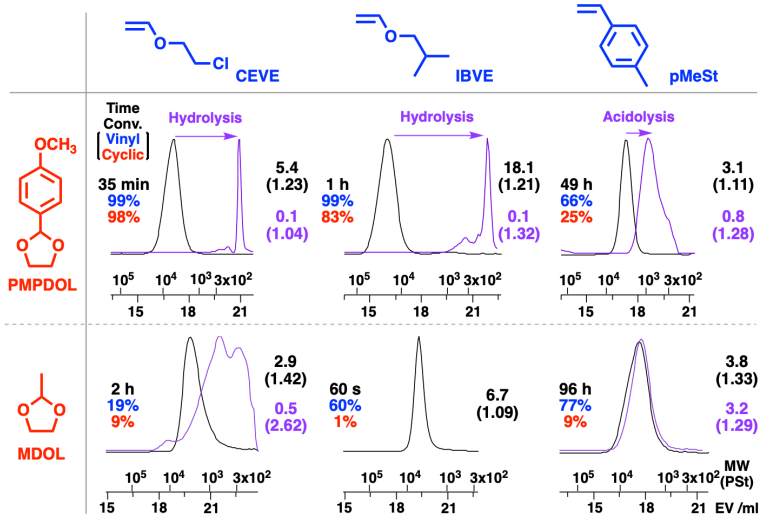

Figure 2. MWD curves of the copolymerization of vinyl monomers and cyclic acetals (black) and their acid hydrolysis products (purple). The data correspond to entries 1–6 in Table 1.

The ^{1}H NMR analysis of vinyl monomer–PMPDOL copolymers indicated the frequent occurrence of the crossover reactions between vinyl monomers and PMPDOL. The ^{1}H NMR spectra of a CEVE–PMPDOL copolymer and its acid hydrolysis product are shown in Figure 3 (see Figure S1 for ^{13}C NMR spectrum). Peaks at 4.6 ppm (peak 8) were assigned to the acetal structure generated by the crossover reaction from CEVE to PMPDOL. The peak at 4.3 ppm (peak 3) was attributed to the *sec*-benzyl ether structure generated by the crossover reaction from PMPDOL to CEVE. Interestingly, peaks assignable to an aromatic acetal structure of the PMPDOL–PMPDOL homosequence were not observed at 5–6 ppm, indicating that the homopropagation of PMPDOL did not occur in the copolymerization (Table S1), corresponding to the absence of the homopropagation. From the integral ratio of the aromatic peaks (peak 4 and 5), the acetal and *sec*-benzyl ether peaks (peak 8 and 3), and the CEVE-derived methylene proton in the main chain (peak 7), the average number of CEVE and PMPDOL units per block was estimated to be 1.0_5 and 1.0, respectively, indicating the occurrence of an alternating copolymerization. DSC measurements of the CEVE–PMPDOL copolymer showed the T_g value of –5 ºC, which is higher than CEVE homopolymer (Figure S2; –21 ºC ($M_n = 2.9 \times 10^3$)).[32] In addition, the lower T_g value of the CEVE–PMPDOL alternating copolymer than that of CEVE–benzaldehyde alternating copolymer (38 ºC)[33] reflected the incorporation of oxyethylene units in the main chains.

The alternating copolymerization of CEVE and PMPDOL was also corroborated by acid hydrolysis of the obtained copolymers. In the ^{1}H NMR spectrum of the hydrolysis product (Figure 3B), the peaks assigned to *p*-methoxycinnamaldehyde, which was derived from the alternating sequences of CEVE and PMPDOL, were exclusively observed. This product was generated via acid hydrolysis of acid-labile acetal and *sec*-benzyl structures of the CEVE–PMPDOL–CEVE sequence and subsequent dehydration reaction (Scheme 3). Ethylene glycol and 2-chloroethanol, which were derived from PMPDOL and CEVE units, respectively, were removed during the purification process. Moreover, the disappearance of the peaks of the CEVE-derived methylene protons in the main chain (peak 7) after hydrolysis indicated the selective generation of acid-

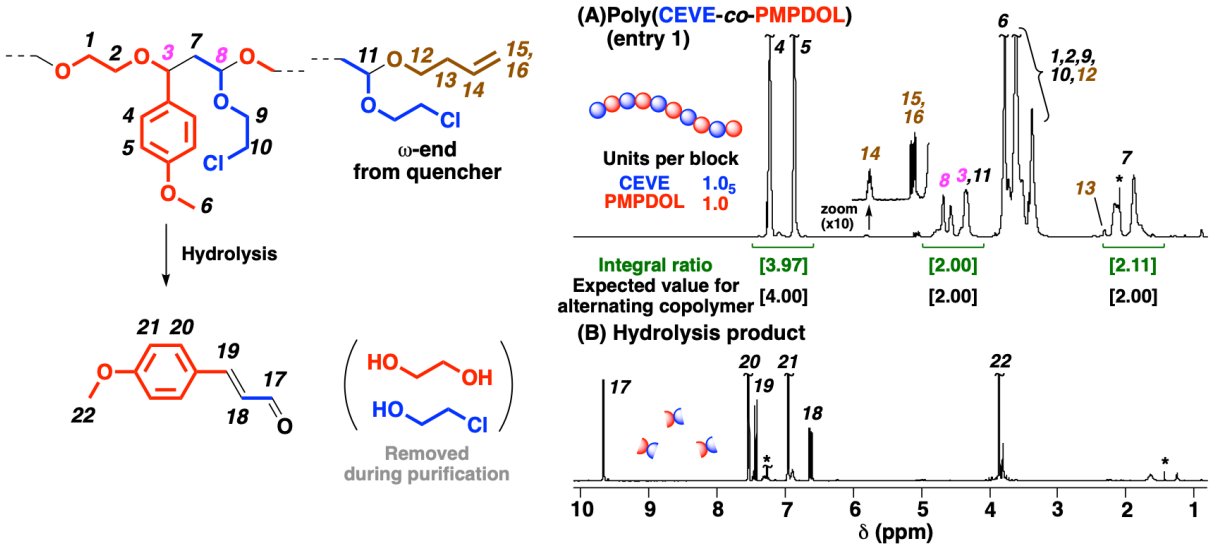

Figure 3. ^{1}H NMR spectra of (A) poly(CEVE-*co*-PMPDOL) and (B) its hydrolysis product (in $CDCl_3$ at 30 ºC); * water, $CHCl_3$. The data correspond to entry 1 in Table 1.

Scheme 3. Acid Hydrolysis of Copolymers via Cleavage of Acetal Moieties

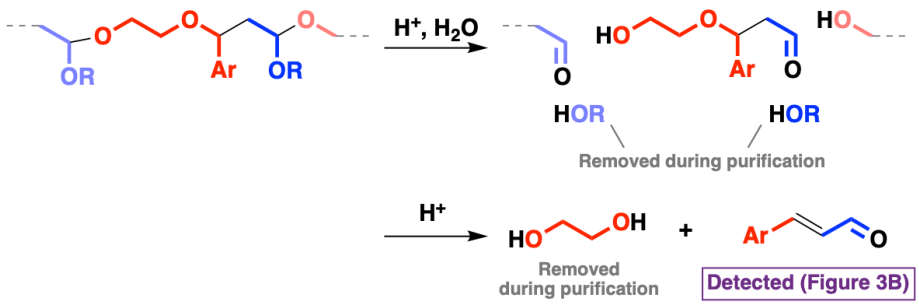

degradable PMPDOL–CEVE–PMPDOL sequence and negligible occurrence of CEVE homopropagation. The very sharp peak in the low-MW region of the MWD curves of the hydrolysis products also supported the selective generation of PMPDOL–CEVE–PMPDOL alternating sequences (Figure 1C).

The livingness of the copolymerization was confirmed by the incorporation of a quencher into the chain ends of the obtained copolymers. The peaks at 2.3, 5.1, and 5.8 ppm in the ^{1}H NMR spectra of the copolymers (peak 13–16, Figure 3A) were assigned to the ω-end structure derived from 3-buten-1-ol used as a quencher. Moreover, the M_n calculated from the integral ratios of the peaks of the main chain and this ω-end (5.4×10^3; Figure 1B triangle) was consistent with the value measured by GPC analysis (5.4×10^3; Figure 1B circle), indicating efficient introduction of the quencher into the chain ends. This result also suggests that the copolymerization proceeded in a controlled manner via an appropriate dormant-active equilibrium at the propagating chain ends. The addition of a fresh supply of CEVE into the reaction solution at the late stage of the copolymerization reaction resulted in copolymers with higher-MWs without residual peaks in the MWD curves, indicating the livingness of the copolymerization (Figure S3).

The Effects of the Substituents of Cyclic Acetals on the Copolymerization Behavior.

Controlled cationic copolymerization of CEVE and cyclic acetals other than PMPDOL also proceeded effectively (Table 2 and Figure 4). A series of aryl-substituted cyclic acetals (Scheme 2; PhDOL (with a phenyl group substituted at the 2-position), PMPDOX (a six-membered cyclic acetal), and PMPDOP (a seven-membered cyclic acetal)) were synthesized by condensation reaction of the corresponding aldehydes and diols. Moreover, alkyl-substituted cyclic acetals (Scheme 2; TMDOL (with a methyl group substituted at the 4-position), CyDOL (with a cyclohexane ring directly substituted at the 2-position), and Cy-DMDOL (with a cyclohexane ring introduced as a fused-ring structure)) were also prepared to investigate the effects of bulkiness around the propagating species on copolymerizability. The cationic copolymerization of these cyclic acetals and CEVE successfully produced copolymers with relatively narrow MWDs. The MWD curves of the copolymers shifted to the higher-MW region as the copolymerization proceeded, indicating the generation of long-lived species. The generation of low-MW products after acid hydrolysis of the obtained copolymers indicated that the acetal moieties were introduced into the main chain by the crossover reaction from CEVE to cyclic acetals. The average number of monomer units per block determined by ^{1}H NMR analysis of the obtained copolymers was independent of the conversion of both monomers, suggesting that the crossover reactions occurred at constant frequencies throughout the copolymerization reaction. As in the case of

Table 2. Cationic Copolymerization of CEVE and Cyclic Acetals[a]

			conv (%)[c]				units per block[f]	
entry	cyclic acetal	time	CEVE	cyclic	$M_n \times 10^{-3}$ [e]	M_w/M_n [e]	CEVE	cyclic
1[b]	MDOL	2 h	19	9	2.9	1.42	2.7	1.0
2	DMDOL	13 min	75	34	9.9	1.19	2.5	1.0
3	PhDOL	2 h	91[d]	79[d]	8.3	1.13	1.2	1.0
4[b]	PMPDOL	35 min	99[d]	98[d]	5.4	1.23	1.0_5	1.0
5	PMPDOX	10 min	63[d]	36[d]	3.4	1.27	1.2	1.0
6	PMPDOP	10 min	62[d]	98[d]	1.7	1.59	1.4	1.2
7	TMDOL	10 min	91	56	7.8	1.13	3.2	1.0
8	CyDOL	3 min	46	44	8.4	1.08	3.3	1.0
9	Cy-DMDOL	5 min	82	54	5.4	1.22	2.9	1.0
10	BnDOL	2 h	61	2[g]	7.4	1.11	11	1.0

[a] $[CEVE]_0$ = 0.40 M, $[cyclic\ acetal]_0$ = 0.40 M, $[IBEA]_0$ = 4.0 mM, $[TiCl_4]_0$ = 5.0 mM, $[SnCl_4]_0$ = 20 mM, [ethyl acetate] = 20 mM, $[DTBP]_0$ = 10 mM, in dichloromethane (entry 4) or toluene/dichloromethane (9/1 v/v) (except for entry 4) at −78 °C. Hydrolysis conditions: 1.0 M HCl in 1,2-dimethoxyethane (0.5 wt % polymer) at room temperature for 3 h. [b] Entries 1 and 4 correspond to entries 2 and 1 in Table 1, respectively. [c] Determined by gas chromatography. [d] Determined by ^{1}H NMR analysis. [e] Determined by GPC (polystyrene standards). [f] Evaluated by ^{1}H NMR analysis. [g] Determined by gravimetry and ^{1}H NMR analysis.

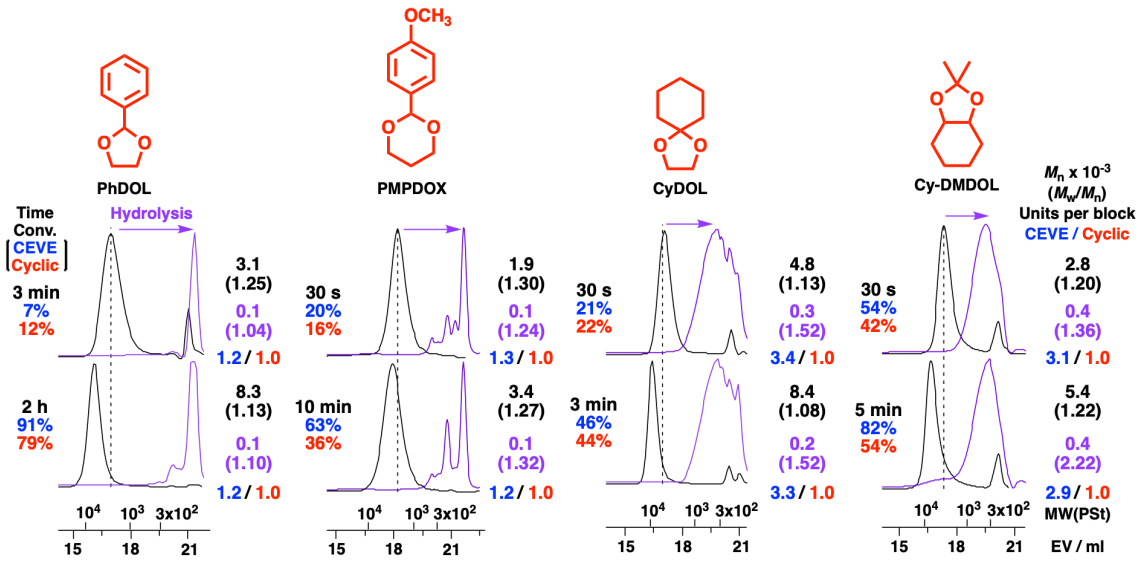

Figure 4. MWD curves of poly(CEVE-*co*-cyclic acetal)s (black) and acid hydrolysis products (purple).

PMPDOL, the cationic homopolymerization of these 2-substituted cyclic acetals did not proceed (Table S1). The absence of the aromatic acetal structures (at 5–6 ppm) in ^{1}H NMR analysis of the obtained copolymer revealed that the homopropagation of cyclic acetals did not occur in the copolymerization with cyclic acetals except for PMPDOP. In the case of PMPDOP, the aromatic acetal structures derived from the homopropagation of PMPDOP was partly generated in the main chain (entry 6 in Table 2; CEVE/PMPDOL = 1.4/1.2 units per block).

The difference in substituents on cyclic acetals mainly affected the frequency of the crossover reactions in the controlled copolymerization with CEVE. Figure 5 summarizes the cyclic acetal composition in the obtained copolymers. The maximum value of cyclic acetal content in Figure 5 is 50 % because the cyclic

acetals used in this study, except for PMPDOP, did not generate homopropagation in the copolymerization. The use of aryl-substituted cyclic acetals such as PhDOL, PMPDOL, PMPDOX, and PMPDOP exhibited a much larger content of cyclic acetals than when using methyl-substituted cyclic acetals such as MDOL and DMDOL, resulting in copolymers with alternating-like sequences (cyclic acetal content; PhDOL = 46%, PMPDOL = 50%, PMPDOX = 46%, PMPDOP = 46%, MDOL = 27%, DMDOL = 28%). The cyclic acetals with bulky substituents, such as TMDOL, CyDOL, and Cy-DMDOL, exhibited slightly lower contents of cyclic acetals in the products compared to MDOL and DMDOL (cyclic acetal content; TMDOL = 24%, CyDOL = 18%, Cy-DMDOL = 26%). In addition, the copolymerization with 2-benzyl-1,3-dioxolane (BnDOL) inefficiently proceeded (entry 10 in Table 2; cyclic acetal content; BnDOL = 8%).

The M_n values of the products obtained by acid hydrolysis obviously reflected the frequency of crossover reactions (Figure 5, purple). For example, acid hydrolysis of PhDOL, PMPDOL, PMPDOX, or PMPDOP copolymers produced compounds with M_n values of approximately 100 (with the products assigned to cinnamaldehyde or *p*-methoxy cinnamaldehyde by ^{1}H NMR analysis), which corresponded to the preferential introduction of CEVE–cyclic acetal–CEVE alternating sequences in main chains. In the case of TMDOL, CyDOL, and Cy-DMDOL copolymers, the generation of hydrolysis products with M_n values of 200–500 was consistent with the number of CEVE units per block calculated by ^{1}H NMR analysis.

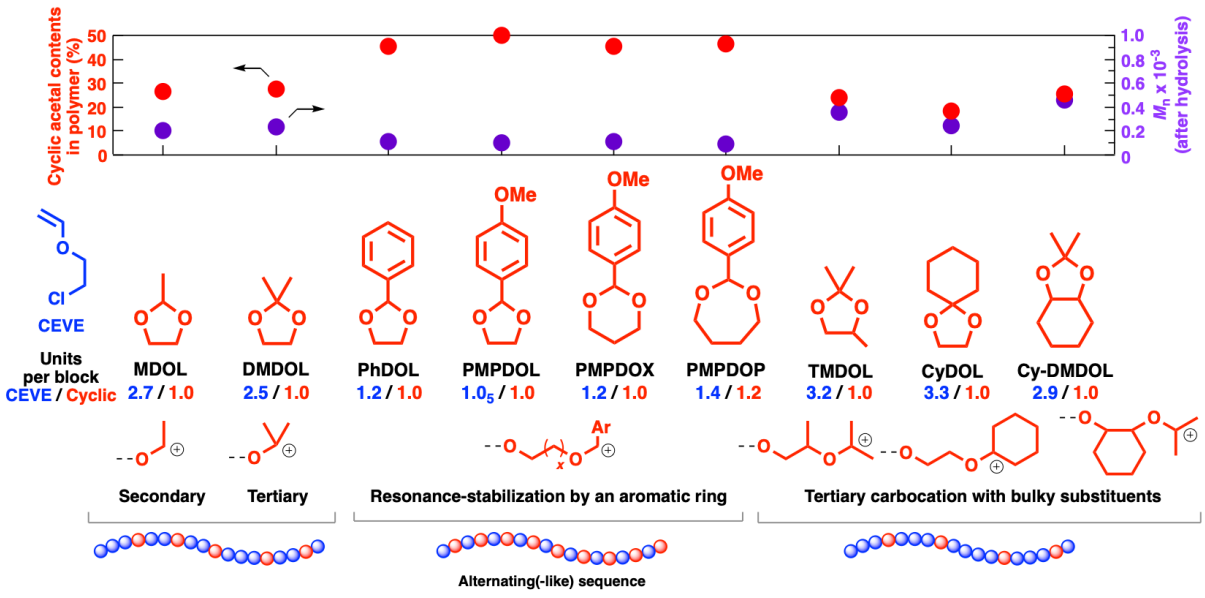

Figure 5. Cyclic acetal contents in the copolymers obtained by the copolymerization with CEVE. The data correspond to entries 1–9 in Table 2. (Counteranions are omitted)

The differences in the copolymerization behavior of cyclic acetals are discussed based on the reaction mechanisms in the propagating step (Scheme 4). A cyclic acetal adds to the propagating species to form an oxonium ion and subsequently generates a carbocation via ring-opening (b and c in Scheme 4). The frequent crossover reactions using PhDOL, PMPDOL, PMPDOX, or PMPDOP compared to MDOL most likely stemmed from aryl-derived resonance stabilization of the carbocation (Figure 5 and Scheme 5B). The efficient generation of the stable carbocation via ring-opening of the cyclic acetal-derived oxonium ion accelerates the subsequent occurrence of the crossover reaction with CEVE (d in Scheme 4). Moreover, in the case of

PMPDOL, which has a methoxy group at the *p*-position of the aromatic ring, the preferential addition of PMPDOL to the CEVE-derived propagating end occurred due to its high reactivity, resulting in the alternating copolymerization. These trends were also consistent with the result that acid hydrolysis of cyclic acetals was accelerated with aryl substituents rather than alkyl substituents in organic reaction.[34–36]

In contrast to these cases, the absence of the stabilization effects is obviously disadvantageous for crossover reactions, as exemplified by the case of 1,3-dioxolane (DOL).[20] An inefficient ring-opening reaction of DOL-derived oxonium ions, which is due to the instability of the primary carbocation generated via the ring-opening reaction, leads to an elimination of a cyclic acetal from the propagating end (b' and c' in Scheme 4). The reaction between the generated CEVE-derived propagating end and CEVE (a in Scheme 4) resulted in CEVE–CEVE homopropagation, and consequently, the crossover reactions between CEVE and DOL did not proceed. The use of MDOL, which generates a relatively stable secondary carbocation, results in the crossover reactions to yield CEVE–MDOL copolymers (d in Scheme 4; Scheme 5A). In addition, copolymerization proceeded in a controlled manner via the dormant-active equilibrium consisting of the reversible activation of carbon–chlorine bonds at the propagating ends derived from both monomers in a similar manner to the living cationic polymerization of vinyl monomers (f and g in Scheme 4).[19,22]

The homopropagation of cyclic acetals did not proceeded except for PMPDOP (Table 2). The instability of aromatic acetal structures, which stemmed from the homopropagation of cyclic acetals, is most likely responsible for the negligible homopropagation (e' in Scheme 4). Indeed, in a previous study, 1,3-dioxolanes with substituents at the 2-position, such as PhDOL, were reported to be ineffective for homopolymerization.[37] In the copolymerization, therefore, the selective addition of CEVE to the cyclic acetal-derived propagating end occurred, generating CEVE–cyclic acetal–CEVE sequences. The PMPDOP homosequence most likely resulted from the disturbance of the reverse reaction (Scheme 4e') due to the inefficient generation of a strained seven-membered oxonium ion by the ring-closing reaction of the carbocation.[38,39]

The bulkiness around the carbocation disturbed the crossover reaction from the cyclic acetal-derived carbocation to CEVE due to the steric hindrance (d in Scheme 4), which increased the relative rate of the reverse reaction (b' and c' in Scheme 4). The addition of CEVE to the CEVE-derived propagating end after elimination of a cyclic acetal (a in Scheme 4) led to the decreased frequency of the crossover reaction.

Scheme 4. Copolymerization Mechanisms (Counteranions are omitted)

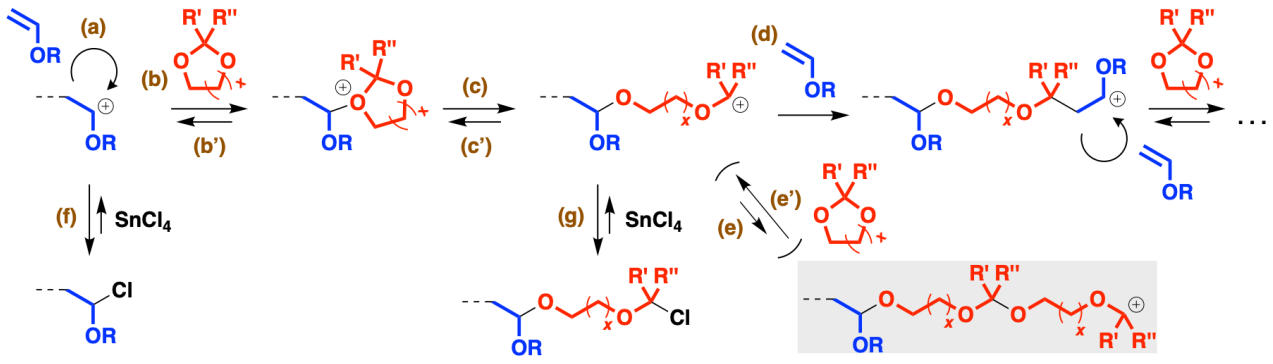

Scheme 5. Propagating Species Generated from (A) Alkyl-Substituted Cyclic Acetal and (B) Aryl-Substituted Cyclic Acetal (Counteranions are omitted)

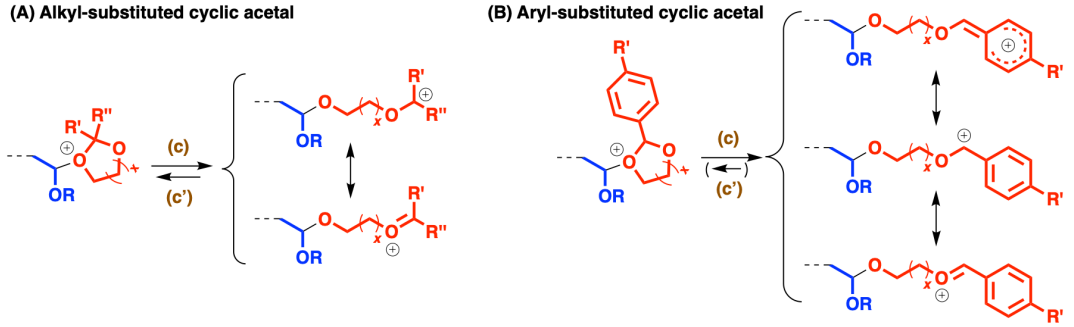

The Effects of Aryl-Substituted Cyclic Acetals on the Copolymerization with Various Vinyl Monomers.

The resonance stabilization of the propagating species notably increased the frequency of the crossover reactions in the copolymerization with other VEs or pMeSt. The average number of monomer units per block in the products obtained from various vinyl monomers and cyclic acetals is summarized in Figure 6 (Table 1 and S2). PMPDOL was efficiently copolymerized with IBVE or IPVE, which are more reactive VEs than CEVE, to yield copolymers with narrow MWDs (entry 3 in Table 1; Figure 2 upper; IBVE/PMPDOL = 1.0_5/1.0 units per block, IPVE/PMPDOL = 2.6/1.0 units per block). The generation of low-MW products after acid hydrolysis of the obtained copolymers also supported the efficient occurrence of the crossover reactions between the VEs and PMPDOL. pMeSt, which is a styrene derivative that is less reactive than CEVE,[40] also underwent the copolymerization with PMPDOL (entry 5 in Table 1; Figure 2 upper; pMeSt/PMPDOL = 2.5/1.0 units per block). In contrast, the copolymerization of MDOL with IBVE, IPVE, or pMeSt indicated the negligible occurrence of the crossover reactions (entries 4 and 6 in Table 1; Figure 2 lower). The homopropagation of highly reactive VEs most likely disrupted the crossover reaction from VEs to MDOL. Sharp differences between aryl- and alkyl-substituted cyclic acetals were also observed when PhDOL and

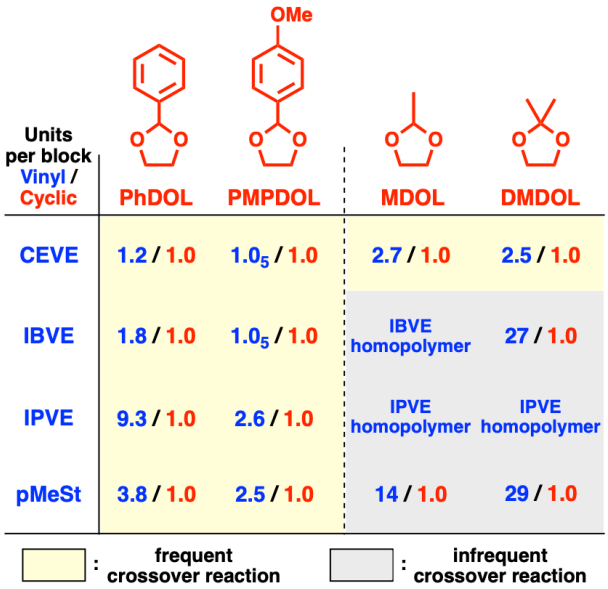

Figure 6. Average number of monomer units per block in the copolymerization of equimolar amounts of vinyl monomers and cyclic acetals (determined by ^{1}H NMR analysis of the obtained copolymers). The data correspond to Table 1 and S2.

DMDOL were used (Figure 6).

The monomer reactivity ratios determined by the Kelen–Tüdõs method were also consistent with the copolymerizability difference of the aryl- and alkyl-substituted cyclic acetals (Table 3, Figure 7, Table S3 for the copolymerization data).[41,42] The r_1 and r_2 values (M_1: vinyl monomer, M_2: cyclic acetal) of approximately zero in the copolymerization of CEVE and PMPDOL indicated the exclusive occurrences of crossover reactions (b in Scheme 4) and the absence of the homopropagation (a in Scheme 4) (Figure 7, left; CEVE/PMPDOL: $r_1 = 0.15$, $r_2 = 0.01$). The smaller r_1 value in the copolymerization with PMPDOL than that with MDOL is in accordance with the more frequent crossover reactions with PMPDOL (CEVE/PMPDOL: $r_1 = 0.15$, CEVE/MDOL: $r_1 = 2.6$). A drastic difference between PMPDOL and MDOL was observed in the copolymerization with IBVE (Figure 7, center; IBVE/PMPDOL: $r_1 = 0.32$, $r_2 = 0.06$, IBVE/MDOL: $r_1 = 93$, $r_2 = 0.01$). The smaller r_1 values in the copolymerization of PMPDOL with pMeSt than that of MDOL also reflected the efficient occurrence of the crossover reaction from pMeSt to PMPDOL (Figure 7, right; $r_1 = 1.81$ for pMeSt/PMPDOL, $r_1 = 9.4$ for pMeSt/MDOL). Interestingly, the larger r_1 value in the copolymerization of pMeSt and PMPDOL than that of CEVE and PMPDOL (CEVE/PMPDOL: $r_1 = 0.15$, pMeSt/PMPDOL: $r_1 = 1.81$) was inconsistent with the order of reactivity of vinyl monomers[40] (pMeSt < CEVE) because the use of less reactive pMeSt instead of CEVE was expected to suppress the homopropagation of pMeSt and lead to the decrease of r_1 value. These results suggest that the difference in reactivity of the carbocations derived from VEs or pMeSt affects the crossover reactions from vinyl monomers to cyclic acetals.

Table 3. Monomer Reactivity Ratio[a]

M_1	M_2	r_1	r_2
CEVE	PMPDOL	0.15	0.01
	MDOL	2.6[b]	0.06[b]
IBVE	PMPDOL	0.32	0.06
	MDOL	93	0.01
pMeSt	PMPDOL	1.81	0.01
	MDOL	9.4	~0

[a] Determined by Kelen–Tüdõs method. The data used for the determination of the monomer reactivity ratios are shown in Table S3. [b] Values reported in ref. 20.

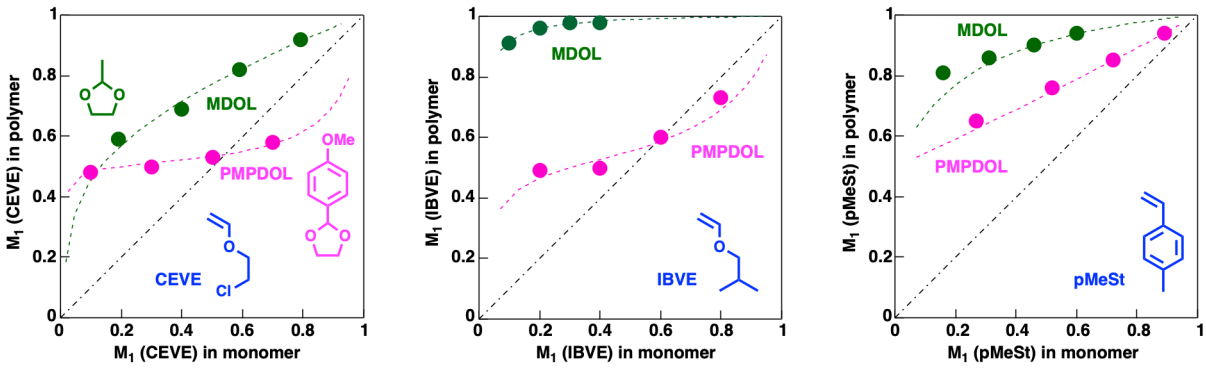

Figure 7. Copolymer compositions for the cationic copolymerizations of vinyl monomers and PMPDOL or MDOL (broken curves: curves that were drawn using the *r* values obtained by the Kelen–Tüdõs method; dashed-dotted lines: azeotropic lines). The copolymerization data used for the plots are summarized in Table S3. The data for the copolymerization of CEVE and MDOL are the same to those shown in ref. 20.

In the copolymerization of pMeSt and cyclic acetals, the presence of the ring-opening reaction in the propagating reaction was notably related to the frequent crossover reactions. The cyclic acetal content in the obtained polymers is showed in Figure 8 (Table 4). The use of PhDOL, FurylDOL, and NpDOL, which generated aryl group-adjacent carbocation or furyl group-adjacent carbocation by ring-opening reaction, indicated efficient incorporation of cyclic acetals into the copolymers in a similar manner to the case of PMPDOL (entries 3, 5, and 6 in Table 4; pMeSt/PhDOL = 3.8/1.0 units per block, pMeSt/FurylDOL = 2.5/1.0 units per block, pMeSt/NpDOL = 3.0/1.0 units per block). In contrast, copolymerization with *p*-methoxy benzaldehyde, which generates a propagating species that is structurally similar to that form PMPDOL, negligibly proceeded under the conditions examined in this study (entry 7 in Table 4; pMeSt/pMeOBzA = 26/1.0 units per block). These results possibly stemmed from the difference in reaction mechanisms during the propagating step (Scheme 6). The addition and dissociation of a comonomer to the pMeSt-derived propagating end establishes addition-ring elimination equilibrium, as described in Scheme 4. The dissociation of a PMPDOL monomer from the propagating end occurs by both ring-closing of the oxonium ion species and the subsequent elimination reaction, while that of pMeOBzA proceeded by the elimination reaction alone (Scheme 6). Therefore, the occurrence of the ring-opening reaction during the crossover reactions from pMeSt to a cyclic acetal possibly suppressed the reverse reaction and consequently contributed to efficient crossover reactions. Moreover, the difference in cyclic acetal content in the copolymerization of pMeSt and PMPDOL or MDOL probably reflected both the stability and the similarity of the structures of propagation species. In addition to the high stability of the resonance-stabilized carbocation derived from PMPDOL, the similarity of the carbocation to the pMeSt-derived propagating carbocation contributed to improving the crossover reaction from PMPDOL to pMeSt.

Table 4. Cationic Copolymerizations of pMeSt and Aryl-Substituted Cyclic Acetals[a]

				conv (%)[b]				units per block[e]	
entry	vinyl	comonomer	time	vinyl	cyclic	$M_n \times 10^{-3}$ [d]	M_w/M_n[d]	vinyl	cyclic
1	pMeSt	MDOL	96 h	77[c]	9[c]	3.8	1.33	14	1.0
2		DMDOL	96 h	56[c]	7[c]	2.1	1.29	29	1.0
3		PhDOL	96 h	39	54	3.7	1.33	3.8	1.0
4		PMPDOL	49 h	66	25	3.1	1.11	2.5	1.0
5		FurylDOL	72 h	12	15	1.8	1.34	2.5	1.0
6		NpDOL	72 h	48	20	1.8	1.26	3.0	1.0
7		pMeOBzA	90 h	87[c]	3	3.2	1.20	26	1.0

[a] $[pMeSt]_0$ = 1.0 (entries 1–3) or 0.50 M (entries 4–7), $[\text{cyclic acetal}]_0$ = 1.0 (entries 1 –3) or 0.50 M (entries 4–6), $[pMeOBzA]_0$ = 0.50 M (entry 7), $[EtSO_3H]_0$ = 20 (entries 1–3) or 10 mM (entries 4–7), $[SnCl_4]_0$ = 20 mM, $[n\text{Bu}_4\text{NCl}]_0$ = 10 (entries 1–3) or 8.0 mM (entries 4–7) in dichloromethane at 0 °C. Acidolysis conditions: 0.50 M trifluoroacetic acid in dichloromethane (0.5 wt% polymer) at room temperature for 1 h. [b] Determined by ^{1}H NMR analysis. [c] Determined by gas chromatography. [d] Determined by GPC (polystyrene standards). [e] Evaluated by ^{1}H NMR analysis.

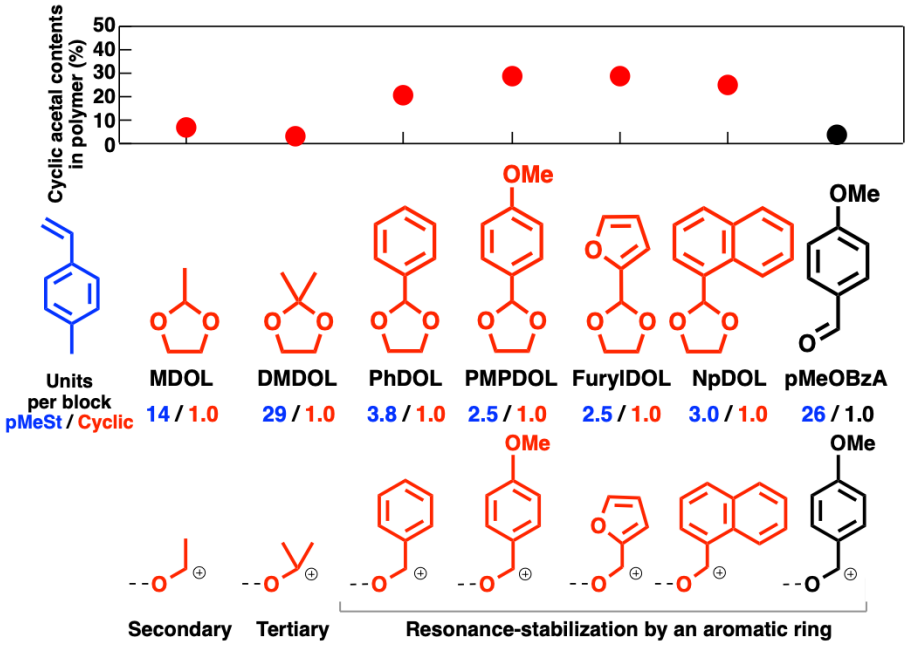

Figure 8. Cyclic acetal contents in copolymers of pMeSt and cyclic acetals. The data correspond to Table 4. (Counteranions are omitted.)

Scheme 6. Mechanisms of the Crossover Reactions from pMeSt to (A) PMPDOL or (B) pMeOBzA (Counteranions are omitted.)

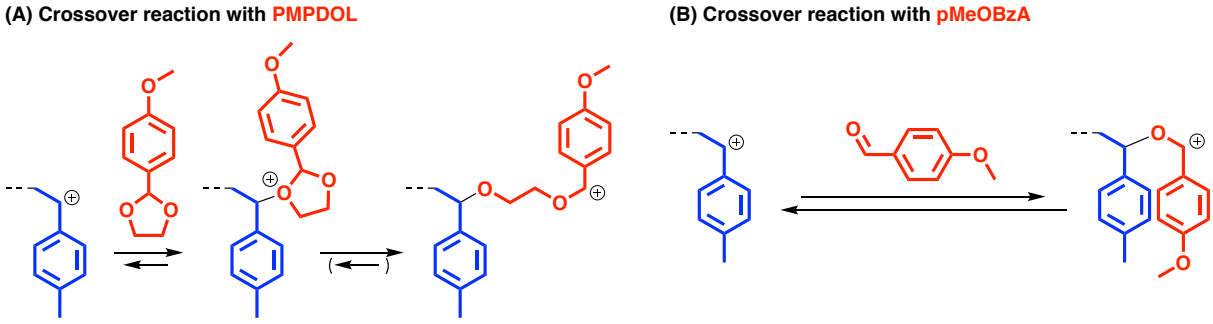

Conclusion

The effects of the difference in electronic and steric factors around the propagating species on the copolymerization behavior were investigated in the concurrent vinyl-addition and ring-opening cationic copolymerization of vinyl monomers and cyclic acetals. A series of cyclic acetals with various substituents were designed and synthesized from the corresponding aldehydes, acetals, and diols. The controlled cationic copolymerization of CEVE and cyclic acetals produced the copolymers with different cyclic acetal contents. Importantly, alternating copolymerization was feasible using aryl-substituted cyclic acetals. The electronic and steric effects derived from their substituents affected the reactivity and stability of the carbocation generated by the ring-opening reaction of the oxonium ion derived from cyclic acetals, which was significantly related to the frequency of the crossover reactions. In addition, the difference in the copolymerization behavior between PMPDOL and pMeOBzA suggested that the presence of the ring-opening reaction in the propagating reaction is related to the efficiency of the crossover reactions. These results will contribute to the sophisticated

design of copolymers consisting of vinyl monomers and cyclic monomers and the application of functionalities based on their unique structures.

References

1. Grubbs, R. B.; Grubbs, R. H. *Macromolecules* **2017**, *50*, 6979–6997.
2. Webster, O. W. *Science* **1991**, *251*, 887–893.
3. Walsh, D. J.; Hyatt, M. G.; Miller, S. A.; Guironnet, D. *ACS Catal.* **2019**, *9*, 11153–11188.
4. Alfrey, T.; Price, C. C. *J. Polym. Sci.* **1947**, *2*, 101–106.
5. Leonard, J. In *Polymer Handbook 4th Edition*; Brandrup, J.; Immergut, E. H.; Grulke, E. A. Eds.; Wiley, New York, **1999**.
6. Young, L. J. *J. Polym. Sci.* **1961**, *54*, 411–455.
7. Fischer, H.; Radom, L. *Angew. Chem. Int. Ed.* **2001**, *40*, 1340–1371.
8. Lutz, J.-F.; Lehn, J.-M.; Meijer, E. W.; Matyjaszewski, K. *Nat. Rev. Mater.* **2016**, *1*, 16024.
9. Bates, C. M.; Bates, F. S. *Macromolecules* **2017**, *50*, 3–22.
10. Polymeropoulos, G.; Zapsas, G.; Ntetsikas, K.; Bilalis, P.; Gnanou, Y.; Hadjichristidis, N. *Macromolecules* **2017**, *50*, 1253–1290.
11. Perry, S. L.; Sing, C. E. *ACS Macro Lett.* **2020**, *9*, 216–225.
12. Rempp, P. *Makromol. Chem. Macromol. Symp.* **1992**, *60*, 209–218.
13. Matyjaszewski, K. *Prog. Polym. Sci.* **2005**, *30*, 858–875.
14. Beyer, V. P.; Kim, J.; Becer, C. R. *Polym. Chem.* **2020**, *11*, 1271–1291.
15. Guo, X.; Choi, B.; Feng, A.; Thang, S. H. *Macromol. Rapid Commun.* **2018**, *39*, 1800479.
16. Kanazawa, A.; Kanaoka, S.; Aoshima, S. *J. Am. Chem. Soc.* **2013**, *135*, 9330–9333.
17. Okada, M.; Yamashita, Y.; Ishii, Y. *Makromol. Chem.* **1966**, *94*, 181–193.
18. Okada, M.; Yamashita, Y. *Makromol. Chem.* **1969**, *126*, 266−275.
19. Shirouchi, T.; Kanazawa, A.; Aoshima, S *Macromolecules* **2016**, *49*, 7184–7195.
20. Maruyama, K.; Kanazawa, A.; Aoshima, S. *Polym. Chem.* **2019**, *10*, 5304–5314.
21. Smith, M. B.; Kubczyk, M. T.; Graham, E. A. *Tetrahedron*, **2012**, *68*, 7775-7781.
22. Kimura, R.; Yamada, M.; Kanazawa, A.; Kanaoka, S.; Aoshima, S. *Polym. Prepr., Jpn.* **2013**, *62*, 2412.
23. Kanazawa, A.; Kanaoka, S.; Aoshima, S. *Macromolecules* **2009**, *42*, 3965–3972.
24. Higashimura, T.; Ishihama, Y.; Sawamoto, M. *Macromolecules* **1993**, *26*, 744–751.
25. Aoshima, S.; Kanaoka, S. *Chem. Rev.* **2009**, *109*, 5245–5287.
26. Kennedy, J. P.; Chou, R. T. *J. Macromol. Sci., Chem.* **1982**, *18*, 11–16.
27. Bae, Y. C.; Faust, R. *Macromol. Symp.* **1998**, *132*, 11–23.
28. Van Meirvenne, D.; Haucourt, N.; Goethals, E. J. *Polym. Bull.* **1990**, *23*, 185–190.
29. Satoh, K.; Kamigaito, M.; Sawamoto, M. *Macromolecules* **2000**, *33*, 748–753.
30. Yokoyama, N.; Kanazawa, A.; Kanaoka, S.; Aoshima, S. *Macromolecules* **2018**, *51*, 884–894.
31. Shimomoto, H.; Yoshida, H.; Kanaoka, S.; Aoshima, S. *J. Polym. Sci. Part Polym. Chem.* **2012**, *50*, 3703–3709.
32. Schappacher, M.; Deffieux, A. *Makromol. Chem. Rapid Commun.* **1991**, *12*, 447–453.
33. Ishido, Y.; Kanazawa, A.; Kanaoka, S.; Aoshima, S. *J. Polym. Sci., Part A: Polym. Chem.* **2014**, *52*, 1334–1343.
34. Vitullo, V. P.; Pollack, R. M.; Faith, W. C.; Keiser, M. L. *J. Am. Chem. Soc.* **1974**, *96*, 6682–6685.
35. Fife, T. H.; Jao, L. K. *J. Org. Chem.* **1965**, *30*, 1492–1495.

36. Liu, B.; Thayumanavan, S. *J. Am. Chem. Soc.* **2017**, *139*, 2306–2317.
37. Okada, M.; Yamashita, Y.; Ishii, Y. *Makromol. Chem.* **1964**, *80*, 196–207.
38. Okada, M.; Yagi, K.; Sumitomo, H. *Makromol. Chem.* **1973**, *163*, 225–234.
39. Pantiru, M.; Vuluga, D. M.; Vasilescu, D. S.; Abadie, M. J. M. *Polym. Bull.* **2002**, *47*, 485–492.
40. Masuda, T.; Higashimura, T.; Okamura, S. *Polym. J.* **1970**, *1*, 19–26.
41. Kelen, T.; Tüdős, F. *React. Kinet. Catal. Lett.* **1974**, *1*, 487–492.
42. Kennedy, J. P.; Kelen, T.; Tüdös, F. *J. Polym. Sci., Polym. Chem. Ed.* **1975**, *13*, 2277–2289.

Supporting Information

Table S1. Cationic Homopolymerization of Cyclic Acetals[a]

entry	cyclic (M)	time	conv[b] (%) cyclic	$M_n \times 10^{-3}$ [c]	M_w/M_n [c]
1	MDOL	24 h	7	–	–
2	DMDOL	13 min	0	–	–
3	PhDOL	24 h	6	–	–
4	PMPDOL	48 h	2	–	–
5	PMPDOX	2 h	2	–	–
6	PMPDOP	2 h	14	–	–
7	TMDOL	48 h	0	–	–
8	CyDOL	10 h	19	–	–
9	Cy-DMDOL	2 h	0	–	–
10	BnDOL	72 h	6	–	–

[a] $[\text{cyclic acetal}]_0 = 0.40$ M, $[\text{IBEA}]_0 = 4.0$ mM, $[TiCl_4]_0 = 5.0$ mM, $[SnCl_4]_0 = 20$ mM, [ethyl acetate] = 20 mM, $[\text{DTBP}]_0 = 10$ mM, in toluene/dichloromethane (9/1 v/v) at −78 °C. [b] Determined by gravimetry. [c] Determined by GPC (polystyrene standards).

Scheme S1. Possible Mechanism of the Initiation Reaction of the Cationic Copolymerization of Cyclic Acetals and Vinyl Ether

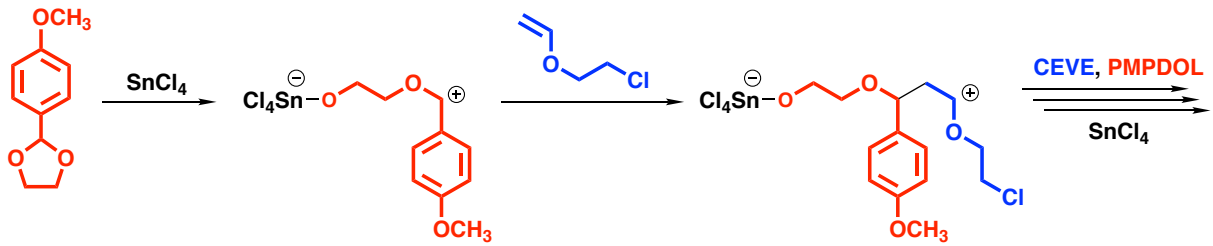

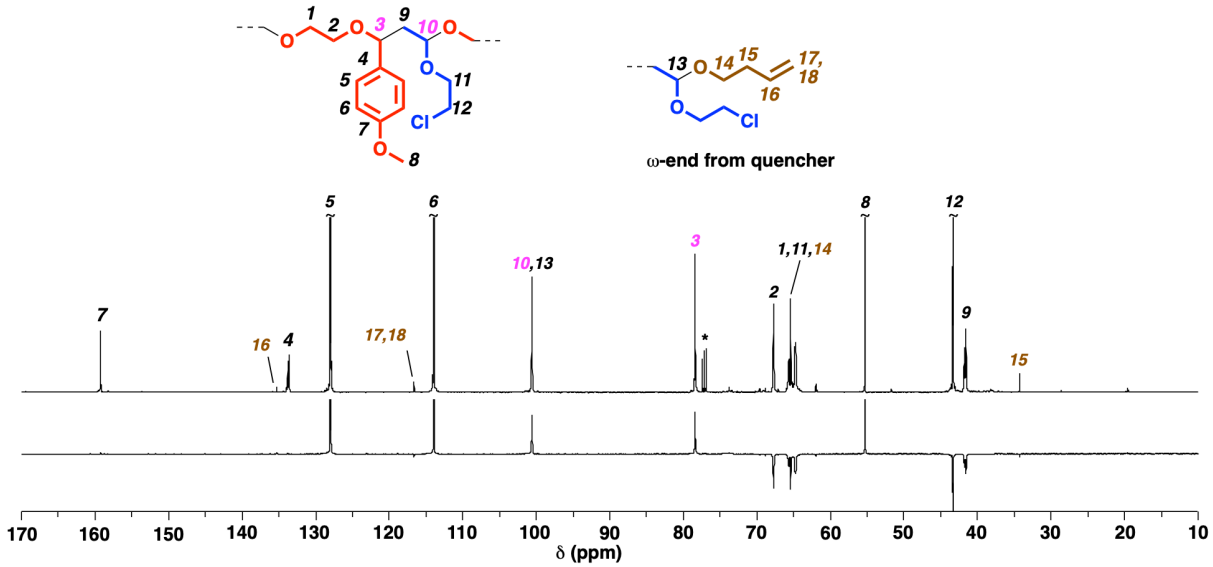

Figure S1. ^{13}C and DEPT 135 NMR spectra of CEVE–PMPDOL copolymer (entry 1 in Table 1, entry 4 in Table 2) (in $CDCl_3$ at 30 ºC). * $CDCl_3$.

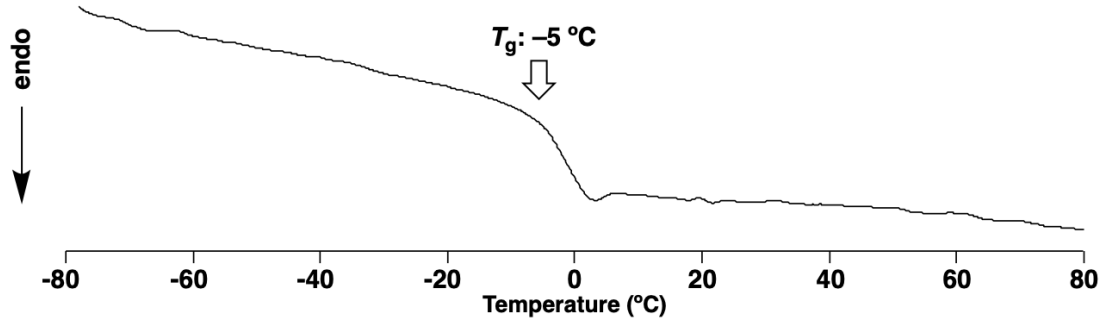

Figure S2. DSC thermogram of CEVE–PMPDOL copolymer (entry 1 in Table 1, entry 4 in Table 2) (the second heating scan; heating rate: 10 ºC/min).

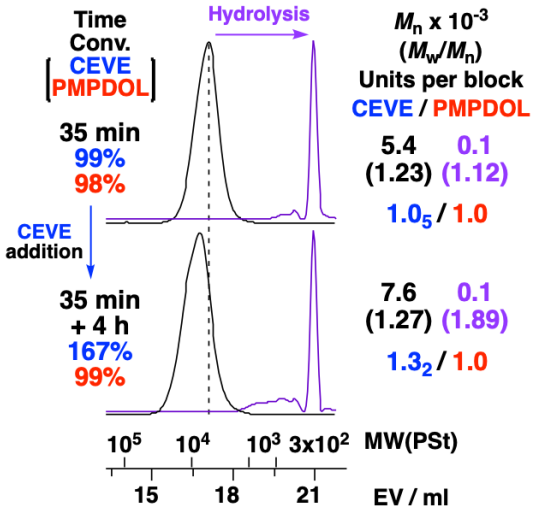

Figure S3. MWD curves of poly(CEVE-*co*-PMPDOL)s (black) and acid hydrolysis products (purple) obtained in the monomer-addition experiment. Polymerization conditions: $[CEVE]_0$ = $[CEVE]_{add}$ = 0.40 M, $[PMPDOL]_0$ = 0.40 M, $[IBEA]_0$ = 4.0 mM, $[TiCl_4]_0$ = 5.0 mM, $[SnCl_4]_0$ = 20 mM, [ethyl acetate] = 20 mM, $[DTBP]_0$ = 10 mM, in dichloromethane at −78 °C. Hydrolysis conditions: 1.0 M HCl (aq.) in 1,2-dimethoxyethane (0.5 wt% polymer) at room temperature for 3 h.

Table S2. Cationic Copolymerization of Various VEs and Cyclic Acetals[a]

				conv (%)[b]				units per block[f]	
entry	vinyl	cyclic acetal	time	vinyl	cyclic	$M_n \times 10^{-3}$ [e]	M_w/M_n[e]	vinyl	cyclic
1	IBVE	PhDOL	60 s	99	83	14.1	1.16	1.8	1.0
2		PMPDOL	1 h	99	83	18.1	1.21	1.0_5	1.0
3[g]		MDOL	60 s	60[c]	1[c]	6.7	1.09	–	–
4[g]		DMDOL	3 min	84[c]	3[d]	9.9	1.09	27	1.0
5	IPVE	PhDOL	8 s	99	15	8.5	1.57	9.3	1.0
6		PMPDOL	10 s	93	40	8.7	1.47	2.6	1.0
7		MDOL	4 s	99[c]	0[c]	8.8	1.33	–	–
8		DMDOL	4 s	99[c]	0[c]	8.2	1.35	–	–
9	pMeSt	PhDOL	96 h	39	54	3.7	1.33	3.8	1.0
10		PMPDOL	49 h	66	25	3.1	1.11	2.5	1.0
11		MDOL	96 h	77[c]	9[c]	3.8	1.33	14	1.0
12		DMDOL	96 h	56[c]	7[c]	2.1	1.29	29	1.0

[a] Polymerization conditions for entries 1–8: $[IBVE]_0 = 0.50$ M (entries 1–4), $[IPVE]_0 = 0.50$ M (entries 5–8), $[\text{cyclic acetal}]_0 = 0.50$ M, $[IBVE–HCl]_0 = 5.0$ mM, $[SnCl_4]_0 = 5.0$ mM, [ethyl acetate] = 1.0 M, in dichloromethane at −78 °C. Polymerization conditions for entries 9–12: $[pMeSt]_0 = 0.50$ (entry 5) or 1.0 M (entry 6), $[\text{cyclic acetal}]_0 = 0.50$ (entry 5) or 1.0 M (entry 6), $[EtSO_3H]_0 = 10$ (entry 5) or 20 mM (entry 6), $[SnCl_4]_0 = 20$ mM, $[n\text{Bu}_4\text{NCl}]_0 = 8.0$ (entry 5) or 10 mM (entry 6) in dichloromethane at 0 °C. Hydrolysis conditions for entries 1–8: 0.50 M HCl in 1,2-dimethoxyethane (0.5 wt% polymer) at room temperature for 3 h. Acidolysis conditions for entries 9–12: 0.50 M trifluoroacetic acid in dichloromethane (0.5 wt% polymer) at room temperature for 1 h. [b] Determined by ^{1}H NMR analysis. [c] Determined by gas chromatography. [d] Determined by gravimetry and ^{1}H NMR analysis. [e] Determined by GPC (polystyrene standards). [f] Evaluated by ^{1}H NMR analysis. [g] Reported in reference 20.

Table S3. The Data for Determination of Monomer Reactivity Ratio[a]

entry	vinyl	(M)	cyclic (M)	(M)	time	conv[b] (%) vinyl	conv[b] (%) cyclic	$M_n \times 10^{-3}$ [c]	M_w/M_n[c]	vinyl in copolymer[b]
1	CEVE	0.10	PMPDOL	0.90	5 min	5	15	2.7	1.16	0.48
2		0.30		0.70	3 min	4	25	2.5	1.21	0.50
3		0.50		0.50	2 min	20	9	2.0	1.48	0.53
4		0.70		0.30	2 s	14	14	2.0	1.49	0.58
5	IBVE	0.20	PMPDOL	0.80	3 min	17	7	5.6	1.20	0.49
6		0.40		0.60	90 s	10	8	3.9	1.36	0.50
7		0.60		0.40	10 s	13	9	5.6	1.37	0.60
8		0.80		0.20	1 s	18	7	4.6	1.31	0.70
9	IBVE	0.10	MDOL	0.90	10 s	26	~0	0.9	1.10	0.91
10		0.20		0.80	10 s	13	~0	1.5	1.15	0.96
11		0.30		0.70	10 s	17	~0	2.1	1.14	0.98
12		0.40		0.60	5 s	23	~0	2.0	1.19	0.98
13	pMeSt	0.27	PMPDOL	0.73	20 min	19	10	1.3	1.32	0.65
14		0.52		0.48	5 min	19	8	1.4	1.23	0.76
15		0.72		0.28	10 s	4	15	1.4	1.25	0.85
16		0.89		0.11	2 s	3	12	1.3	1.44	0.94
17	pMeSt	0.15	MDOL	0.85	10 min	26	1	1.4	1.13	0.81
18		0.30		0.70	5 min	16	1	1.7	1.19	0.86
19		0.45		0.55	5 min	15	~0	1.7	1.15	0.90
20		0.60		0.40	1 min	17	~0	2.4	1.27	0.94

[a] Polymerization conditions for entries 1–4: $[CEVE]_0 + [PMPDOL]_0 = 1.0$ M, $[IBEA]_0 = 4.0$ mM, $[TiCl_4]_0 = 5.0$ mM, $[SnCl_4]_0 = 20$ mM, [ethyl acetate] = 20 mM, $[DTBP]_0 = 10$ mM, in toluene/dichloromethane (9/1 v/v) at −78 °C. Polymerization conditions for entries 4–12: $[IBVE]_0 + [\text{cyclic acetal}]_0 = 1.0$ M, $[IBVE–HCl]_0 = 5.0$ mM, $[SnCl_4]_0 = 5.0$ mM, [ethyl acetate] = 1.0 M, in dichloromethane at −78 °C. Polymerization conditions for entries 13–20: $[pMeSt]_0 + [\text{cyclic acetal}]_0 = 1.0$ M , $[EtSO_3H]_0 = 10$ mM, $[SnCl_4]_0 = 20$ mM, $[n\text{Bu}_4\text{NCl}]_0 = 8.0$ mM in dichloromethane at 0 °C. [b] Determined by ^{1}H NMR analysis.

Part II

Synthesis of Sequence-Controlled Polymers via One-Pot Approach Consisting of Selective Generation of Cyclic Monomers and Subsequent Alternating Copolymerization with Vinyl Monomers

Chapter 4.

ABC-Type Periodic Terpolymer Synthesis by a One-Pot Approach Consisting of Oxirane- and Carbonyl-Derived Cyclic Acetal Generation and Subsequent Living Cationic Alternating Copolymerization with a Vinyl Monomer

Introduction

Monomer sequences are important structural factors of polymers.[1–4] Natural macromolecules such as peptides and proteins exhibit sophisticated functions due to their perfectly regulated monomer sequences. In synthetic polymers, various methods have been developed to control the monomer sequences. One of the most reliable strategies is iterative single unit monomer addition (Scheme 1A), such as polypeptide synthesis with the Merrifield resin, although considerable time and effort are required to prepare long polymers.[5–8] The polymerization of monomers containing a specific sequence (Scheme 1B) effectively produces sequence-regulated polymers;[9–19] however, the preparation of sequence-incorporated monomers generally requires a multistep reaction and challenging purification steps and/or results in low yield. The direct chain-growth polymerization of several monomers (Scheme 1C) is the simplest approach, although extremely high selectivity during the propagation reactions is indispensable for sequence regulation.[20–23] A simpler and more sophisticated method is desirable for facile access to sequence-controlled polymers.

A promising strategy for facile synthesis of sequence-controlled polymers is a successive one-pot process consisting of the synthesis of a sequence-incorporated monomer and subsequent polymerization with another monomer (Scheme 1D). A relevant and important study on the copolymerization of a sequence-incorporated monomer with another monomer describes the cycloaddition of an electron-deficient olefin and vinyl ether (VE) and the subsequent copolymerization of the cycloaddition product with oxirane,[24,25] although this example is not a one-pot process and requires purification and isolation of the cycloaddition product before polymerization with oxirane. To achieve a one-pot method, quantitative synthesis of a sequence-incorporated monomer without residual starting materials, the absence of byproducts, and the use of catalysts that do not disturb either the monomer synthesis or the polymerization are required.

Scheme 1. Schematic Illustration for (A), (B), (C) Synthesis of Sequence-Regulated Polymers and (D) the Method Designed in This Study: *In situ* Synthesis of a Sequence-Programmed Monomer and Subsequent Copolymerization with Another Monomer

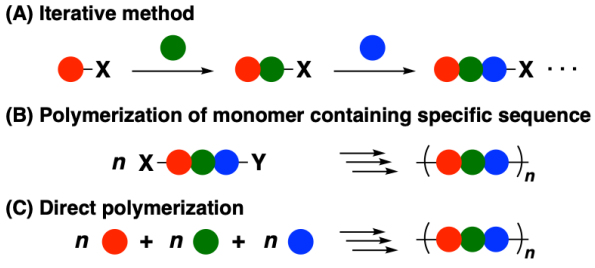

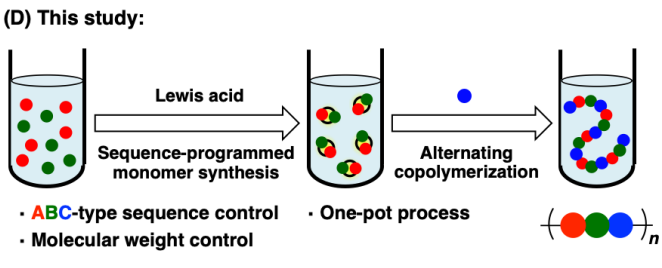

To satisfy these requirements, we devised a one-pot method that consists of the synthesis of a sequence-programmed cyclic acetal via selective cyclodimerization of oxirane and a carbonyl compound and the subsequent copolymerization of the cyclic acetal with a vinyl monomer. The cyclic acetal formation was reported to proceed from oxirane and acetone with the aid of a Lewis acid catalyst.[26–29] In addition, in our previous study, a cyclic acetal was generated as a byproduct in the cationic terpolymerization of oxirane, ketone, and VE,[23] which suggests that the cyclization reaction of oxirane and a carbonyl compound occurs even under the conditions required for cationic polymerization. The cationic copolymerization of cyclic acetals and vinyl monomers via the cationic mechanism was reported several decades ago.[30,31] Recently, we reported the controlled cationic copolymerization of VEs and cyclic acetals using a carefully designed initiating system based on the living cationic polymerization of vinyl monomers.[32] We also systematically investigated the structural effects of cyclic acetals on copolymerization behavior.[33] The elaborate design of reaction conditions that enable both the quantitative synthesis of a sequence-programmed cyclic acetal and the subsequent alternating copolymerization of the cyclic acetal with a vinyl monomer can potentially afford ABC-type periodic terpolymers by a one-pot method.

In this study, we examined the one-pot synthesis of sequence-controlled terpolymers composed of oxiranes, carbonyl compounds, and vinyl monomers via the above-explained strategy (Scheme 2). Suitable combinations of aldehydes or ketones with oxiranes underwent selective and quantitative cyclodimerization reactions and yielded cyclic acetals without any byproducts under appropriately designed conditions. The generated cyclic acetals were successively copolymerized with VEs or styrene derivatives in a living manner, which afforded ABC-type periodic terpolymers with controlled molecular weights (MWs), molecular weight distributions (MWDs), and chain end structures. Furthermore, the sequential addition of VEs with different substituents, such as chloride or acetoxy moieties, produced unique block polymers consisting of blocks with different ABC-type periodic sequences.

Scheme 2. Synthesis of Sequence-Regulated Polymers via Selective Cyclodimerization of Oxiranes and Carbonyl Compounds and Subsequent Controlled Cationic Copolymerization with Vinyl Monomers (upper). Monomers Used in This Study (lower)

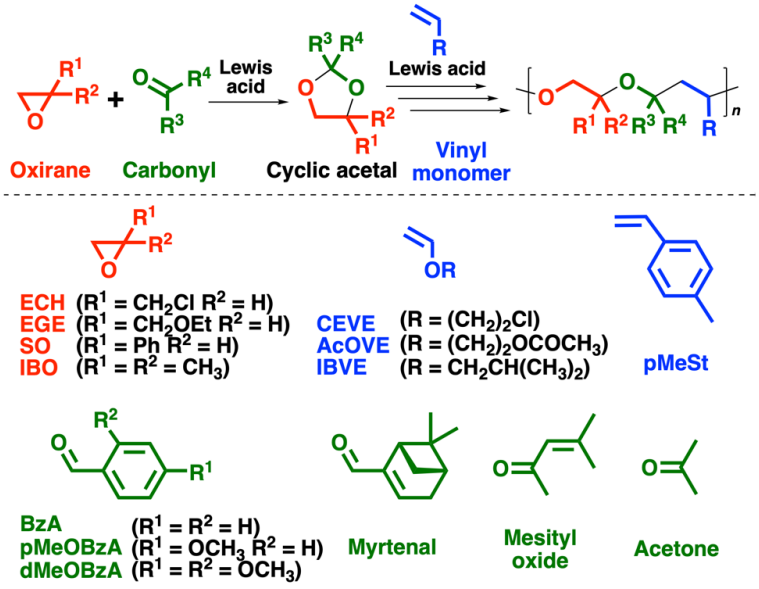

Experimental Section

Materials

Epichlorohydrin (ECH; TCI; >99.0%), ethyl glycidyl ether (EGE; TCI; >98.0%), styrene oxide (SO; Aldrich; 97.0%), *p*-methoxybenzaldehyde (pMeOBzA; Nacalai Tesque; ≥99.0%), benzaldehyde (BzA; Wako; >98.0%), and (1*R*)-(–)-myrtenal (myrtenal; Aldrich; ≥97.0%) were distilled twice over calcium hydride under reduced pressure. Mesityl oxide (Nacalai Tesque; ≥96.0%), isobutylene oxide (IBO; TCI; >97.0%), and ethyl acetate (Wako; >99.5%) were distilled twice over calcium hydride. 2-Acetoxyethyl VE (AcOVE) was synthesized by the substitution reaction of CEVE with sodium acetate and then distilled twice over calcium hydride under reduced pressure.[34] 2,4-Dimethoxybenzaldehyde (dMeOBzA; TCI; >98.0%) was recrystallized from hexane and dried under reduced pressure. $In(OTf)_3$ (Sigma-Aldrich), potassium *tert*-butoxide (Wako; >85.0%), sodium iodide (Wako; >99.5%), *N*,*N*-dimethylformamide (Nacalai Tesque; >99.5%), and toluene (Nacalai Tesque; ≥99.5%) were used without further purification. Stock solutions of $FeCl_3$ in diethyl ether and $GaCl_3$ in hexane were prepared from $FeCl_3$ (Sigma-Aldrich; 99.99%) and $GaCl_3$ (Sigma-Aldrich; >99.999%), respectively. Other compounds were prepared and used as described in Part I.

Synthesis of Cyclic Acetals via Selective Cyclodimerization

A typical reaction for the cyclodimerization of an oxirane and a carbonyl compound is as follows. A glass tube equipped with a three-way stopcock was dried using a heat gun (Ishizaki, PJ-206A; the air temperature was approximately 450 °C) under dry nitrogen. Dichloromethane and pMeOBzA were added into the tube using dry syringes. After cooling the solution to 0 °C, a solution of $SnCl_4$ (containing a small amount of heptane) in dichloromethane kept at 0 °C was added to the tube. The reaction was initiated by dropwise addition of a solution of ECH in dichloromethane (2 M). After 24 h, the reaction was terminated with methanol containing a small amount of an aqueous ammonia solution. The monomer conversion and the amount of cyclic acetal generated were determined by ^{1}H NMR spectroscopy of the quenched mixture. The quenched solution was diluted with dichloromethane and washed with water. The volatiles were then removed under reduced pressure to yield a colorless cyclic acetal. In the case of the one-pot process for the synthesis of a terpolymer, the reaction mixture was subjected to subsequent copolymerization with a vinyl monomer without quenching by methanol, as described below.

4-Chloromethyl-2-(4-methoxyphenyl)-1,3-dioxolane (the product of entry 1 in Table 1)

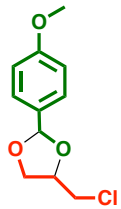

A mixture of diastereomers (58/42).^{1}H NMR ($CDCl_3$; 500 MHz): Major diastereomer: δ 7.41 (2H, d, *J* = 9.0 Hz), 6.91 (2H, d, *J* = 9.0 Hz), 5.79 (1H, s), 4.43 (1H, dddd, *J* = 7.0, 6.5, 4.5, 4.5 Hz), 4.14 (1H, dd, *J* = 8.5, 6.5 Hz), 4.12 (1H, dd, *J* = 8.5, 4.5 Hz), 3.81 (3H, s), 3.66 (1H, dd, *J* = 11, 4.5 Hz), 3.56 (1H, dd, *J* = 11, 7.0 Hz), Minor diastereomer: δ 7.39 (2H, d, *J* = 9.0 Hz), 6.90 (2H, d, *J* = 9.0 Hz), 5.93 (1H, s), 4.48 (1H, dddd, *J* = 7.0, 6.5, 4.5, 4.5 Hz), 4.32 (1H, dd, *J* = 8.5, 6.5 Hz), 3.91 (1H, dd, *J* = 8.5, 4.5 Hz), 3.81 (3H, s), 3.72 (1H, dd, *J* = 11, 4.5 Hz), 3.61 (1H, dd, *J* = 11, 7.0 Hz). ^{13}C NMR ($CDCl_3$; 125 MHz): Major diastereomer: δ 160.6, 129.0, 128.0, 114.0, 105.0, 75.4, 69.0, 55.5, 44.7, Minor diastereomer: δ 160.8, 129.0, 128.0, 114.0, 104.4, 75.7, 68.7, 55.5, 44.4. MS (ESI) *m/z* $[M + Na]^+$, calcd: 251.0445, observed: 251.0445.

4-Chloromethyl-2-(2,4-dimethoxyphenyl)-1,3-dioxolane (the product of entry 2 in Table 1)

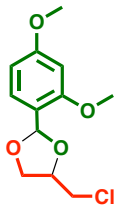

A mixture of diastereomers (60/40). ^{1}H NMR ($CDCl_3$; 500 MHz): Major diastereomer: δ 7.48 (1H, d, *J* = 8.5 Hz), 6.51 (1H, dd, *J* = 8.5, 2.5 Hz), 6.45 (1H, d, *J* = 2.5 Hz), 6.12 (1H, s), 4.42 (1H, dddd, *J* = 7.5, 7.0, 4.5, 4.5 Hz), 4.14 (1H, dd, *J* = 9.0, 4.5 Hz), 4.11 (1H, dd, *J* = 9.0, 7.0 Hz), 3.82 (3H, s), 3.81 (3H, s), 3.66 (1H, dd, *J* = 11, 4.5 Hz), 3.57 (1H, dd, *J* = 11, 7.5 Hz), Minor diastereomer: δ 7.41 (1H, d, *J* = 8.5 Hz), 6.49 (1H, dd, *J* = 8.5 Hz, 2.5 Hz), 6.45 (1H, d, *J* = 2.5 Hz), 6.25 (1H, s), 4.49 (1H, dddd, *J* = 7.5, 6.5, 6.5, 5.0 Hz), 4.32 (1H, dd, *J* = 8.5, 6.5 Hz), 3.90 (1H, dd, *J* = 8.5, 6.5 Hz), 3.82 (3H, s), 3.81 (3H, s), 3.73 (1H, dd, *J* = 11, 5.0 Hz), 3.61 (1H, dd, *J* = 11, 7.5 Hz). ^{13}C NMR ($CDCl_3$; 125 MHz): Major diastereomer: δ 162.0, 159.0, 128.1, 117.5, 104.7, 100.4, 98.6, 75.6, 68.6, 55.8, 55.5, 44.6, Minor diastereomer: δ 161.9, 159.0, 128.0, 118.1, 104.4, 100.2, 98.7, 75.4, 69.0, 55.8, 55.5, 44.3. MS (ESI) *m/z* $[M + Na]^+$, calcd: 281.0551, observed: 281.0550.

4-Chloromethyl-2-phenyl-1,3-dioxolane (the product of entry 3 in Table 1)

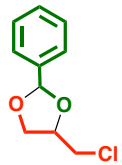

A mixture of diastereomers (59/41). ^{1}H NMR ($CDCl_3$; 500 MHz): Major diastereomer: δ 7.47–7.49 (2H, m), 7.37–7.39 (3H, m), 5.83 (1H, s), 4.44 (1H, dddd, *J* = 8.0, 5.0, 5.0, 5.0 Hz), 4.13 (2H, d, *J* = 5.0 Hz), 3.65 (1H, dd, *J* = 11, 5.0 Hz), 3.55 (1H, dd, *J* = 11, 8.0 Hz), Minor diastereomer: δ 7.47–7.49 (2H, m), 7.37–7.39 (3H, m), 5.99 (1H, s), 4.48 (1H, dddd, *J* = 7.5, 6.0, 6.0, 5.0 Hz), 4.30 (1H, dd, *J* = 8.5, 6.0 Hz), 3.92 (1H, dd, *J* = 8.5, 6.0 Hz), 3.72 (1H, dd, *J* = 11, 5.0 Hz), 3.61 (1H, dd, *J* = 11, 7.5 Hz). ^{13}C NMR ($CDCl_3$; 125 MHz): Major diastereomer: δ 136.9, 129.7, 129.5, 126.7, 105.0, 75.9, 68.9, 44.5, Minor diastereomer: δ 137.6, 129.6, 128.6, 126.5, 104.4, 75.5, 68.8, 44.3. MS (ESI) *m/z* $[M + Na]^+$, calcd: 221.0340, observed: 221.0345.

4-Chloromethyl-2-(6,6-dimethyl-bicyclo[3.1.1]-hept-2-ene-2-yl)-1,3-dioxolane (the product of entry 4 in Table 1)

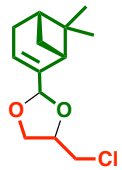

A mixture of diastereomers (55/45). ^{1}H NMR ($CDCl_3$; 400 MHz): Major diastereomers: δ 5.74–5.77 (1H, m); 5.18, 5.20 (1H, s); 4.23–4.28 (1H, m); 3.96, 3.97 (2H, probably d); 3.57, 3.66 (1H, dd, *J* = 11.2, 4.8 Hz); 3.42, 3.43, 3.51 (1H, dd, *J* = 11.2, 8.0 Hz; 11.2, 8.4 Hz); 2.41–2.46 (1H, m); 2.32–2.37 (1H, m); 2.24–2.29 (2H, m); 2.11 (1H, m); 1.30 (3H, s); 1.16–1.20 (1H, m); 0.82 (3H, s); Minor diastereomers: δ 5.74–5.77 (1H, m); 5.31, 5.31 (1H, s); 4.28–4.35 (1H, m); 4.19, 4.21 (1H, dd, *J* = 13.2, 4.8 Hz; 15.2, 6.4 Hz); 3.76, 3.77 (1H, dd, *J* = 8.8, 6.0 Hz; 8.8, 6.4 Hz); 3.53, 3.56 (1H, dd, *J* = 15.2, 4.4 Hz; 13.2 Hz, 5.2 Hz); 3.51–3.54 (overlap), 3.50 (1H, dd, *J* = 6.0, 4.8 Hz); 2.41–2.46 (1H, m); 2.32–2.37 (1H, m); 2.24–2.29 (2H, m); 2.11 (1H, m); 1.30 (3H, s); 1.16–1.20 (1H, m); 0.82 (3H, s). ^{13}C NMR ($CDCl_3$; 125 MHz): Major diastereomer: δ 144.6, 125.5, 105.9, 75.3, 68.9, 44.5, 41.0, 40.7, 38.0, 31.8, 31.5, 26.2, 21.3, Minor diastereomer: δ 144.1, 125.4, 105.4, 75.2, 68.8, 44.4, 41.0, 40.7, 38.0, 31.7, 31.4, 26.2, 21.3. MS (ESI) *m/z* $[M + Na]^+$, calcd: 265.0966, observed: 265.0966.

Note: Multiple diastereomers exist because the alicyclic moiety at the 2-position of the cyclic acetal also has stereocenters.

4-Chloromethyl-2-methyl-2-(2-methyl-1-propene-1-yl)-1,3-dioxolane (the product of entry 5 in Table 1)

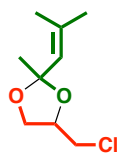

A mixture of diastereomers (65/35). ^{1}H NMR ($CDCl_3$; 500 MHz): Major diastereomer: δ 5.20 (1H, s), 4.22 (1H, dddd, *J* = 7.5, 6.5, 4.5, 4.5 Hz), 3.96 (1H, dd, *J* = 8.5, 6.5 Hz), 3.84 (1H, dd, *J* = 8.5, 4.5 Hz), 3.57 (1H, dd, *J* = 11, 4.5 Hz), 3.45 (1H, dd, *J* = 11, 7.5 Hz), 1.79 (6H, s), 1.51 (3H, s), Minor diastereomer: δ 5.30 (1H, s), 4.29 (1H, dddd, *J* = 7.5, 6.0, 5.0, 4.5 Hz), 4.16 (1H, dd, *J* = 8.5, 6.0 Hz), 3.75 (1H, dd, *J* = 8.5, 4.5 Hz), 3.61 (1H, dd, *J* = 11, 5.0 Hz), 3.40 (1H, dd, *J* = 11, 7.5 Hz), 1.70 (6H, s), 1.46 (3H, s). ^{13}C NMR ($CDCl_3$; 125 MHz): Major diastereomer: δ 136.7, 126.5, 109.6, 75.0, 68.3, 45.0, 26.7, 26.1, 18.2, Minor diastereomer: δ 136.7, 127.5, 109.6, 75.6, 67.3, 44.8, 26.6, 25.7, 18.7. MS (ESI) *m/z* $[M + Na]^+$, calcd: 213.0653, observed: 213.0654.

4-Ethoxymethyl-2-(4-methoxyphenyl)-1,3-dioxolane (the product of entry 1 in Table S1)

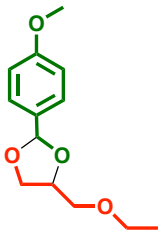

A mixture of diastereomers (52/48). ^{1}H NMR ($CDCl_3$; 500 MHz): Major diastereomer: δ 7.42 (2H, d, *J* = 8.5 Hz), 6.90 (2H, d, *J* = 8.5 Hz), 5.76 (1H, s), 4.37 (1H, dddd, *J* = 7.0, 6.0, 5.5, 5.5 Hz), 4.08 (1H, dd, *J* = 8.0, 7.0 Hz), 3.95 (1H, dd, *J* = 8.0, 5.5 Hz), 3.804 (3H, s), 3.63 (1H, dd, *J* = 10, 5.5 Hz), 3.57 (2H, probably q (overlap)), 3.52 (1H, dd, *J* = 10, 6.0 Hz), 1.22 (3H, t, *J* = 7.0 Hz), Minor diastereomer: δ 7.41 (2H, d, *J* = 8.5 Hz), 6.89 (2H, d, *J* = 8.5 Hz), 5.89 (1H, s), 4.42 (1H, probably dddd, *J* = 7.0, 6.5, 6.0, 5.5 Hz), 4.25 (1H, dd, *J* = 8.5, 7.0 Hz), 3.806 (1H, probably dd (overlap), *J* = 8.5, 6.5 Hz), 3.805 (3H, s), 3.63 (1H, dd, *J* = 10, 5.5 Hz), 3.57 (2H, probably q (overlap)), 3.57 (1H, probably dd (overlap), *J* = 10, 6.0 Hz), 1.23 (3H, t, *J* = 7.0 Hz). ^{13}C NMR ($CDCl_3$; 125 MHz): Major diastereomer: δ 160.4, 129.6, 128.2, 113.8, 103.8, 75.1, 71.6, 68.0, 67.2, 55.4, 15.2, Minor diastereomer: δ 160.6, 130.2, 128.0, 114.4, 104.4, 75.4, 71.1, 67.9, 67.1, 55.7, 15.3. MS (ESI) *m/z* $[M + Na]^+$, calcd: 261.1097, observed: 261.1096.

4-Ethoxymethyl-2-(2,4-dimethoxyphenyl)-1,3-dioxolane (the product of entry 8 in Table 1)

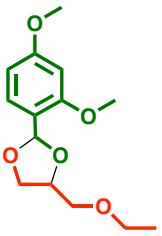

A mixture of diastereomers (60/40). ^{1}H NMR ($CDCl_3$; 500 MHz): Major diastereomer: δ 7.49 (1H, d, *J* = 8.0 Hz), 6.50 (1H, dd, *J* = 8.0, 2.0 Hz), 6.44 (1H, d, *J* = 2.0 Hz), 6.10 (1H, s), 4.36 (1H, dddd, *J* = 6.5, 6.0, 5.5, 5.0 Hz), 4.07 (1H, dd, *J* = 8.5, 6.5 Hz), 3.95 (1H, dd, *J* = 8.5, 5.0 Hz), 3.82 (3H, s), 3.805 (3H, s), 3.64 (1H, dd, *J* = 9.5, 5.5 Hz), 3.53–3.60 (2H, probably q (overlap)), 3.50 (1H, dd, *J* = 9.5, 6.0 Hz), 1.21 (3H, t, *J* = 7.0 Hz), Minor diastereomer: δ 7.44 (1H, d, *J* = 8.0 Hz), 6.48 (1H, dd, *J* = 8.0, 2.0 Hz), 6.44 (1H, d, *J* = 2.0 Hz), 6.20 (1H, s), 4.43 (1H, probably dddd), 4.24 (1H, dd, *J* = 8.0, 6.5 Hz), 3.82 (3H, s), 3.801 (3H, s), 3.799 (1H, probably dd (overlap), *J* = 8.5, 6.5 Hz), 3.66 (1H, dd, *J* = 10, 5.5 Hz), 3.53–3.60 (2H, probably q (overlap)), 3.51 (1H, probably dd (overlap)), 1.22 (3H, t, *J* = 7.0 Hz). ^{13}C NMR ($CDCl_3$; 125 MHz): Major diastereomer: δ 161.8, 159.0, 128.2, 118.1, 104.6, 99.6, 98.5, 75.1, 71.6, 68.1, 67.2, 55.7, 55.5, 15.7, Minor diastereomer: δ 161.7, 159.0, 128.1, 118.7, 104.3, 99.7, 98.6, 75.0, 71.2, 68.1, 67.1, 55.7, 55.5, 15.3. MS (ESI) *m/z* $[M + Na]^+$, calcd: 291.1203, observed: 291.01204.

4-Phenyl-2-(4-methoxyphenyl)-1,3-dioxolane (the product of entry 2 in Table S1)

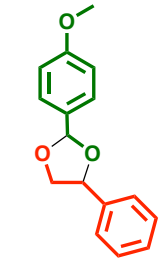

A mixture of diastereomers (89/11). ^{1}H NMR ($CDCl_3$; 500 MHz): Major diastereomer: δ 7.50 (2H, d, *J* = 8.5 Hz), 7.27–7.41 (5H, m), 6.92 (2H, d, *J* = 8.5 Hz), 5.92 (1H, s), 5.14 (1H, dd, *J* = 7.5, 7.0 Hz), 4.32 (1H, dd, *J* = 8.0, 7.5 Hz), 3.90 (1H, dd, *J* = 8.0, 7.0 Hz), 3.77 (3H, s), Minor diastereomer: δ 7.47 (2H, d, *J* = 8.5 Hz), 7.27–7.41 (5H, m), 6.91 (2H, d, *J* = 8.5 Hz), 6.12 (1H, s), 5.19 (1H, dd, *J* = 7.5, 7.0 Hz), 4.50 (1H, dd, *J* = 8.0, 7.5 Hz), 3.82 (1H, dd, *J* = 8.0, 7.0 Hz), 3.77 (3H, s). ^{13}C NMR ($CDCl_3$; 125 MHz): Major diastereomer: δ 160.0, 139.2, 129.4, 128.1, 127.8, 127.6, 126.0, 113.3, 104.0, 78.0, 71.6, 54.5, Minor diastereomer: δ 160.0, 139.5, 129.5, 128.1, 127.8, 127.6, 125.6, 113.8, 104.1, 77.3, 72.2, 54.8. MS (ESI) *m/z* $[M + Na]^+$, calcd: 279.0992, observed: 279.0993.

4,4-Dimethyl-2-(4-methoxyphenyl)-1,3-dioxolane (the product of entry 4 in Table S1)

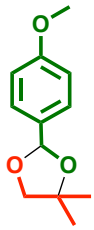

^{1}H NMR ($CDCl_3$; 500 MHz): δ 7.41 (2H, d, *J* = 8.5 Hz), 6.87 (2H, d, *J* = 8.5 Hz), 5.83 (1H, s), 3.84 (1H, d, *J* = 8.0 Hz), 3.75 (3H, s), 3.72 (1H, d, *J* = 8.0 Hz), 1.40 (3H, s), 1.38 (3H, s). ^{13}C NMR ($CDCl_3$; 125 MHz): δ 159.9, 131.4, 127.7, 113.8, 102.7, 78.4, 76.0, 55.0, 26.5. MS (ESI) *m/z* $[M + Na]^+$, calcd: 231.0992, observed: 231.0993.

Note

Comparison of chemical shifts in ^{1}H NMR spectra of the cyclic acetals with those of similar structures previously reported[35] suggests that major diastereomers are *trans* isomers and minor diastereomers are *cis* isomers.

Polymerization Procedure

The following is a typical procedure for the copolymerization of a cyclic acetal and a vinyl monomer by a one-pot method. The glass tube containing the reaction mixture for cyclic acetal synthesis (explained above) was cooled at –96 °C. The polymerization was started by sequentially adding ethyl acetate, CEVE, and a solution of $SnCl_4$ in dichloromethane to the tube. After a predetermined interval, the polymerization was terminated with methanol or 3-buten-1-ol containing a small amount of aqueous ammonia or triethylamine, respectively. The quenched reaction mixture was diluted with dichloromethane and then washed with water. The volatiles were evaporated under reduced pressure at 50 °C. The residual cyclic acetal was removed by reprecipitation with methanol to yield a terpolymer. Monomer conversion was determined by ^{1}H NMR spectroscopy of the quenched reaction mixture using heptane as an internal standard.

Acid Hydrolysis

Acid hydrolysis was conducted in a manner similar to that described in Part I.

Formation of Vinyl Acetal Structure by Elimination of HCl

The polymer (15 mg) was dissolved in *N*,*N*-dimethylformamide (2 mL). Potassium *tert*-butoxide (50 mg) and sodium iodide (65 mg) were added to the reactor, and the reaction mixture was stirred for 16 h at room temperature. The reaction mixture was then diluted with toluene and washed with water. The volatiles were removed under reduced pressure.

Characterization

The MWD, NMR spectra, and electrospray ionization mass spectra (ESI-MS) of the obtained products were determined as described in Chapter 2. The absolute M_n values were determined with a GPC system composed of a Viscotek VE 1122 pump, polystyrene gel columns (TSKgel GMH_{HR}-M × 2; flow rate = 0.7 mL/min), and a Viscotek TDA 305 triple detector [refractive index, laser light scattering (λ = 670 nm; 90° RALS and 7° LALS), and differential pressure viscometer] in tetrahydrofuran. The thermal properties of the polymers were examined with a Shimadzu DSC-60 Plus differential scanning calorimeter for differential scanning calorimetry (DSC) analysis and PerkinElmer STA 6000 for thermal gravimetric analysis (TGA).

Results and Discussion

Selective and Quantitative Synthesis of Sequence-Programmed Cyclic Acetal.

To synthesize sequence-regulated monomers, the cyclodimerization reaction of various oxiranes and carbonyl compounds was examined using $SnCl_4$ as a Lewis acid in dichloromethane at 0 °C. $SnCl_4$ was used because this Lewis acid is highly effective for the living cationic polymerization of various VEs and styrene derivatives.[36] During the cyclodimerization reaction, complete consumption of both oxirane and carbonyl compounds is required because residual oxirane and carbonyl compounds would potentially react with VE during the subsequent cationic copolymerization.[37,38]

Very high selectivity was attained in the cyclodimerization of epichlorohydrin (ECH) with various aromatic aldehydes or conjugated ketones, among various combinations of monomers. The reactions

effectively proceeded with almost complete consumption of both monomers, resulting in cyclic acetals consisting of ECH and a carbonyl compound (entries 1–5 in Table 1). In the case of *p*-methoxybenzaldehyde (pMeOBzA; entry 1 in Table 1), the ^{1}H NMR spectrum of the reaction mixture (Figure 1), which was recorded after quenching with an excess amount of methanol, exhibited peaks attributed to a cyclic acetal (98%) and a very small amount of residual pMeOBzA (2%; this resulted from the experimental error when using equimolar amounts of pMeOBzA and ECH), while no peaks attributed to residual ECH and undesired products, such as oxirane homopolymer, were observed. Similar results were obtained with 2,4-dimthoxybenzaldehyde (dMeOBzA; entry 2) and benzaldehyde (BzA; entry 3), which are more and less reactive aromatic aldehydes than pMeOBzA, respectively. Moreover, the acyclic conjugated aldehyde (1*R*)-(–)-myrtenal (myrtenal; entry 4) and the conjugated ketone mesityl oxide (entry 5) also underwent an efficient cyclodimerization reaction with ECH.[39] However, the use of acetone resulted in the incomplete generation of a cyclic acetal and the partial formation of an ECH oligomer (entry 6), probably due to the smaller nucleophilicity of acetone than the conjugated aldehydes and ketones.

Table 1. Selective Cyclodimerization of Various Oxiranes and Carbonyl Compounds[a]

			conv (%)[b]		
entry	oxirane	carbonyl	oxirane	carbonyl	CE(%)[c]
1	ECH	pMeOBzA	100	98	>99
2		dMeOBzA	100	99	>99
3		BzA	100	99	>99
4		myrtenal	100	97	>99
5		mesityl oxide	100	98	>99
6		acetone	90	97	72
7	EGE	pMeOBzA	100	68	64
8		dMeOBzA	100	94	98
9	SO	pMeOBzA	100	82	83
10		dMeOBzA	87	70	71
11	IBO	pMeOBzA	100	75	78
12		dMeOBzA	100	83	88

[a] $[\text{oxirane}]_0 = 0.50$ (except for entry 8) or 1.0 (entry 8) M, $[\text{carbonyl compound}]_0 = 0.50$ (except for entry 8) or 1.0 (entry 8) M, $[SnCl_4]_0 = 20$ (entries 1, 2, 7, and 9–12) or 5.0 (entries 3–6, and 8) mM in dichloromethane at 0 ºC (except for entries 9 and 10) or –78 ºC (entries 9 and 10) for 24 h. [b] Determined by ^{1}H NMR analysis. [c] Cyclization efficiency: the ratio of the generated cyclic acetal to the feeds of oxiranes ($[\text{cyclic}]/[\text{oxirane}]_0$) determined by ^{1}H NMR analysis.

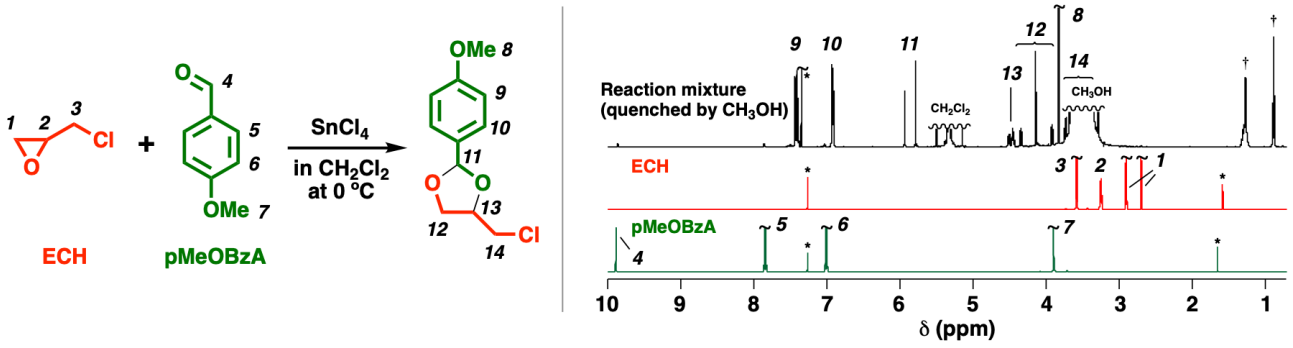

Figure 1. ^{1}H NMR spectra of the reaction mixture quenched by methanol (upper; entry 1 in Table 1), ECH monomer (middle), and pMeOBzA monomer (lower). In $CDCl_3$ at 30 ºC. * $CHCl_3$ and water. † heptane.

Oxiranes other than ECH also generated cyclic acetals when combined with appropriate carbonyl compounds, although the selectivity was inferior to that of ECH. The reaction of ethyl glycidyl ether (EGE) and dMeOBzA produced a cyclic acetal without any byproducts (entry 8 in Table 1). However, when pMeOBzA was used, the selectivity of the cyclodimerization reaction was relatively low because the oligomerization of EGE also occurred (entry 7). The selective cyclodimerization of EGE and pMeOBzA proceeded when the amount of pMeOBzA was twice that of EGE (entry 1 in Table S1). The cyclodimerization of pMeOBzA with styrene oxide (SO), which generates a benzyl-type carbocation by a ring-opening reaction, effectively proceeded at a lower temperature (–78 °C), although a slight amount of SO oligomer was also produced (entry 9 in Table 1, entry 3 in Table S1). In the case of isobutylene oxide (IBO), which generates a tertiary carbocation by the ring-opening reaction, IBO oligomers containing a homodimer were partly generated at an equimolar feed of both monomers (entries 11 and 12 in Table 1). When an excess of pMeOBzA (2 equiv. with respect to SO or 4 equiv. with respect to IBO) was charged, selective cyclodimerization proceeded successfully (entries 2 and 4 in Table S1). The ESI-MS spectra of the obtained products also corroborated the generation of the corresponding cyclic acetals. As demonstrated here, various oxiranes were used for cyclodimerization; however, equimolar amounts of both oxirane and carbonyl compounds need to be used because residual monomers disturb the sequence control of the subsequent copolymerization.

An appropriate choice of a Lewis acid catalyst is important for the efficient cyclodimerization reaction (Table S2). Among the various Lewis acids examined, $SnCl_4$ was superior in terms of activity and selectivity in the cyclodimerization reaction of SO and BzA. Lewis acids such as $FeCl_3$, $TiCl_4$, and $GaCl_3$ did not result in complete consumption of SO (Table S2). These differences probably stemmed from the difference in the interaction between the Lewis acids and BzA, partly arising from the difference in oxophilicity of the Lewis acids.[37,40]

Synthesis of an ABC-Type Periodic Terpolymer: Controlled Cationic Copolymerization of a Sequence-Programmed Cyclic Acetal and a Vinyl Monomer.

Cationic copolymerization of the above-obtained cyclic acetal and CEVE was subsequently conducted to synthesize an ABC-type sequence-regulated terpolymer with an initiating system that is effective for the controlled cationic copolymerization of CEVE and cyclic acetals (entries 1 and 2 in Table 2; Figure 2).[32,41] First, the selective cyclodimerization of ECH and pMeOBzA was performed as explained above. After cooling the reaction solution to –96 °C, without any purification processes, ethyl acetate, CEVE, and $SnCl_4$ were added to the solution. Ethyl acetate was used as a Lewis basic additive to suppress side reactions such as chain transfer reactions during cationic polymerization.[36] The additional $SnCl_4$ was used to compensate for the deficiency of the catalytic activity at lower temperatures. Milder reaction conditions, such as higher temperatures and lower catalyst loading, would be feasible by tuning reaction conditions, such as the amount of ethyl acetate. The copolymerization proceeded with the consumption of both monomers, yielding a polymer with a unimodal MWD (Figure 2A and 2C).[42] Interestingly, the MWD curves of the terpolymers shifted to the high-MW region as copolymerization proceeded, indicating the generation of long-lived species (Figure 2C). The M_n values measured by GPC with polystyrene standards (circle symbols in Figure 2B) or light-scattering detectors (square symbols) were consistent with the values calculated from the conversion of both monomers

Table 2. Controlled Cationic Copolymerization of Sequence-Programmed Cyclic Acetals and Vinyl Monomers[a]

					conv (%)[b]				units per block[d]		
entry	oxirane	carbonyl	vinyl	time	cyclic	vinyl	$M_n \times 10^{-3}$[c]	M_w/M_n[c]	oxirane	carbonyl	vinyl
1	ECH	pMeOBzA	CEVE	15 min	8	32	5.4	1.26	1.0	1.0_5	1.0_5
2				50 min	25	95	12.4	1.51	1.0	1.0_0	1.0_5
3		dMeOBzA		50 min	13	49	4.3	1.19	1.0	1.0_1	1.0_9
4		BzA		24 h	12	42	5.3	1.69	1.0	1.0_7	1.2_0
5		myrtenal		40 min	24	99	9.5	1.54	1.0	1.0_0	1.2_4
6		mesityl oxide		24 h	1	68	2.1	1.21	1.0	1.0	4.1
7	ECH	pMeOBzA	AcOVE	30 min	24	81	12.8	1.43	1.0	1.0_0	1.0_3
8			IBVE	46 h	9	73	15.7	1.71	1.0	0.9_9	2.1
9			pMeSt	93 h	6	68	3.0	1.18	1.0	1.0	3.4
10	EGE	pMeOBzA	pMeSt	96 h	30	76	2.4	1.19	1.0	1.0	4.8
11	IBO	pMeOBzA	pMeSt	96 h	36	38	2.3	1.15	1.0	1.0	13

[a] Reaction conditions for the synthesis of cyclic acetals: $[\text{oxirane}]_0$ = 1.0 (entries 1–9), 0.50 (entry 10), or 0.25 (entry 11) M; $[\text{carbonyl compound}]_0$ = 1.0 M; $[SnCl_4]_0$ = 5.0 (entries 1–8) or 20 (entries 9–11) mM; in dichloromethane at 0 °C for 24 h. Polymerization conditions: $[\text{cyclic acetal}]_0$ = 1.0 (entries 1–9), 0.50 (entry 10), or 0.25 (entry 11) M; $[\text{vinyl monomer}]_{add}$ = 0.25 (entries 1–9) or 0.50 (entries 10 and 11) M; $[\text{ethyl acetate}]_{add}$ = 0.25 (entries 1, 2, 5, and 7) or 1.0 (entry 8) M; $[SnCl_4]_{add}$ = 10 (entries 1–5 and 7), 20 (entry 6), or 5.0 (entry 8) mM; $[EtSO_3H]_{add}$ = 10 mM (entries 10 and 11); in dichloromethane at –96 (entries 1, 2, 5, 7, and 8), –78 (entries 3, 4, and 6), or 0 (entries 9–11) ºC. [b] Determined by ^{1}H NMR analysis. [c] Determined by GPC (polystyrene standards). [d] Evaluated by ^{1}H NMR analysis.

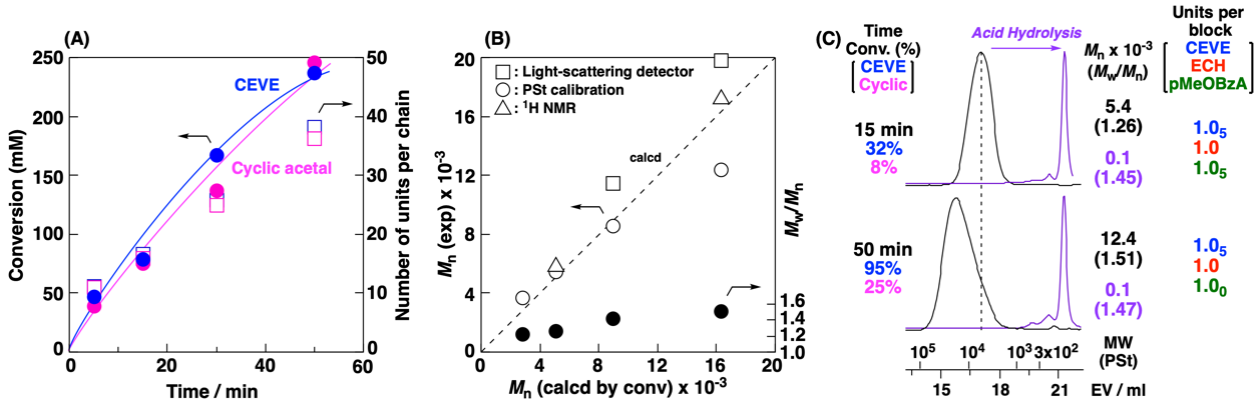

Figure 2. (A) Time–conversion curves for the copolymerization of CEVE and the cyclic acetal synthesized by the selective cyclodimerization of ECH and pMeOBzA (circle) and the average number of monomer units per chain (square; calculated from ^{1}H NMR analysis and MW values measured by GPC analysis), (B) the M_n (open) determined by GPC (circle; polystyrene standards, square; light-scattering detector) or NMR (triangle; from the main chain and the ω-ends) and M_w/M_n (filled) values of the polymers, and (C) MWD curves of poly(CEVE-*co*-cyclic acetal)s (black) and acid hydrolysis products (purple). The data correspond to entries 1 and 2 in Table 2.

and the amounts of the first portion of $SnCl_4$ (5.0 mM), which also suggests propagation in a living manner. Livingness of the copolymerization is slightly inferior to that of the homopolymerization of CEVE under similar conditions, as indicated by the slight broadening of MWDs of the high MW terpolymers. The broadening probably resulted from the additional initiation from the cyclic acetal via the interaction with $SnCl_4$. Polymers with higher MWs are potentially obtained by an increase in the feed of oxiranes, carbonyl compounds, and vinyl monomers.

The ^{1}H NMR analysis of the obtained terpolymers indicated the occurrence of extremely frequent crossover reactions between CEVE and the cyclic acetal (Figure 3A; Figure S1 for ^{13}C NMR spectra). Peaks assigned to acetal and *sec*-benzyl ether structures, which were generated by the crossover reaction from CEVE to the cyclic acetal and from the cyclic acetal to CEVE, respectively, were detected (peaks 9 and 4). Moreover, a peak attributed to an aromatic acetal was not observed at 5–6 ppm, indicating that homopropagation of the cyclic acetal did not occur. The absence of homopropagation is consistent with the result that the homopolymerization of the cyclic acetal did not proceed under the same conditions (Table S3, $[\text{cyclic acetal}]_0$ = 1.0 M). From the integral ratios of the aromatic peaks (peaks 5 and 6), the peaks of acetal and *sec*-benzyl ether (peaks 9 and 4), and the peaks of the CEVE-derived methylene group in the main chain (peak 8), the average number of ECH, pMeOBzA, and CEVE units per block was estimated to be 1.0, 1.0_5, 1.0_5, respectively (entry 1 in Table 2), suggesting that the copolymerization of CEVE and the cyclic acetal occurred in an alternating manner; thus, the terpolymer has ABC-type periodic sequences. The terpolymers obtained at different degrees of monomer conversion also had similar ABC-type periodic sequences (entries 1 and 2 in Table 2; Figure 2).

The ABC-type periodic sequences derived from alternating copolymerization were also corroborated by acid hydrolysis of the obtained terpolymers. In the ^{1}H NMR spectrum of the hydrolysis product, peaks assigned to *p*-methoxycinnamaldehyde, which was derived from one CEVE unit and one pMeOBzA unit, were exclusively observed (Figure 3B). This compound was generated via acid hydrolysis of the acid-labile acetal and *sec*-benzyl ether structures of the ECH–pMeOBzA–CEVE–ECH sequence and the subsequent dehydration reaction (Scheme 3A). 3-Chloro-1,2-propanediol and 2-chloroethanol, which are derived from the ECH and CEVE units, respectively, were most likely removed during purification. Importantly, other possible hydrolysis products, such as compounds derived from two or more CEVE units, were not observed in the ^{1}H NMR spectrum (Scheme 3B), which indicates the negligible occurrence of CEVE homopropagation during alternating copolymerization. The very sharp peaks in the low-MW region of the

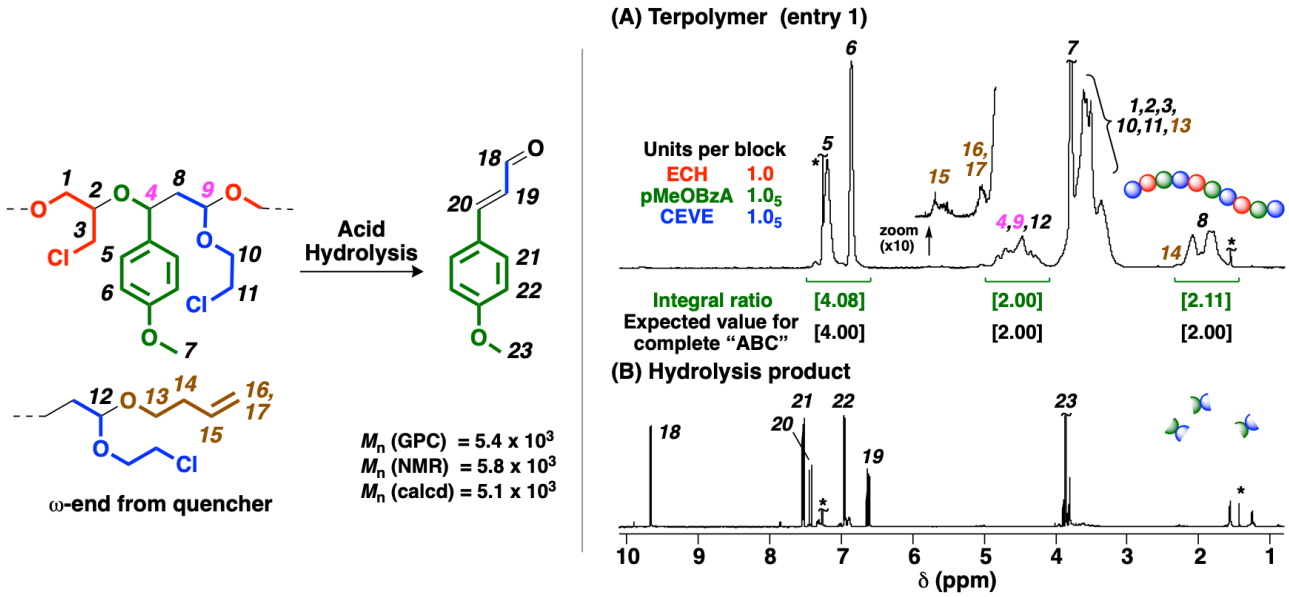

Figure 3. ^{1}H NMR spectra of (A) ECH–pMeOBzA–CEVE terpolymer (entry 1 in Table 2) and (B) its hydrolysis product. In $CDCl_3$ at 30 ºC. * $CHCl_3$ and water.

Scheme 3. Possible Mechanism of Acid Hydrolysis of the Terpolymers with ABC-Type Periodic Sequences

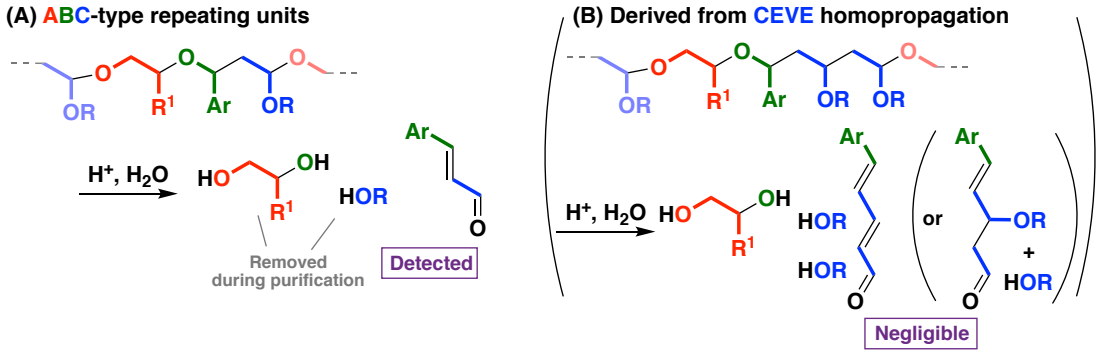

MWD curves of the hydrolysis products also suggest the ABC-type periodic sequences of the original terpolymer (Figure 2C, purple).

The livingness of the copolymerization was confirmed by the incorporation of a quencher into the chain ends and the monomer-addition experiment. In the ^{1}H NMR spectrum (Figure 3A), the peaks at 2.3, 5.1, and 5.8 ppm (peaks 14–17) were assigned to the ω-end structure derived from 3-buten-1-ol, which was used as a quencher.[43] The M_n value calculated from the integral ratio of the peaks of the main chain to those of the ω-end (5.8×10^3; Figure 2B triangle) was comparable to both the theoretical value based on the conversion of both monomers (5.1×10^3) and the value measured by GPC analysis (5.4×10^3; Figure 2B open circle, Figure 2C upper). This result suggests that copolymerization proceeded in a highly controlled manner via an appropriate dormant-active equilibrium at the propagating chain ends. Moreover, when the second portion of CEVE was added to the reaction mixture after almost complete consumption of the first portion of CEVE (conversion = 95%), the unimodal MWD curve shifted smoothly to the high-MW region without any tailings (Figure S2), indicating the occurrence of living polymerization.

The copolymerization mechanism is summarized in Scheme 4. Successful regulation of the ABC-type periodic sequence was achieved as a result of the nonhomopolymerizability of the cyclic acetal and the frequent crossover reactions from VE to cyclic acetal. A cyclic acetal adds to the VE-derived propagating carbocation to form an oxonium ion (Scheme 4a), which is subsequently converted to a carbocation via a ring-opening reaction (Scheme 4b). The selective scission of an acetal moiety rather than an ether moiety during the ring-opening reaction occurs because an alkoxy-adjacent carbocation is more stable than an alkyl-adjacent carbocation.[44,45] At the cyclic acetal-derived propagating end, the homopropagation of cyclic acetals did not proceed (Scheme 4e), which is consistent with the nonhomopolymerizability of 2-aryl-1,3-dioxolanes under the adopted conditions (Table S3).[46] The instability of an aromatic acetal structure in the main chain, which results from the homopropagation of the cyclic acetal, may be responsible for the nonhomopolymerizability. Therefore, the selective addition of VE to the cyclic acetal-derived propagating end proceeds (Scheme 4c), exclusively generating an oxirane–carbonyl–VE sequence. The acid hydrolysis of the obtained terpolymer (Figure 3B) also suggested an ABC-type periodic sequence, as explained above. The frequent crossover reactions from VE to cyclic acetal (Scheme 4a), which is also consistent with the copolymerization of VEs and 2-aryl-1,3-dioxolanes,[47] most likely stem from the higher reactivity of the cyclic acetal than of CEVE and the efficient occurrence of the ring-opening reaction. The monomer reactivity ratios determined by the Kelen–

Scheme 4. Copolymerization Mechanisms (Counteranions are omitted; $R^1 = CH_2Cl$, $R^2 = C_6H_4OCH_3$, R = CH_2CH_2Cl)

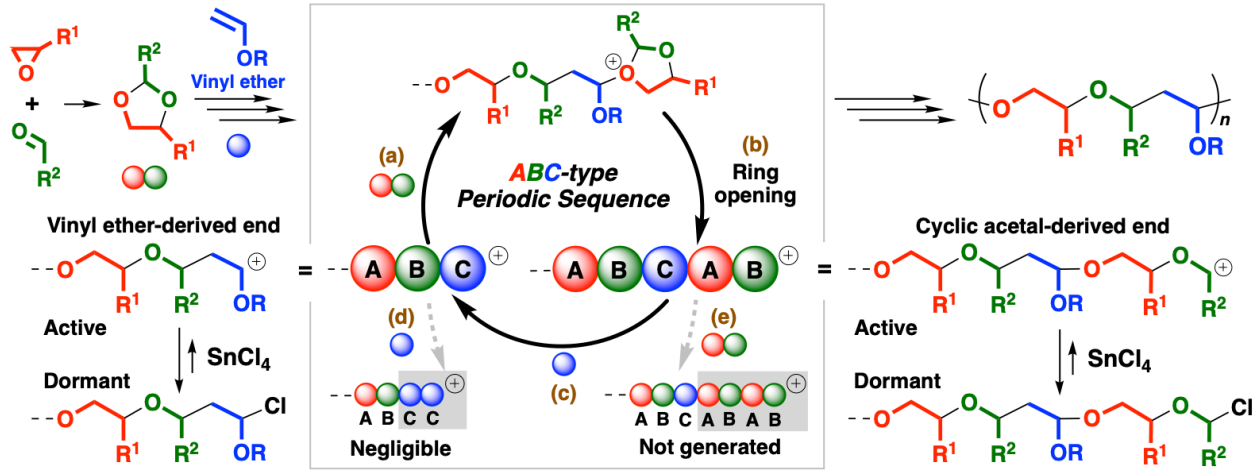

Tüdõs method also supported the frequent occurrence of crossover reactions (Table S4; M_1 = CEVE, M_2 = cyclic acetal consisting of ECH and pMeOBzA).[48,49] An r_1 value of less than 1 ($r_1 = 0.41$) and an r_2 value of approximately zero ($r_2 = 0.03$) indicate the favorable crossover from VE to cyclic acetal (Scheme 4a) over the homopropagation (Scheme 4d) and the nonhomopolymerizability of the cyclic acetal (Scheme 4e), respectively. To completely suppress the homopropagation of CEVE (Scheme 4d), the charged amount of CEVE was one-fourth the amount of cyclic acetal (Figure 2), resulting in alternating copolymerization. The initiation reaction most likely occurs via ring opening of the cyclic acetal with the first portion of $SnCl_4$ in a manner similar to the acetal-initiated living cationic polymerization of VEs or styrene derivatives.[50–54] The reaction of CEVE with the cyclic acetal-derived carbocation generates the CEVE-derived propagating end, which is followed by smooth propagation reactions as explained above (Scheme S1). The living copolymerization most likely proceeded via a dormant-active equilibrium consisting of the reversible activation of carbon–chlorine bonds at the propagating ends in a similar manner to the living cationic polymerization of vinyl monomers.[32,41]

The microstructures of the ABC-type periodic terpolymer were investigated with a focus on the ring-opening mode of the cyclic acetal. The cyclodimerization reaction of an oxirane and a carbonyl compound generates a 2,4-disubstituted asymmetric cyclic acetal via the α-scission or β-scission of an oxirane (Scheme S2). During copolymerization, the asymmetric cyclic acetal reacts with a VE-derived propagating species via the reaction of the oxygen atom at the 1-position or that at the 3-position, resulting in different microstructures (Scheme 5). The ratio of the two microstructures in the main chain was determined by the transformation of the VE–ECH sequence into vinyl acetal (i) and divinyl acetal (ii) structures with *t*BuOK (Scheme 6). The (i)/(ii) ratio was calculated to be 63/37 by ^{1}H NMR (Figure S3) and 64/36 by ^{13}C NMR (Figure S4), which indicates that the reaction of the cyclic acetal at the 1-position was preferential over that at the 3-position probably due to the less steric hindrance around the 1-position (Scheme 5). The main chains of the obtained terpolymers were not cleaved by the transformation under the basic conditions.

Scheme 5. The Addition Mode of the Cyclic Acetal in the Copolymerization with a VE (Counteranions are omitted)

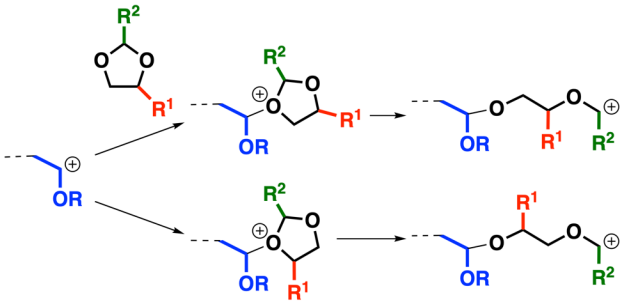

Scheme 6. Determination of Microstructure Distribution by Elimination Reaction (R = $C_6H_4OCH_3$)

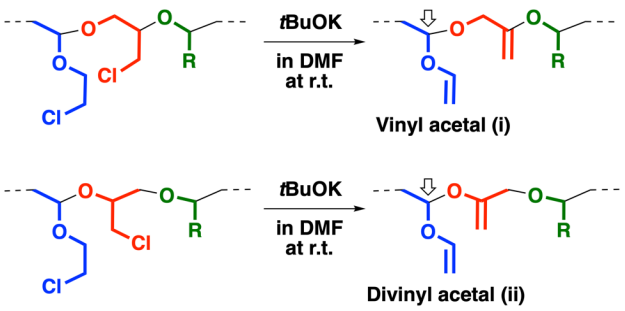

The one-pot synthesis of the ABC-type terpolymer demonstrated above exhibited adequate controllability in terms of sequences and MWs, even when compared with the polymerization of an isolated cyclic acetal and CEVE, whereas this method was obviously superior to the direct terpolymerization of ECH, pMeOBzA, and CEVE. The cationic copolymerization of CEVE and the cyclic acetal that was isolated and purified after the cyclodimerization reaction of ECH and pMeOBzA resulted in an ABC-type periodic terpolymer with similar degrees of sequence and MW control (Figure S5). In contrast, the direct cationic terpolymerization of ECH, pMeOBzA, and CEVE did not proceed under the same conditions as those used for the copolymerization of the cyclic acetal and CEVE (entries 2 and 3 in Table S5), likely because the Lewis basicities of the ECH and pMeOBzA monomers suppressed the catalytic activity of $SnCl_4$ at –96 °C. At a higher temperature (0 °C), terpolymerization proceeded; however, both ECH and pMeOBzA reacted with the CEVE-derived propagating species, resulting in a statistical sequence rather than an ABC-type periodic sequence (entry 1 in Table S5, Figure S6). These results indicate that the selective synthesis of the sequence-incorporated monomer is significantly important for the sequence regulation of the terpolymer.

The use of other monomers was also effective for the synthesis of ABC-type periodic terpolymers. When dMeOBzA was used instead of pMeOBzA, frequent crossover reactions between CEVE and the cyclic acetals generated quantitatively from ECH and dMeOBzA occurred, yielding ABC-type periodic terpolymers (entry 3 in Table 2; ECH/dMeOBzA/CEVE = $1.0/1.0_1/1.0_9$ units per block). The use of BzA or myrtenal-derived cyclic acetal also generated ABC-type sequence-controlled terpolymers, although CEVE homosequences were partly generated (entries 4 and 5 in Table 2; ECH/BzA/CEVE = $1.0/1.0_7/1.2_0$ units per block, ECH/myrtenal/CEVE = $1.0/1.0_0/1.2_4$ units per block). In the case of mesityl oxide, however, the number

of CEVE units per block was obviously large (entry 6 in Table 2; ECH/mesityl oxide/CEVE = 1.0/1.0/4.1 units per block). The difference in the substituents at the 2-position of cyclic acetals most likely affected the efficiency of the crossover reaction from VEs to cyclic acetals.

The difference in vinyl monomers mainly affected the length of vinyl monomer units. The use of 2-acetoxyethyl VE (AcOVE), which has an electron-withdrawing ester group and exhibits reactivity comparable to that of CEVE, also generated an ABC-type periodic terpolymer by copolymerization with ECH- and pMeOBzA-derived cyclic acetals (entry 7 in Table 2; ECH/pMeOBzA/AcOVE = $1.0/1.0_0/1.0_3$ units per block). In addition, the M_n values corresponded to the calculated values, indicating the livingness of the copolymerization (Figure 4). Copolymerization with isobutyl VE (IBVE), which is a more reactive VE than CEVE, resulted in a terpolymer containing a larger number of IBVE units per block (entry 8 in Table 2; ECH/pMeOBzA/IBVE = $1.0/0.9_9/2.1$ units per block). These results indicate that the use of VEs with low reactivity is important for the construction of ABC-type periodic sequences. The copolymerization of *p*-methylstyrene (pMeSt), which exhibits a smaller reactivity than CEVE,[55] and the cyclic acetal resulted in a terpolymer with several pMeSt units per block (entry 9 in Table 2; ECH/pMeOBzA/pMeSt = 1.0/1.0/3.4 units per block), which probably stemmed from the difference in the reactivity of the carbocations derived from pMeSt and VEs. The longer reaction time was required for the copolymerization with less reactive pMeSt. Faster polymerization is possibly achieved by tuning reaction conditions (e.g., higher reaction temperatures, larger amounts of the catalyst, etc.) without losing controllability. Interestingly, in the case of pMeSt, terpolymers with ABC-type sequences were successfully generated even when an excess amount of pMeOBzA was charged for the selective cyclodimerization with EGE or IBO. Unreacted pMeOBzA did not disturb the subsequent copolymerization (entries 10 and 11 in Table 2; EGE/pMeOBzA/pMeSt = 1.0/1.0/4.8 units per block, IBO/pMeOBzA/pMeSt = 1.0/1.0/13 units per block). Indeed, during the copolymerization of pMeSt and pMeOBzA under similar conditions, negligible crossover reactions occurred between pMeSt and pMeOBzA.[47]

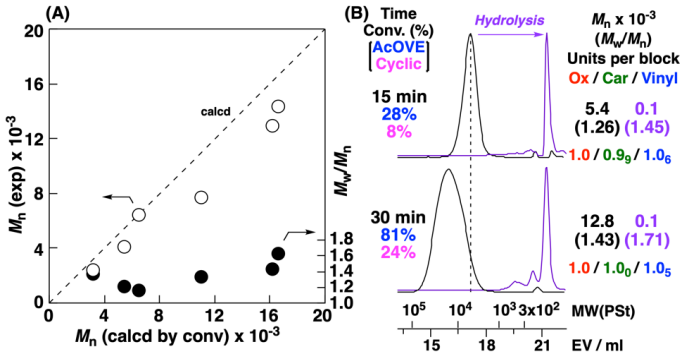

Figure 4. (A) M_n (open) and M_w/M_n (filled) values (by GPC) of the copolymers obtained and (B) MWD curves of poly(AcOVE-*co*-cyclic acetal)s (black) and acid hydrolysis products (purple). The data correspond to entry 7 in Table 2.

Synthesis of a Block Quaterpolymer with Periodic Sequences.

The livingness of the copolymerization was effective for the synthesis of block polymers consisting of blocks with different ABC-type periodic sequences, such as an ABC-*b*-ABD quaterpolymer, by a one-pot process (Figure S7). The alternating cationic copolymerization of the ECH- and pMeOBzA-derived cyclic

acetal with CEVE was conducted using four equivalents of the cyclic acetal with respect to CEVE (Figure S7 upper; CEVE/ECH/pMeOBzA = $1.0_3/1.0/1.0_1$ units per block). At the late stage of copolymerization, a fresh portion of AcOVE was added to the reaction mixture, which triggered the subsequent copolymerization of AcOVE and the residual cyclic acetal. The sequential monomer addition afforded a high-MW polymer via frequent crossover reactions between AcOVE and the cyclic acetal (Figure S7 lower; CEVE/ECH/pMeOBzA/AcOVE = $1.0_3/1.0/1.0_0/1.3_3$ units per block), resulting in a block polymer consisting of blocks with ECH–pMeOBzA–CEVE and ECH–pMeOBzA–AcOVE periodic sequences.

Thermal Properties of an ABC-Type Periodic Terpolymer.

The thermal properties of the ECH–pMeOBzA–CEVE terpolymers with different sequences were examined by DSC analysis (Figure 5). The glass transition temperature (T_g) of the ABC-type periodic terpolymer (T_g = –3 °C; Figure 5A; see Figure S8 for TGA) was lower than that of the statistical terpolymer (T_g = 9 °C; Figure 5C). The ABC-type periodic monomer sequences probably affected the lower T_g value than that of the statistical sequences. In copolymerization of two kinds of monomers, the differences of T_g between alternating and statistical sequences were reported in several past studies.[56–59] However, whether alternating copolymers exhibit higher or lower T_g than statistical copolymers depends on the combinations of monomers. Further investigation is needed to clarify the T_g difference in the present study. Interestingly, the T_g of the ABC_n-type sequence-controlled terpolymer containing CEVE homosequences (T_g = –2 °C; Figure 5B) was comparable to that of the ABC-type periodic-sequence terpolymer, which suggests that regular incorporation rather than statistical incorporation of the three monomers in the order of ECH, pMeOBzA, and CEVE into polymer chains also affected the thermal properties.

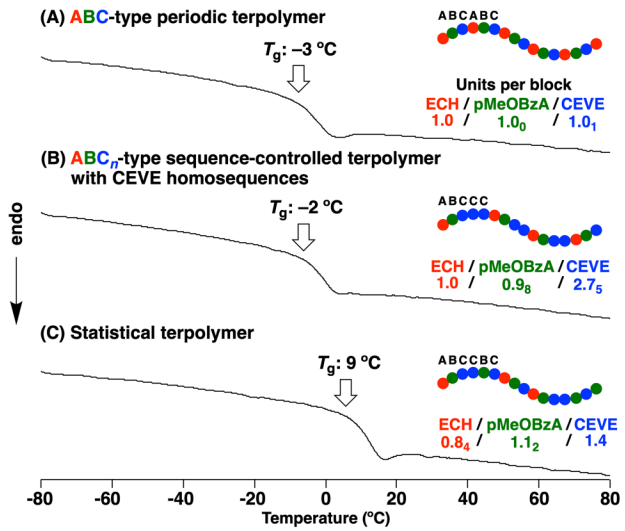

Figure 5. DSC thermogram of the ECH–pMeOBzA–CEVE terpolymers with (A) ABC-type periodic sequences (entry 1 in Table S5), (B) ABC_n-type sequences with CEVE homosequences (entry 4 in Table S4), and (C) statistical sequences (Figure S6) (the second heating scan; heating rate: 10 ºC/min).

Conclusion

A one-pot strategy consisting of the quantitative synthesis of a sequence-programmed monomer and the subsequent copolymerization reaction was developed using oxiranes, carbonyl compounds, and vinyl monomers as monomers. The selective cyclodimerization reaction of oxiranes and carbonyl compounds

quantitatively produced sequence-programmed cyclic acetals, even when both monomers were charged in equimolar amounts. The subsequent cationic copolymerization with vinyl monomers proceeded in an alternating manner to give terpolymers with an ABC-type periodic monomer sequence. Moreover, the livingness of the copolymerization enabled the simultaneous control of the MW, MWD, and chain end structures. The sequential addition of vinyl monomers yielded unique ABC-*b*-ABD-type quaterpolymers. The use of oxiranes with sufficient reactivity and low tendency to homocyclization, aldehydes with an electron-donating group, and VEs with low reactivity is of great importance for the selective cyclodimerization and alternating polymerization reactions. This strategy is expected to provide a concept for the simple conversion of various types of commercially available monomers, such as vinyl, cyclic, and carbonyl monomers, into ter- or quaterpolymers with a high degree of sequence and MW control. Further progress in both the efficient synthesis of sequence-programmed monomers and the occurrence of exclusive crossover reactions between different types of monomers will contribute to the construction of polymers with unique properties from various types of monomers and to the development of novel technologies with sequence-controlled polymers.

References and Notes

1. Lutz, J.-F.; Ouchi, M.; Liu, D. R.; Sawamoto, M. *Science* **2013**, *341*, No. 1238149.
2. Lutz, J.-F. *Macromol. Rapid Commun.* **2017**, *38*, No. 1700582.
3. Szymański, J. K.; Abul-Haija, Y. M.; Cronin, L. *Acc. Chem. Res.* **2018**, *51*, 649–658.
4. Meier, M. A. R.; Barner-Kowollik, C. *Adv. Mater.* **2019**, *31*, No. 1806027.
5. Merrifield, R. B. *J. Am. Chem. Soc.* **1963**, *85*, 2149–2154.
6. Trinh, T. T.; Laure, C.; Lutz, J.-F. *Macromol. Chem. Phys.* **2015**, *216*, 1498–1506.
7. Solleder, S. C.; Schneider, R. V.; Wetzel, K. S.; Boukis, A. C.; Meier, M. A. R. *Macromol. Rapid Commun.* **2017**, *38*, No. 1600711.
8. Hill, S. A.; Gerke, C.; Hartmann, L. *Chem. Asian J.* **2018**, *13*, 3611–3622.
9. Cho, I.; Hwang, K. M. *J. Polym. Sci., Part A: Polym. Chem.* **1993**, *31*, 1079–1081.
10. Cho, I. *Prog. Polym. Sci.* **2000**, *25*, 1043−1087.
11. Zhang, J.; Matta, M. E.; Hillmyer, M. *ACS Macro Lett.* **2012**, *1*, 1383–1387.
12. Yokota, K. *Prog. Polym. Sci.* **1999**, *24*, 517−563.
13. Satoh, K.; Ozawa, S.; Mizutani, M.; Nagai, K.; Kamigaito, M. *Nat. Commun.* **2010**, *1*, 6.
14. Miyajima, M.; Satoh, K.; Horibe, T.; Ishihara, K.; Kamigaito, M. *J. Am. Chem. Soc.* **2020**, *142*, 18955–18962.
15. Zhang, C.; Ling, J.; Wang, Q. *Macromolecules* **2011**, *44*, 8739–8743.
16. Schulz, M. D.; Wagener, K. B. *Macromol. Chem. Phys.* **2014**, *215*, 1936–1945.
17. Gutekunst, W. R.; Hawker, C. J. *J. Am. Chem. Soc.* **2015**, *137*, 8038–8041.
18. Yang, C.; Flynn, J. P.; Niu, J. *Angew. Chem. Int. Ed.* **2018**, *57*, 16194–16199.
19. Kreye, O.; Tóth, T.; Meier, M. A. R. *J. Am. Chem. Soc.* **2011**, *133*, 1790–1792.
20. Saegusa, T.; Kobayashi, S.; Kimura, Y. *Macromolecules* **1977**, *10*, 68–72.
21. Hsieh, H. L. *J. Macromol. Sci., Part A: Chem.* **1973**, *7*, 1525−1535.
22. Kanazawa, A.; Aoshima, S. *ACS Macro Lett.* **2015**, *4*, 783–787.
23. Mimura, M.; Kanazawa, A.; Aoshima, S. *Macromolecules* **2019**, *52*, 7572–7583.
24. Yokozawa, T.; Suzuki, T. *Macromolecules* **1996**, *29*, 22–25.
25. Yokozawa, T.; Tagami, M.; Takehana, T.; Suzuki, T. *Tetrahedron* **1997**, *53*, 15603–15616.

26. Krompiec, S.; Penkala, M.; Szczubiałka, K.; Kowalska, E. *Coord. Chem. Rev.* **2012**, *256*, 2057–2095.
27. Bogert, M. T.; Roblin, R. O. *J. Am. Chem. Soc.* **1933**, *55*, 3741–3745.
28. Saha, S.; Mandal, S. K.; Roy, S. C. *Tetrahedron Lett.* **2008**, *49*, 5928–5930.
29. Nagata, T.; Takai, T.; Yamada, T.; Imagawa, K.; Mukaiyama, T. *Bull. Chem. Soc. Jpn.* **1994**, *67*, 2614–2616.
30. Okada, M.; Yamashita, Y.; Ishii, Y. *Makromol. Chem.* **1966**, *94*, 181–193.
31. Okada, M.; Yamashita, Y. *Makromol. Chem.* **1969**, *126*, 266−275.
32. Shirouchi, T.; Kanazawa, A.; Aoshima, S. *Macromolecules* **2016**, *49*, 7184–7195.
33. Maruyama, K.; Kanazawa, A.; Aoshima, S. *Polym. Chem.* **2019**, *10*, 5304–5314.
34. Aoshima, S.; Nakamura, T.; Uesugi, N.; Sawamoto, M.; Higashimura, T. *Macromolecules* **1985**, *18*, 2097–2101.
35. Park, Y. J.; Yang, J. W. *Green Chem.* **2019**, *21*, 2615–2620.
36. Aoshima, S.; Kanaoka, S. *Chem. Rev.* **2009**, *109*, 5245–5287.
37. Ishido, Y.; Aburaki, R.; Kanaoka, S.; Aoshima, S. *J. Polym. Sci., Part A: Polym. Chem.* **2010**, *48*, 1838–1843.
38. Ishido, Y.; Aburaki, R.; Kanaoka, S.; Aoshima, S. *Macromolecules* **2010**, *43*, 3141–3144.
39. The slightly different values between the conversion of carbonyl compounds and cyclization efficiency were due to the experimental errors in using equimolar amounts of carbonyl compounds and oxiranes.
40. Kanazawa, A.; Kanaoka, S.; Aoshima, S. *Macromolecules* **2009** *42*, 3965–3972.
41. Kimura, R.; Yamada, M.; Kanazawa, A.; Kanaoka, S.; Aoshima, S. *Polym. Prepr., Jpn.* **2013**, *62*, 2412.
42. Each diastereomer of the cyclic acetal was equally consumed as indicated by ^{1}H NMR analysis of the quenched reaction mixtures.
43. To characterize the end groups of the obtained terpolymers, ESI-MS and MALDI-TOF-MS analysis were conducted under various conditions. However, the analysis of the samples was difficult because the signal intensity was very small.
44. Goethals, E.; Duprez, F. *Prog. Polym. Sci.* **2007**, *32*, 220–246.
45. Deslongchamps, P.; Dory, Y. L.; Li, S. *Tetrahedron* **2000**, *56*, 3533–3537.
46. Okada, M. *Makromol. Chem.* **1964**, *80*, 196–207.
47. See chapter 3 in this thesis.
48. Kelen, T.; Tüdõs, F. *Kinet. Catal. Lett.* **1974**, *1*, 487−492.
49. Kennedy, J. P.; Kelen, T.; Tüdõs, F. *J. Polym. Sci., Polym. Chem. Ed.* **1975**, *13*, 2277−2289.
50. Van Meirvenne, D.; Haucourt, N.; Goethals, E. J. *Polym. Bull.* **1990**, *23*, 185–190.
51. Haucourt, N. H.; Goethals, E. J.; Schappacher, M.; Deffieux, A. *Makromol. Chem. Rapid Commun.* **1992**, *13*, 329–336.
52. Satoh, K.; Kamigaito, M.; Sawamoto, M. *Macromolecules* **2000**, *33*, 748–753.
53. Shimomoto, H.; Yoshida, H.; Kanaoka, S.; Aoshima, S. *J. Polym. Sci., Part A: Polym. Chem.* **2012**, *50*, 3703–3709.
54. Yokoyama, N.; Kanazawa, A.; Kanaoka, S.; Aoshima, S. *Macromolecules* **2018**, *51*, 884–894.
55. Masuda, T.; Higashimura, T.; Okamura, S. *Polym. J.* **1970**, *1*, 19–26.
56. Hirooka, M.; Kato, T. *J. Polym. Sci. Polym. Lett. Ed.* **1974**, *12*, 31–37.
57. Mori, Y.; Sumi, H.; Hirabayashi, T.; Inai, Y.; Yokota, K. *Macromolecules* **1994**, *27*, 1051–1056.
58. Denizli, B. K.; Lutz, J.-F.; Okrasa, L.; Pakula, T.; Guner, A.; Matyjaszewski, K. *J. Polym. Sci., Part A: Polym. Chem.* **2005**, *43*, 3440–3446.
59. Liu, G.; Meng, Z.; Wang, W.; Zhou, Y.; Zhang, L. *J. Phys. Chem. B* **2008**, *112*, 93–99.

Supporting Information

Table S1. Selective Cyclodimerization of Various Oxiranes and pMeOBzA[a]

entry	oxirane (M)	pMeOBzA (M)	conv (%)[b]		CE(%)[c]
			oxirane	aldehyde	
1	EGE, 0.50	1.0	100	46	>99
2	SO, 0.50	1.0	100	46	>99
3	SO, 0.50	0.50	100	64	73
4	IBO, 0.25	1.0	100	21	98

[a] $[SnCl_4]_0$ = 20 mM in dichloromethane at 0 (except for entry 2) or –78 (entry 2) ºC for 24 h. [b] Determined by ^{1}H NMR analysis. [c] Cyclization efficiency: the ratio of the generated cyclic acetal to the feed of oxirane ([cyclic]/ $[oxirane]_0$) determined by ^{1}H NMR analysis.

Table S2. Cyclodimerization of Styrene Oxide and Benzaldehyde Using Various Lewis Acids[a]

entry	catalyst	time	conv (%)[b]		CE(%)[c]
			SO	BzA	
1	$FeCl_3$	48 h	54	13	25
2	$TiCl_4$	72 h	42	14	28
3	$GaCl_3$	72 h	86	33	60
4	$SnCl_4$	24 h	100	40	82

[a] $[SO]_0$ = 0.50 M, $[BzA]_0$ = 1.0 M, $[catalyst]_0$ = 20 mM in dichloromethane at 0 (entry 1) or –78 ºC (except for entry 1). [b] Determined by ^{1}H NMR analysis. [c] Cyclization efficiency: the ratio of the generated cyclic acetal to the feed of oxirane ([cyclic]/ $[oxirane]_0$) determined by ^{1}H NMR analysis.

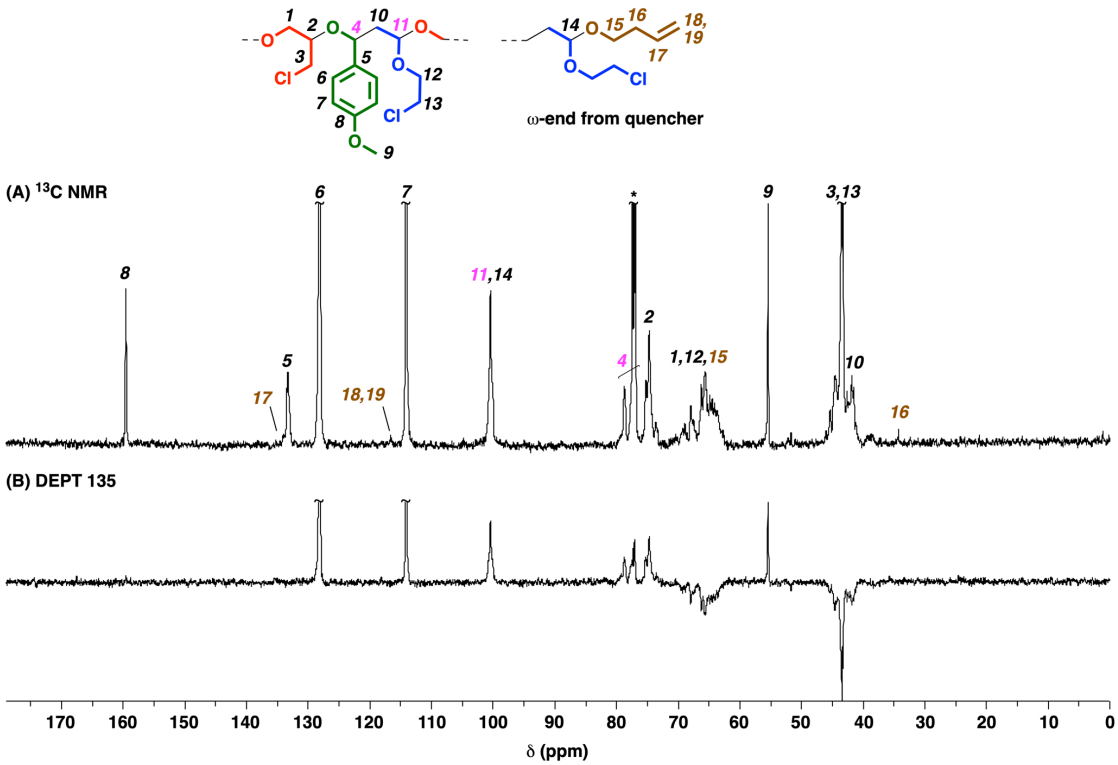

Figure S1. ^{13}C and DEPT 135 NMR spectra of the ECH–pMeOBzA–CEVE terpolymer (entry 1 in Table 2) (in $CDCl_3$ at 30 ºC). * $CDCl_3$.

Table S3. Homopolymerization of Cyclic Acetal Consisting of ECH and pMeOBzA[a]

			conv (%)[b]			
entry	cyclic (M)	time	cyclic	$M_n \times 10^{-3}$ [c]	M_w/M_n[c]	
1	1.0	24 h	0	–	–	

[a] Reaction conditions for the synthesis of the cyclic acetal: $[ECH]_0$ = 1.0 M, $[pMeOBzA]_0$ = 1.0 M, $[SnCl_4]_0$ = 5.0 mM, in dichloromethane at 0 °C for 24 h. Polymerization conditions: [cyclic acetal]$_0$ = 1.0 M, [ethyl acetate]$_{add}$ = 0.25 M, $[SnCl_4]_{add}$ = 10 mM in dichloromethane at –96 °C. [b] Determined by ^{1}H NMR analysis. [c] Determined by GPC (polystyrene standards).

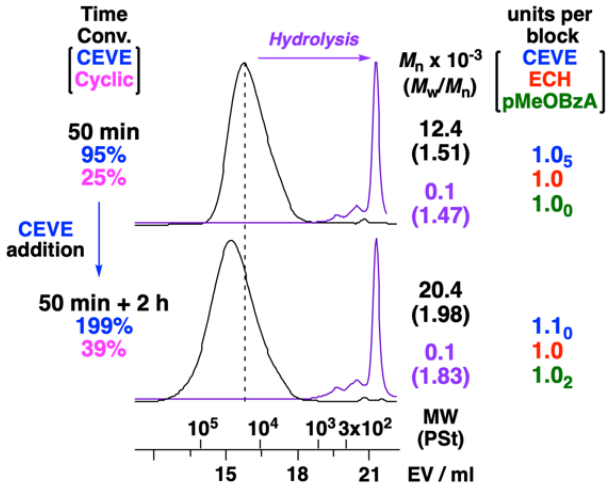

Figure S2. MWD curves of the copolymerization of CEVE and a cyclic acetal consisting of ECH and pMeOBzA (black) and the acid hydrolysis products (purple) in the monomer-addition experiment. Reaction conditions for the synthesis of the cyclic acetal: $[ECH]_0$ = 1.0 M, $[pMeOBzA]_0$ = 1.0 M, $[SnCl_4]_0$ = 5.0 mM in dichloromethane at 0 °C for 24 h. Polymerization conditions: [cyclic acetal (ECH-pMeOBzA)]$_0$ = 1.0 M, $[CEVE]_{add}$ = 0.25 + 0.25 M, [ethyl acetate]$_{add}$ = 0.25 M, $[SnCl_4]_{add}$ = 10 mM in dichloromethane at –96 °C.

Table S4. The Data for Determination of Monomer Reactivity Ratios[a]

				conv (%)[b]				
entry	CEVE (M)	cyclic (M)	time	CEVE	cyclic	$M_n \times 10^{-3}$ [c]	M_w/M_n[c]	CEVE in copolymer[b]
1	0.25	1.0	5 min	19	4	3.7	1.22	0.50
2	0.50	0.75	60 s	6	4	5.8	1.37	0.55
3	0.75	0.50	10 s	9	5	4.2	1.16	0.60
4	1.0	0.25	10 s	11	10	4.1	1.33	0.73

[a] Reaction conditions for the synthesis of the cyclic acetal: $[ECH]_0$ = 0.25—1.0 M, $[pMeOBzA]_0$ = 0.25—1.0 M, $[SnCl_4]_0$ = 5.0 mM, in dichloromethane at 0 °C for 24 h. Polymerization conditions: [cyclic acetal]$_0$ + $[CEVE]_{add}$ = 1.25 M, [ethyl acetate]$_{add}$ = 0.25 M, $[SnCl_4]_{add}$ = 10 mM in dichloromethane at –96 °C. [b] Determined by ^{1}H NMR analysis. [c] Determined by GPC (polystyrene standards).

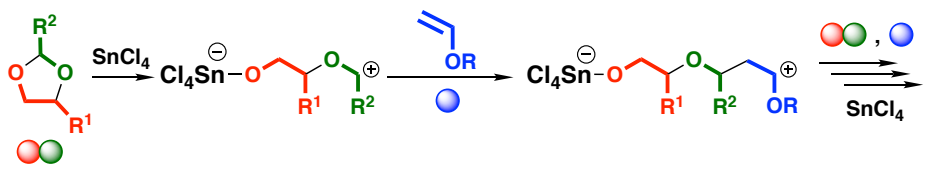

Scheme S1. Possible mechanism of the initiation reaction of the cationic copolymerization of the cyclic acetal and vinyl ether

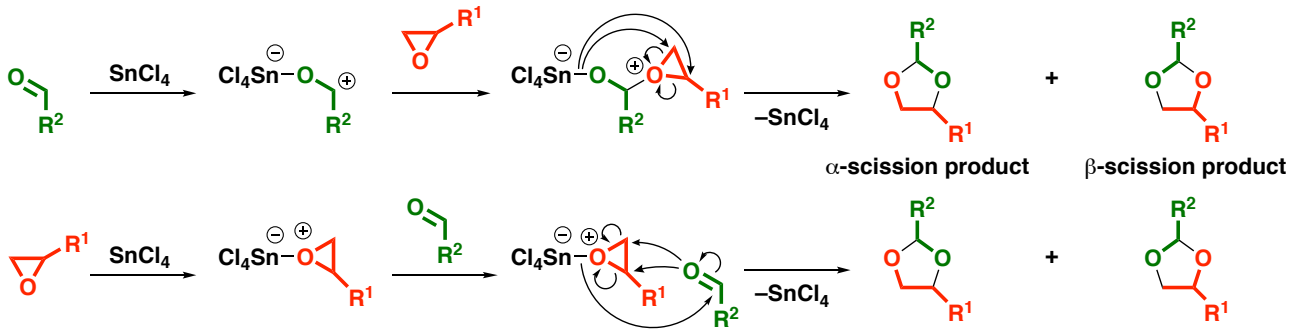

Scheme S2. Possible mechanisms of generation of cyclic acetals via selective cyclodimerization reaction

Note

The oxygen atoms at the 1-position are derived from a carbonyl compound or an oxirane when the α- or β-scission occurs, respectively. The oxygen atom at the 3-position is also derived from either compound. However, the origins of the two oxygen atoms are not distinguished in this study because both the α- and β-scission products have the same structures irrespective of the origin.

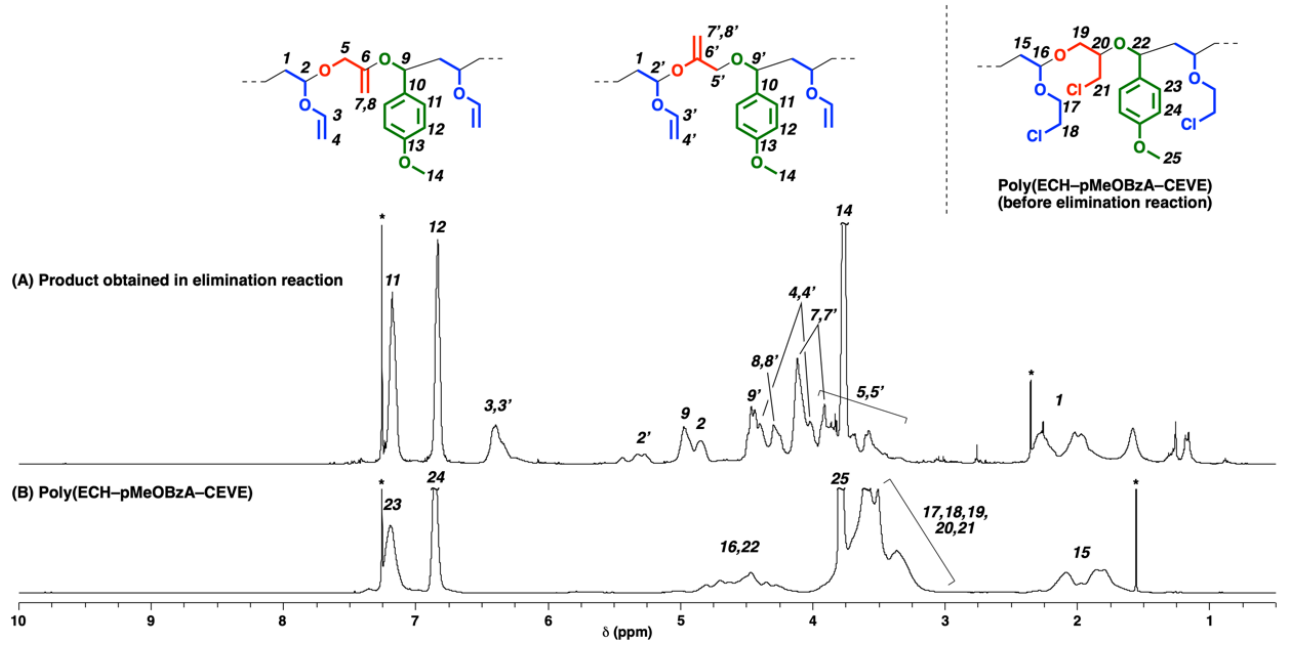

Figure S3. ^{1}H NMR spectra of (A) the product obtained by elimination reaction of the ECH–pMeOBzA–CEVE terpolymer and (B) the original terpolymer (entry 2 in Table 2) (in $CDCl_3$ at 30 ºC). * $CHCl_3$, toluene.

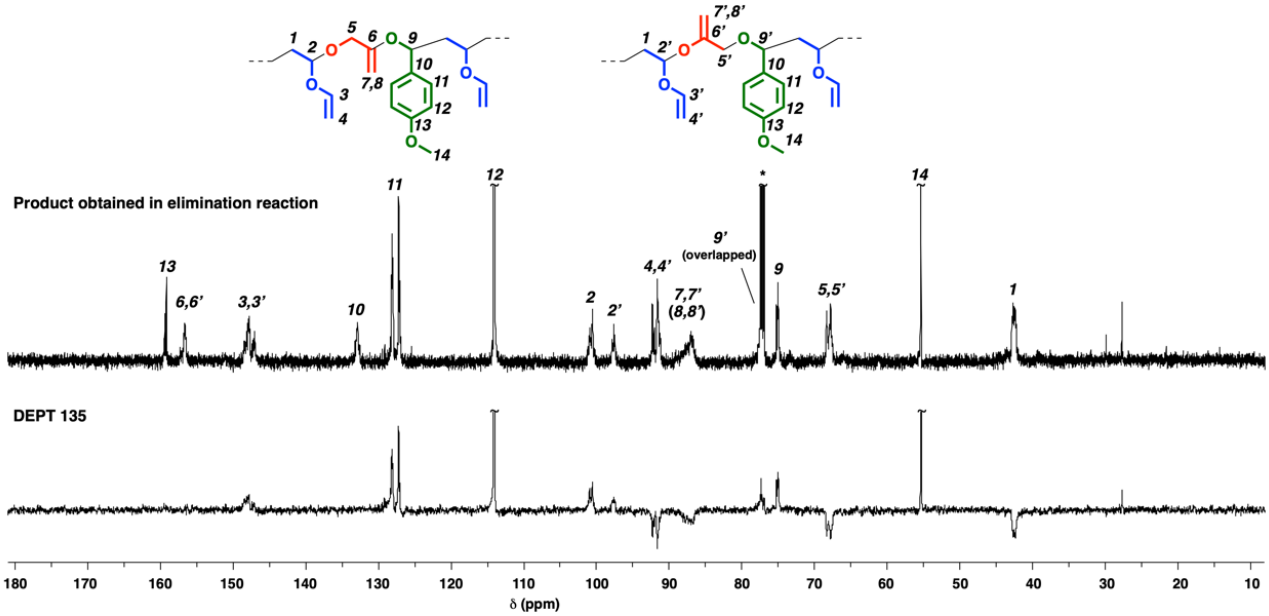

Figure S4. ^{13}C and DEPT 135 NMR spectra of the product obtained by elimination reaction of the ECH–pMeOBzA–CEVE terpolymer (in $CDCl_3$ at 30 ºC). * $CDCl_3$.

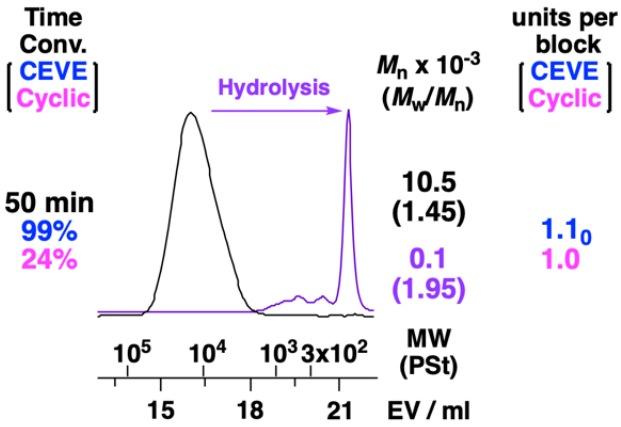

Figure S5. MWD curves of the product obtained by the cationic copolymerization of CEVE and 4-chloromethyl-2-(4-methoxyphenyl)-1,3-dioxolane (the cyclic acetal consisting of ECH and pMeOBzA; isolated before use) (black) and its acid hydrolysis product (purple). Polymerization conditions: $[CEVE]_0$ = 0.25 M, $[\text{cyclic acetal}]_0$ = 1.0 M, [ethyl acetate] = 0.25 M, $[SnCl_4]_0$ = 15 mM in dichloromethane at –96 ºC. Reaction conditions for synthesis of the cyclic acetal: $[ECH]_0$ = 1.0 M, $[pMeOBzA]_0$ = 1.0 M, $[SnCl_4]_0$ = 5.0 mM in dichloromethane at 0 ºC for 24 h.

Table S5. Direct Cationic Terpolymerization of ECH, pMeOBzA, and CEVE[a]

			conv (%)[b]				
entry	time	temp. (ºC)	ECH	pMeOBzA	CEVE	$M_n \times 10^{-3}$[c]	M_w/M_n[c]
1	12 h	0	100	93	100	2.7	1.26
2	50 min	–96	0	0	0	—	—
3	24 h	–96	9	4	0	—	—

[a] $[ECH]_0$ = 1.0 M, $[pMeOBzA]_0$ = 1.0 M, $[CEVE]_0$ = 0.25 M, [ethyl acetate] = 0.25 M, $[SnCl_4]_0$ = 15 mM in dichloromethane. [b] Determined by ^1H NMR analysis. [c] Determined by GPC (polystyrene standards).

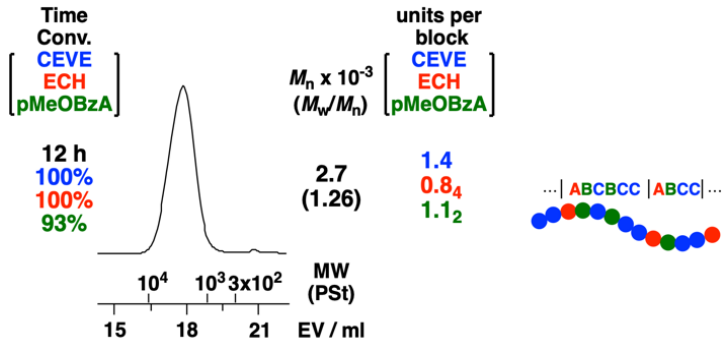

Figure S6. MWD curve of the product obtained by the direct cationic terpolymerization of ECH, pMeOBzA, and CEVE. See entry 1 in Table S5 for the polymerization conditions.

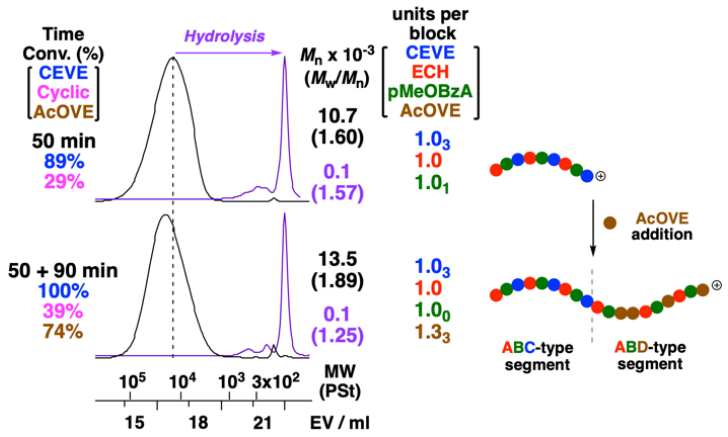

Figure S7. MWD curves of the (ECH–pMeOBzA–CEVE)-*b*-(ECH–pMeOBzA–AcOVE) quaterpolymer. Reaction conditions for the synthesis of the cyclic acetal: $[ECH]_0$ = 1.0 M, $[pMeOBzA]_0$ = 1.0 M, $[SnCl_4]_0$ = 5.0 mM in dichloromethane at 0 °C for 24 h. Polymerization conditions: $[cyclic\ acetal]_0$ = 1.0 M, $[CEVE]_{add}$ = 0.25 M, $[AcOVE]_{add}$ = 0.25 M, $[ethyl\ acetate]_{add}$ = 0.25 M, $[SnCl_4]_{add}$ = 10 mM in dichloromethane at –96 °C.

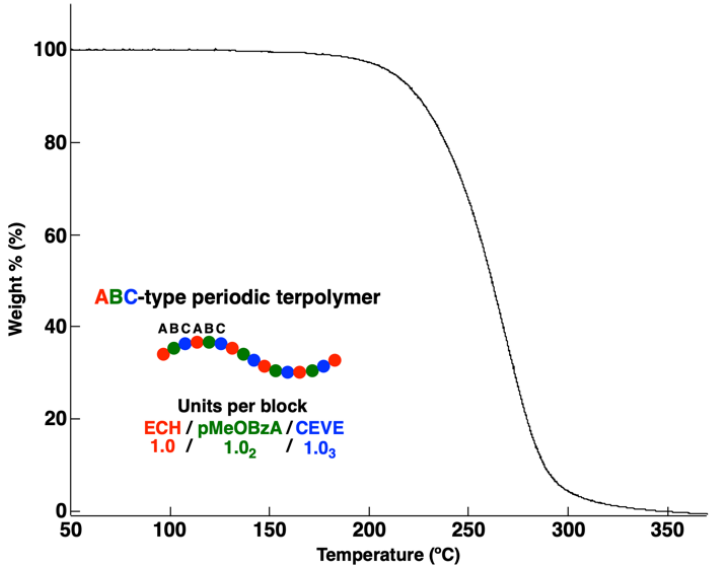

Figure S8. TGA thermogram of the ECH–pMeOBzA–CEVE terpolymer with ABC-type periodic sequences (the sample obtained under the same conditions as those for entries 1 and 2 in Table 2; M_n (GPC) = 8.5 × 10^3, ECH/pMeOBzA/CEVE = $1.0/1.0_2/1.0_3$ units per block) (N_2 atmosphere; heating rate: 10 °C/min).

Chapter 5.

Synthesis of Alternating Copolymers via Selective Generation of Alcohol-Derived 2-Alkoxy Cyclic Ethers and Subsequent Cationic Copolymerization with a Vinyl Ether in One-Pot Process

Introduction

Sequence control of synthetic polymers has attracted great interest, inspired by the possibility of sophisticated functions based on perfectly controlled structures of biopolymers.[1–4] For example, alternating sequences consisting of two types of monomers can uniformly introduce their functionalities throughout the polymer chains, which can lead to unique properties compared to mixtures of homopolymers or block polymers. A well-known method for the synthesis of alternating sequences in chain-growth polymerization is the radical copolymerization of monomers with large difference in electronic densities, such as styrene and maleic anhydride.[5,6] The copolymerization of a bulky monomer with higher reactivity and a less reactive monomer is another route for the preferential occurrence of crossover reactions over homopropagations due to the steric repulsions.[7–11] The homopolymerization of elaborately designed monomers consisting of two or more monomer units also affords sequence-controlled polymers.[9–18] These methods produce specific sequences, although the special selections of monomers or multistep synthesis for the sequence-incorporated monomers are required. Developing a widely applicable approach from a simple compound will provide opportunities for designing sequence-controlled copolymers with various structures.

As a promising resource for polymer synthesis, the author focuses on alcohol, which is abundant in both nature and industrial fields. However, in cationic or anionic polymerization, the hydroxy group of alcohols generally results in chain transfer reaction and/or irreversible termination by the reaction with the propagating species.[19,20] Therefore, the transformation of hydroxy groups into other structures is a practical approach for the participation of alcohols in the polymerization reaction. In synthetic chemistry, acetal structures are widely used for the protection of hydroxy groups. Among the various synthetic approaches for acetal compounds, the synthesis of 2-alkoxy cyclic ether structures via the acid-catalyzed addition reaction of alcohol to 2,3-dihydrofuran (DHF) or 3,4-dihydro-2*H*-pyran (DHP) [87–25] is a promising strategy to obtain an alcohol-derived comonomer that can be used in copolymerization with vinyl monomers. In cationic polymerization, the resulting 2-alkoxy cyclic ether possibly generates an alkoxy group-adjacent carbocation, which is structurally similar to the carbocation derived from a vinyl ether (VE), by the ring-opening reaction of the oxonium ion (Scheme 1). Indeed, in Part I, the author reported the controlled cationic copolymerization of various cyclic acetals and vinyl monomers.[26] Moreover, in Chapter 4, the author devised a one-pot synthesis of ABC-type sequence regulated terpolymers based on a successive process consisting of the selective generation of sequence-incorporated cyclic acetals and subsequent alternating copolymerization.[27] The cationic ring-opening copolymerization of substituted cyclic ethers such as 2-methyltetrahydrofuran (2-methyl-THF) or 3-methyl-THF with 1,3-dioxolane was reported several decades ago, whereas the homopolymerization of the substituted cyclic ethers is negligible because the conformations of the substituted cyclic ethers thermodynamically disfavor the polymerization reaction.[28–30] Therefore, the elaborate design of reaction

conditions affording both selective synthesis of 2-alkoxy cyclic ethers and subsequent alternating copolymerization with a vinyl monomer potentially allows for one-pot synthesis of alternating copolymers using alcohol as a starting material.

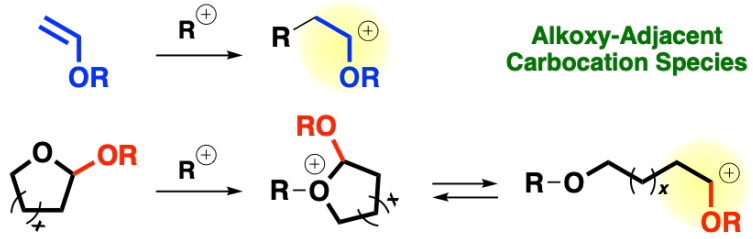

Scheme 1. Propagating Species Derived from 2-Alkoxy Cyclic Ether.

In this chapter, the author aims to develop the one-pot synthesis of sequence-controlled copolymers using various alcohols as monomer precursors. The addition reaction of various alcohols, such as methyl, primary, and secondary alcohols, including naturally-occurring alcohols, to DHF or DHP, which are inexpensive and commercially available cyclic enol ethers, is used to selectively generate the corresponding 2-alkoxy cyclic ethers under suitable reaction conditions. These 2-alkoxy cyclic ethers subsequently copolymerized with 2-chloethyl VE (CEVE) without any purification, yielding alternating copolymers with a well-defined molecular weight (MW), molecular weight distribution (MWD), and chain end fidelity.

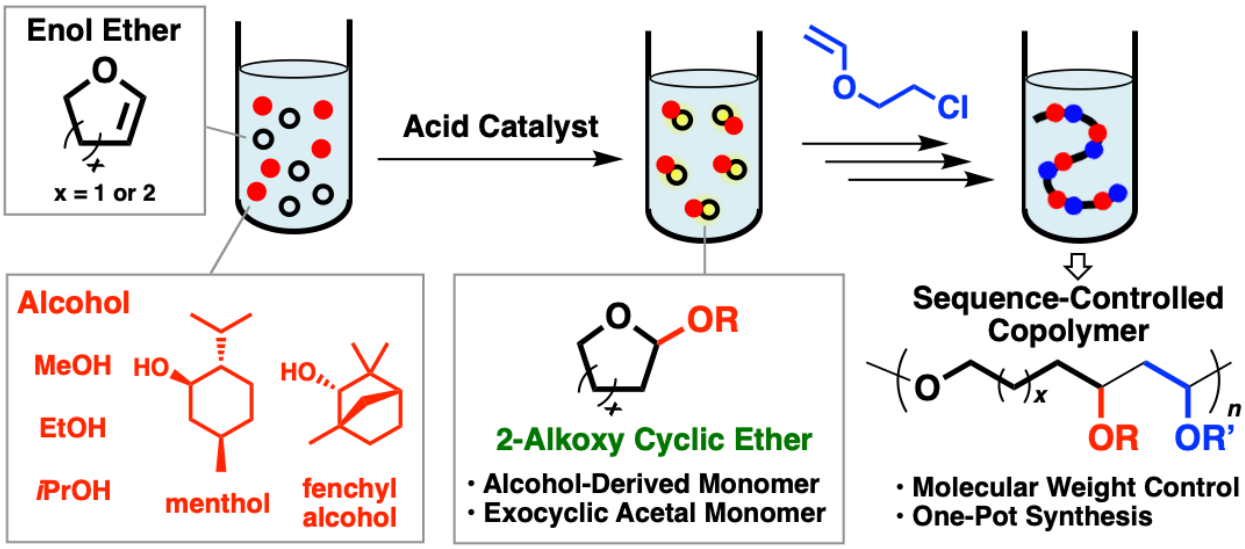

Scheme 2. The Synthesis of Alcohol-Derived Sequence-Controlled Copolymers in One-Pot Approach: *In-situ* Synthesis of 2-Alkoxy Cyclic Ethers and Subsequent Living Cationic Copolymerization with a Vinyl Ether.

Experimental Section

Materials

2,3-Dihydrofuran (DHF; TCI; >98.0%) and 3,4-dihydro-2*H*-pyran (DHP; TCI; >97.0%) were distilled twice over calcium hydride. Methanol (MeOH; Wako; super dehydrated), ethanol (EtOH; Wako; super dehydrated), 2-propanol (*i*PrOH; Aldrich; 99.5%), (–)-menthol (TCI; >99.0%), and (+)-fenchyl alcohol

(Aldrich; 96%) were used without further purification. Stock solutions of *p*-toluenesulfonic anhydride in dichloromethane and $ZrCl_4$ in ethyl acetate were prepared from *p*-toluenesulfonic anhydride (PTSA; Aldrich; 97%) and $ZrCl_4$ (Aldrich; 99.99%), respectively. Other materials were prepared as described in Part I.

Synthesis of 2-Alkoxy Cyclic Ethers via Addition of Alcohol to Enol Ethers

A typical reaction for the addition of alcohol to enol ether is described as follows. A glass tube equipped with a three-way stopcock was dried using a heat gun (Ishizaki, PJ-206A; the air temperature of approximately 450 °C) under a nitrogen atmosphere. Then, dichloromethane, hexane (as an internal standard for calculation of monomer conversion), alcohol, and enol ether were added into the tube using dry syringes. After cooling the solution at 0 ºC for 10 min, a solution of $ZrCl_4$ (containing a small amount of ethyl acetate) in dichloromethane kept at 0 °C was added to the tube to initiate the reaction. After 1 h, an excess amount of methanol containing a small amount of an aqueous ammonia solution was added to the solution to terminate the reaction. The monomer conversion and the amount of 2-alkoxy cyclic ether generated were determined by ^{1}H NMR analysis of the quenched mixture. The quenched mixture was diluted with dichloromethane and washed with water. The volatiles were then removed under reduced pressure to yield the 2-alkoxy cyclic ether. For the case of the one-pot process, the reaction mixture was directly subjected to subsequent copolymerization with a VE without quenching by methanol, as described below.

2-Isopropoxytetrahydrofuran (2-iPrO-THF)

^{1}H NMR ($CDCl_3$; 500MHz): δ 7.41 (1H, dd, J = 5.0, 1.5 Hz), 3.82–3.92 (3H, m), 1.83–2.03 (4H, m), 1.18 (3H, d, J = 6.0 Hz), 1.14 (3H, d, J = 6.0 Hz).^{13}C NMR ($CDCl_3$; 125MHz): δ 102.0, 68.6, 66.7, 32.8, 23.8, 23.7, 21.9.

2-Isopropoxytetrahydropyran

Conformational isomers are observed in NMR analysis (90/10). ^{1}H NMR ($CDCl_3$; 500MHz): Major conformer: δ 4.67 (1H, dd, J = 7.0, 2.5 Hz), 3.95 (1H, sept, J = 6.0 Hz), 3.47–3.91 (2H, m), 1.81–1.88 (1H, m), 1.68–1.74 (1H, m), 1.50–1.60 (2H, m), 1.23 (3H, d, J = 6.0 Hz), 1.14 (3H, d, J = 6.0 Hz), Minor conformer: 4.96 (1H, dd, J = 7.0, 3.0 Hz), 4.03 (1H, sept, J = 6.0 Hz), 3.47–3.91 (2H, m), 1.81–1.88 (1H, m), 1.68–1.74 (1H, m), 1.50–1.60 (2H, m), 1.23 (3H, d, J = 6.0 Hz), 1.14 (3H, d, J = 6.0 Hz). ^{13}C NMR ($CDCl_3$; 125MHz): Major conformer: δ 96.9, 68.4, 62.8, 31.4, 25.7, 23.7, 21.6, 20.1, Minor conformer: δ 94.8, 64.6, 63.1, 30.8, 25.4, 23.7, 21.6, 19.9.

2-Methoxytetrahydrofuran

Conformational isomers are observed in NMR analysis (99/1). ^{1}H NMR ($CDCl_3$; 500MHz): Major conformer: δ 5.01 (1H, dd, J = 5.0, 1.5 Hz), 3.82–3.92 (2H, m), 3.33 (3H, s), 1.80–2.03 (4H, m), Minor conformer: 5.43 (1H, dd, J = 5.0, 1.5 Hz), 3.89 (2H, m) 3.33 (3H, s), 1.80–2.03 (4H, m). ^{13}C NMR ($CDCl_3$; 125MHz): Major conformer: δ 105.1, 67.0, 54.7, 32.4, 23.5, Minor conformer: δ 105.9, 67.0, 54.7, 32.4, 23.5.

2-Ethoxytetrahydrofuran

Conformational isomers are observed in NMR analysis (94/6). ^{1}H NMR ($CDCl_3$; 500MHz): Major conformer: δ 5.13 (1H, dd, J = 5.5, 1.5 Hz), 3.83–3.93 (2H, m), 3.41–3.75 (2H, m), 1.79–2.03 (4H, m), 1.19 (3H, t), Minor conformer: δ 5.43 (1H, dd, J = 5.5, 1.5 Hz), 3.83–3.93 (2H, m), 3.41–3.75 (2H, m), 1.79–2.03 (4H, m), 1.19 (3H, t). ^{13}C NMR ($CDCl_3$; 125MHz): Major conformer: δ 103.8, 66.9, 62.7, 32.5, 23.7, 15.4, Minor conformer: δ 100.2, 67.1, 62.7, 32.4, 23.5, 15.4.

2-((1R,2S,5R)-Menthyl)tetrahydrofuran

A mixture of diastereomer (66/34). ^{1}H NMR ($CDCl_3$; 500MHz): Major diastereomer: δ 5.31 (1H, dd, *J* = 6.0, 3.0 Hz), 3.81–3.96 (2H, m), 3.45 (1H, dd, *J* = 10.5, 6.0 Hz), 1.78–2.19 (6H, m), 1.58–1.66 (2H, m), 1.32–1.44 (1H, m), 1.15–1.20 (1H, m), 0.77–1.01 (12H, m). Minor diastereomer: δ 5.20 (1H, dd, *J* = 6.0, 3.0 Hz), 3.81–3.96 (2H, m), 3.29 (1H, dd, *J* = 10.5, 6.0 Hz), 1.78–2.19 (6H, m), 1.58–1.66 (2H, m), 1.32–1.44 (1H, m), 1.15–1.20 (1H, m), 0.77–1.01 (12H, m). ^{13}C NMR ($CDCl_3$; 125MHz): Major diastereomer: δ 99.5, 73.7, 66.7, 48.2, 40.2, 34.8, 32.7, 31.6, 25.5, 23.8, 23.3, 22.5, 21.2, 15.7, Minor diastereomer: δ 105.5, 78.8, 66.7, 48.9, 43.6, 34.6, 32.7, 31.8, 25.7, 23.6, 23.5, 22.4, 21.3, 16.4.

2-((1R,2R,4S)-Fenchyl)tetrahydrofuran

A mixture of diastereomer (51/49). ^{1}H NMR ($CDCl_3$; 500MHz): Major diastereomer: δ 5.05 (1H, m), 3.79–3.94 (2H, m), 3.29 (1H, s), 1.78–2.03 (4H, m), 1.61–1.69 (3H, m), 1.43–1.46 (1H, m), 1.33–1.39 (1H, m), 1.00–1.11 (7H, m), 0.90–0.95 (1H, m), 0.85 (3H, s), 0.80 (1H, s), Minor diastereomer: δ 5.08 (1H, m), 3.79–3.94 (2H, m), 3.08 (1H, s), 1.78–2.03 (4H, m), 1.61–1.69 (3H, m), 1.43–1.46 (1H, m), 1.33–1.39 (1H, m), 1.00–1.11 (7H, m), 0.90–0.95 (1H, m), 0.85 (3H, s), 0.80 (1H, s). ^{13}C NMR ($CDCl_3$; 125MHz): Major diastereomer: δ 103.4, 87.8, 66.5, 49.0, 48.3, 41.5, 39.2, 32.3, 31.9, 26.3, 26.2, 23.6, 21.4, 19.6, Minor diastereomer: δ 105.6, 90.6, 67.1, 49.2, 48.7, 41.5, 39.2, 32.6, 30.3, 26.2, 26.1, 24.0, 21.4, 19.9.

Polymerization Procedure

The following is a typical procedure for the copolymerization of a 2-alkoxy cyclic ether and a VE by a one-pot process. A glass tube containing the reaction mixture of the 2-alkoxy cyclic ether, which was obtained as described above, was cooled to –78 ºC. The copolymerization was started by sequential addition of CEVE and a solution of $SnCl_4$ in dichloromethane kept at 0 °C to the tube. After a predetermined interval, the polymerization was terminated with methanol or 3-buten-1-ol containing a small amount of aqueous ammonia or triethylamine, respectively. The quenched reaction mixture was diluted with dichloromethane and then washed with water. The volatiles were evaporated under reduced pressure at 50 ºC. When the monomers were insoluble in water, the residual cyclic monomer was removed by reprecipitation with methanol. The monomer conversion was determined by ^{1}H NMR spectroscopy of the quenched reaction mixture using hexane or ethyl acetate as an internal standard.

Alcoholysis

Alcoholysis of the obtained polymers was conducted with 0.50 M HCl(aq) in dichloromethane/*n*-butanol or methanol (1/1 v/v) (sample: 0.5 wt%) at 50 ºC for 3 h. The reaction mixture was diluted with dichloromethane and washed with an aqueous sodium hydroxide solution and then water. The volatiles were removed under reduced pressure to obtain the products.

Characterization

The MWs, MWDs, ^{1}H and ^{13}C NMR spectra, and electrospray ionization mass spectra (ESI-MS) were measured in a similar manner to that described in the preceding chapters.

Results and Discussion

Selective and Quantitative Synthesis of Alcohol-Derived 2-Alkoxy Cyclic Ethers

For the selective generation of 2-alkoxy cyclic ethers from alcohols and cyclic enol ethers, the author examined the effects of various reaction conditions such as catalysts, alcohols, cyclic enol ethers (DHF or DHP), and solvents, on the reaction selectivity (Table 1). In the subsequent copolymerization with a VE, residual alcohol results in chain transfer reaction and/or irreversible termination. In addition, residual cyclic enol ethers potentially react as a monomer with the propagating species to be incorporated into the main chain. Therefore, the complete consumption of both alcohol and cyclic enol ether is highly required for the successive process of 2-alkoxy cyclic ether generation and subsequent copolymerization.

Among various Brønsted and Lewis acids examined, $ZrCl_4$, one of the efficient catalysts for the synthesis of tetrahydropyranyl ether by the addition reaction of alcohol to DHP,[24] provided the best performance in terms of the reaction rate and selectivity (entries 1–3 in Table 1). Other catalysts, such as *p*-toluenesulfonic acid, a conventional Brønsted acid, and $SnCl_4$, which is applied for living cationic polymerization of various vinyl monomers,[19] also induced selective addition reactions, while these acids required a longer time for the reactions (entries 1 and 2 in Table 1). The ^{1}H NMR spectrum of the reaction mixture recorded after quenched with methanol (Figure 1) exhibited peaks attributed to a 2-alkoxy cyclic ether, while peaks attributed to 2-propanol (*i*PrOH), DHF, and other undesired products were not observed. Moreover, the amount of the 2-alkoxy cyclic ether, which was calculated by the integral ratio of the cyclic ether and hexane as an internal standard, corresponded to the original feeds of DHF and 2-propanol (~0.50 M), indicating quantitative generation of the cyclic monomer.

The addition reaction of alcohols with DHP instead of DHF also quantitatively generated 2-alkoxy cyclic ethers (entries 5 and 6 in Table 1). For the case of DHP, the reaction in dichloromethane led to a faster reaction than that in toluene. This difference most likely stems from the lower reactivity of DHP than DHF.

Table 1. Synthesis of 2-Substituted Cyclic Ethers via Addition of Alcohol to Cyclic Enol Ethers[a]

entry	alcohol	enol ether	catalyst	solvent	time	conv. (%)[b]		RE[c]
						alcohol	enol ether	
1	*i*PrOH	DHF	PTSA	tol	24 h	100	100	>99
2			$SnCl_4$	tol	24 h	100	100	>99
3			$ZrCl_4$	tol	1 h	100	100	>99
4			$ZrCl_4$	DCM	1 h	100	100	>99
5	*i*PrOH	DHP	$ZrCl_4$	tol	24 h	100	100	>99
6			$ZrCl_4$	DCM	1 h	100	100	>99
7	MeOH	DHF	$ZrCl_4$	tol	1 h	100	100	>99
8	EtOH		$ZrCl_4$	tol	1 h	100	100	>99
9	menthol		$ZrCl_4$	tol	1 h	100	100	>99
10	fenchyl alcohol		$ZrCl_4$	DCM	1 h	100	100	>99

[a] $[alcohol]_0$ = 0.50 M, $[cyclic\ enol\ ether]_0$ = 0.50 M, $[catalyst]_0$ = 5.0 mM, $[ethyl\ acetate]_0$ = 100 mM (entries 3–10) or 0 mM (entries 1 and 2) at 0 ºC. [b] Determined by ^{1}H NMR analysis. [c] Reaction efficiency: the ratio of the generated 2-alkoxy cyclic ether to the feeds of cyclic enol ether ([2-alkoxy cyclic ether]/$[cyclic\ enol\ ether]_0$) determined by ^{1}H NMR analysis. tol: toluene. DCM: dichloromethane.

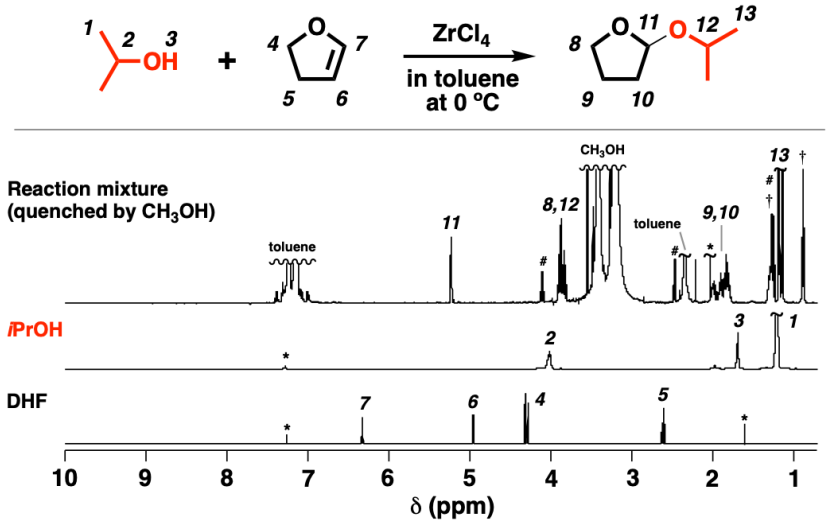

Figure 1. ^{1}H NMR spectra of the reaction mixture quenched by methanol (upper; entry 3 in Table 1), *i*PrOH (middle), and DHF (lower). In $CDCl_3$ at 30 ºC. * $CHCl_3$ and water; † hexane; # ethyl acetate (a solvent for the $ZrCl_4$ stock solution).

The use of a series of alcohols successfully quantitatively generated the corresponding 2-alkoxy cyclic ethers (entries 3 and 7–10 in Table 1). Structural difference, such as methyl (MeOH), primary (EtOH), and secondary (*i*PrOH) alcohols, negligibly affected the selectivity of the addition reaction (entries 3, 7, and 8 in Table 1). Moreover, naturally-occurring alcohols with bulky substituents, such as (–)-menthol and fenchyl alcohol, were also transformed into 2-alkoxy cyclic ethers by reaction with DHF (entries 9 and 10 in Table 1).

Living Cationic Copolymerization of Alcohol-Derived Cyclic Ether and CEVE

The controlled cationic copolymerization of the above-obtained 2-alkoxy cyclic ethers and CEVE successfully proceeded without any isolation or purification of 2-alkoxy cyclic ethers when using an initiating system that is effective for the living cationic polymerization of VEs (Figure 2). The reaction solution containing the obtained 2-isopropoxy-THF was cooled to –78 ºC, without any purification, followed by the addition of CEVE and $SnCl_4$ solutions to start the copolymerization (entry 2 in Table 2). The $SnCl_4$ catalyst was employed to enable fast propagation reactions at low temperatures.[19] The copolymerization proceeded with the consumption of both monomers, generating a copolymer with very narrow MWDs (Figure 2). The MWD curves of the copolymers shifted to the higher MW region as the reaction progressed, indicating the generation of long-lived species. Moreover, the M_n values measured by GPC analysis were consistent with the theoretical values calculated from the monomer conversion and the amounts of $ZrCl_4$ (5.0 mM), suggesting the livingness of the copolymerization.

^{1}H NMR analysis revealed that the obtained copolymers showed alternating sequences of the 2-alkoxy cyclic ether and CEVE (Figure 3, Figure S1 for ^{13}C NMR spectra). The peaks at 4.7 ppm was assigned to the acetal structures derived from the crossover reaction from CEVE to the 2-alkoxy cyclic ether (peak 8), while the peaks at 3.5 ppm was assigned to the structure derived from the crossover reaction from the cyclic ether to CEVE (peak 4). The integral ratio of the methyl protons (peak 6) of the isopropyl group was almost six times that of the acetal proton derived from the crossover reaction (peak 8) and three times that of the

Table 2. Controlled Cationic Copolymerization of 2-Alkoxy Cyclic Ethers and CEVE[a]

entry	alcohol	enol ether	time	conv. (%)[b]		$M_n \times 10^{-3}$[c]	M_w/M_n[c]	units per block[d]	
				cyclic	CEVE			cyclic	CEVE
1	*i*PrOH	DHF	15 min	52	99	8.7	1.20	1.0_1	1.0_0
2			16 h	54	99	11.8	1.10	0.9_8	1.0_1
3	MeOH	DHF	16 h	51	99	0.2	1.42	–	–
4	EtOH		8 h	49	88	6.2	1.26	0.9_9	1.0_9
5	menthol		2 h	50	99	15.0	1.10	1.0_0	1.1_1
6	fenchyl alcohol		2 h	50	99	4.3	1.30	1.0_0	1.0_6
7	*i*PrOH	DHP	2 h	44	99	9.0	1.18	0.9_9	1.1_1
8		DHF	16 h	59	76	15.8	1.11	0.9_9	1.1_7
9[e]	*i*PrOH	DHF	5 h	3	–	–	–	–	–

[a] Reaction conditions for the synthesis of 2-alkoxy cyclic ethers: $[alcohol]_0$ = 0.50 M, $[cyclic\ enol\ ether]_0$ = 0.50 M, $[ZrCl_4]_0$ = 5.0 mM, $[ethyl\ acetate]_0$ = 100 mM (derived from the stock solution of $ZrCl_4$) in dichloromethane (entries 1, 5–7, and 9) or toluene (entries 2–4 and 8) at 0 ºC for 1 h. Polymerization conditions: $[2\text{-alkoxy cyclic ether}]_0$ = 0.50 M, $[CEVE]_{add}$ = 0.25 (entries 1–7), 0.50 (entry 8), or 0 (entry 9) M, $[SnCl_4]_{add}$ = 20 mM in dichloromethane (entries 1, 5–7, and 9) or toluene (entries 2–4 and 8) at –78 ºC. Alcoholysis conditions: 0.50 M HCl in dichloromethane/*n*-butanol (entries 1–4, 7, and 8) or methanol (entries 5 and 6) (1/1 v/v) (0.5 wt% polymer) at 50 ºC for 3 h. [b] Determined by ^{1}H NMR analysis. [c] Determined by GPC (polystyrene standards). [d] Estimated by ^{1}H NMR. [e] CEVE was not added. The 2-alkoxy cyclic ether was used alone.

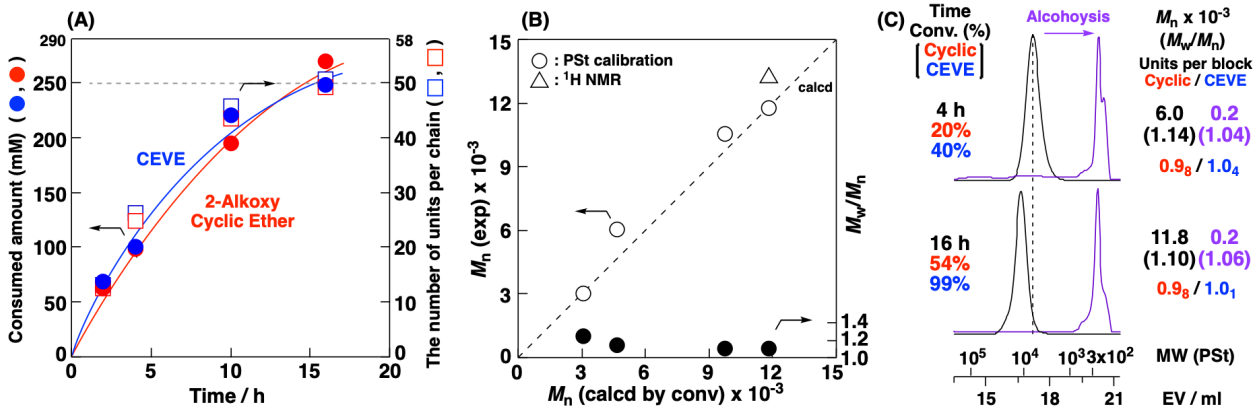

Figure 2. (A) Consumed amounts of CEVE and 2-alkoxy cyclic ether synthesized from *i*PrOH and DHF in the copolymerization (circle) and the average number of monomer units per chain (square: calculated from ^{1}H NMR analysis and MW values measured by GPC), (B) the M_n (open) determined by GPC and M_w/M_n (filled) values of the polymers, and (C) MWD curves of poly(CEVE-*co*-2-alkoxy cyclic ether)s (black) and alcoholysis products (purple). The data correspond to entry 2 in Table 2.

methylene proton of the CEVE units in the main chain (peak 7), indicating the negligible occurrence of homopropagation of the cyclic ether. Indeed, the homopolymerization of 2-*i*PrO-THF did not occur under the same conditions as those for the copolymerization (entry 9 in Table 2). Moreover, from the integral ratios of the acetal peak (peak 8), the methylene peaks of the CEVE units (peak 7), and the peaks for the isopropyl group (peak 6), the average number of the 2-alkoxy cyclic ether and CEVE units per block was calculated to be 0.9_8 and 1.0_1 respectively, indicating the occurrence of alternating copolymerization.

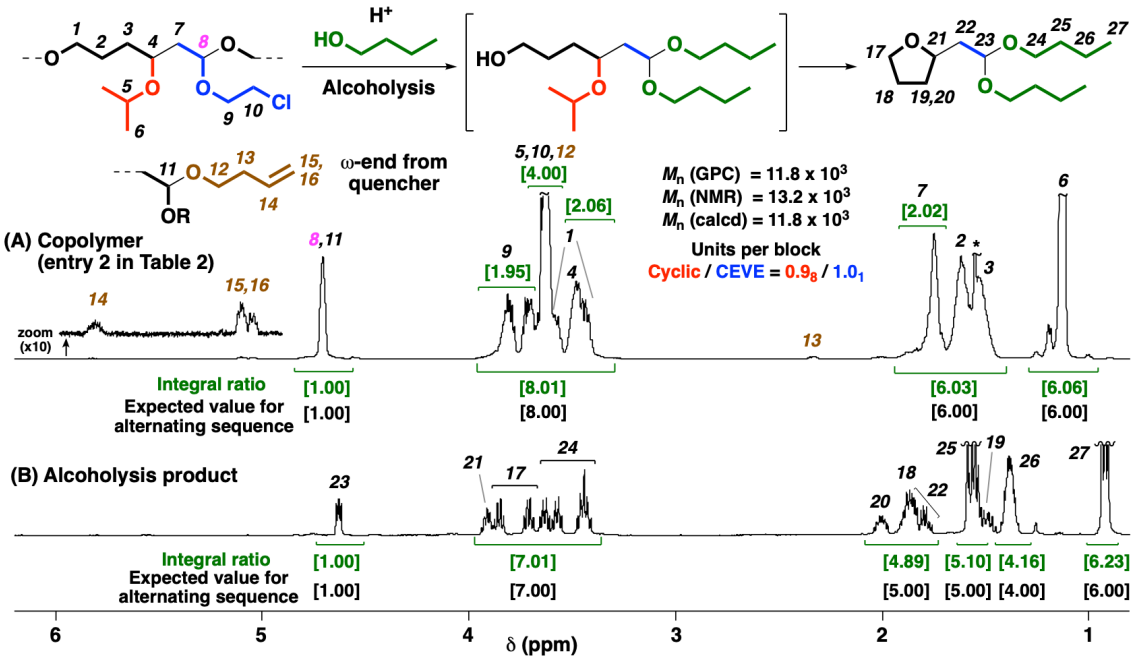

Figure 3. ^{1}H NMR spectra of (A) *i*PrOH–DHF–CEVE copolymer obtained by the copolymerization of CEVE and 2-*i*PrO-THF (entry 2 in Table 2) and (B) its alcoholysis product. In $CDCl_3$ at 30 ºC. * water.

The alcoholysis products of the obtained copolymers also supported the realization of alternating sequences of the copolymers. To examine the structures of the repeating units of the copolymers, a transacetalization reaction was conducted by using hydrochloric acid and 1-butanol as an acid catalyst and an alcohol, respectively. From the ^{1}H NMR spectrum of the alcoholysis products (Figure 3B), peaks assigned to the acetal compound derived from one 2-alkoxy cyclic ether unit and one CEVE unit were selectively observed. This compound is likely generated via the transacetalization of the acetal structures derived from the crossover reaction from CEVE to the cyclic ether and the intramolecular cyclization reaction accompanied by the elimination of isopropyl alcohol (Figures S2 and S3). The MWD curves of the alcoholysis products showed a very sharp peak in the low-MW region, suggesting the occurrence of alternating propagation (Figure 2C purple).

The chain-end analysis of the copolymers indicated the livingness of the copolymerization. From the ^{1}H NMR spectrum of the obtained copolymer (Figure 3A), the peaks at 2.3, 5.1, and 5.8 ppm were assigned to the ω-end structure derived from 3-buten-1-ol, which was used as a quencher. The M_n value calculated from the integral ratio of the ω-end structure (13.2×10^3; Figure 2B triangle) was comparable to both the value measured by GPC analysis (11.8×10^3; Figure 2B circle) and the theoretical value (11.8×10^3; Figure 2B). These results showed the negligible occurrence of side reactions such as chain transfer reactions was confirmed during copolymerization.

The one-pot synthesis of the alternating copolymers demonstrated above indicated the adequate controllability compared with the copolymerization using an isolated 2-alkoxy cyclic ether, while the one-pot method was superior to the direct polymerization of *i*PrOH, DHF, and CEVE (Table 3). The cationic copolymerization of CEVE and 2-isopropoxy-THF, which was obtained via the addition reaction of *i*PrOH to DHF using PTSA as an acid catalyst and subsequent threefold distillation over calcium hydride, smoothly proceeded with similar controllability (entry 2 in Table 3) to that in the one-pot method (entry 1 in Table 3)

Table 3. Cationic Copolymerization of 2-*i*PrO-THF and CEVE[a]

entry	comonomer	time	conv. (%)[b]		$M_n \times 10^{-3}$[c]	M_w/M_n[c]	units per block[d]	
			cyclic	CEVE			cyclic	vinyl
1[e]	2-*i*PrO-THF (*in situ* synthesis)	16 h	54	99	11.8	1.10	0.9_8	1.0_1
2	2-*i*PrO-THF (isolated)	16 h	45	88	13.4	1.12	0.9_8	1.0_3
			conv. (%)[b]					
			*i*PrOH	DHF CEVE				
3	*i*PrOH + DHF	16 h	0	5 5	–	–	–	–

[a] Polymerization conditions for entry 2: $[2\text{-}i\text{PrO-THF}]_0$ = 0.50 M, $[CEVE]_0$ = 0.25 M, $[ZrCl_4]_0$ = 5.0 mM, $[SnCl_4]_0$ = 20 mM in toluene at –78 ºC. Polymerization conditions for entry 3: $[i\text{PrOH}]_0$ = 0.50 M, $[DHF]_0$ = 0.50 M, $[CEVE]_0$ = 0.25 M, $[SnCl_4]_0$ = 20 mM in toluene at –78 ºC. [b] Determined by ^{1}H NMR analysis. [c] Determined by GPC (polystyrene standards). [d] Estimated by ^{1}H NMR. [e] Entry 1 corresponds to entry 2 in Table 2.

in terms of sequences and MWs. In contrast, the direct polymerization of *i*PrOH, DHF, and CEVE did not proceed because *i*PrOH acted as a terminator and/or a chain transfer agent (entry 3 in Table 3). These results showed the selective generation of the alcohol-derived cyclic monomer was significantly important for the one-pot synthesis of the copolymers with well-defined structures.

Copolymerization of 2-Alkoxy Cyclic Ether Using Various Alcohols and Cyclic Enol Ethers with CEVE

The use of other alcohols or cyclic enol ether also resulted in highly controlled copolymerization (entries 3–8 in Table 2). A cyclic ether derived from ethanol and DHF efficiently copolymerized with CEVE (Figure 4; entry 4 in Table 2; cyc(DHF-EtOH)/CEVE = $0.9_9/1.0_9$ units per block). Moreover, the living copolymerization of 2-alkoxy cyclic ethers and CEVE with bulky substituents that were derived from naturally-occurring (–)-menthol and fenchyl alcohol successfully proceeded in an alternating manner (Figure 4; entries 5 and 6 in Table 2; cyc(DHF-menthol)/CEVE = $1.0_0/1.1_1$, cyc(DHF-fenchyl alcohol)/CEVE = $1.0_0/1.0_6$ units per block). A six-membered 2-alkoxy cyclic ether obtained using DHP instead of DHF as a cyclic enol ether also underwent frequent crossover reactions between the 2-alkoxy cyclic ether and CEVE, yielding copolymers with narrow MWDs (Figure 4; entry 7 in Table 2; cyc(DHP-*i*PrOH)/CEVE = $0.9_9/1.1_1$ units per block). The alcoholysis products of the obtained copolymers indicated sharp MWDs in the low-MW region, supporting the efficient occurrence of crossover reactions (Figure 4). In addition, an increased feed of CEVE monomer led to an increase of the M_n values of the alternating copolymers (entry 8 in Table 2). The M_n value obtained from GPC analysis (15.8×10^3) was highly consistent with the theoretical values calculated from the conversion of the both monomers (15.8×10^3), suggesting the generation of high-MW copolymers by the polymerization that occurred in a living manner. The use of dichloromethane instead of toluene enabled faster copolymerization (entry 1 in Table 2).

Interestingly, the cationic copolymerization of a methanol-derived 2-alkoxy cyclic ether and CEVE produced low-MW compounds (entry 3 in Table 2; Figure 4). ^{1}H NMR analysis of the products showed that the major products were oligomers consisting of one or few CEVE units with a THF structure at the α-end and a methoxy group at the ω-end, suggesting that the methanol-derived cyclic ether acted as a chain transfer

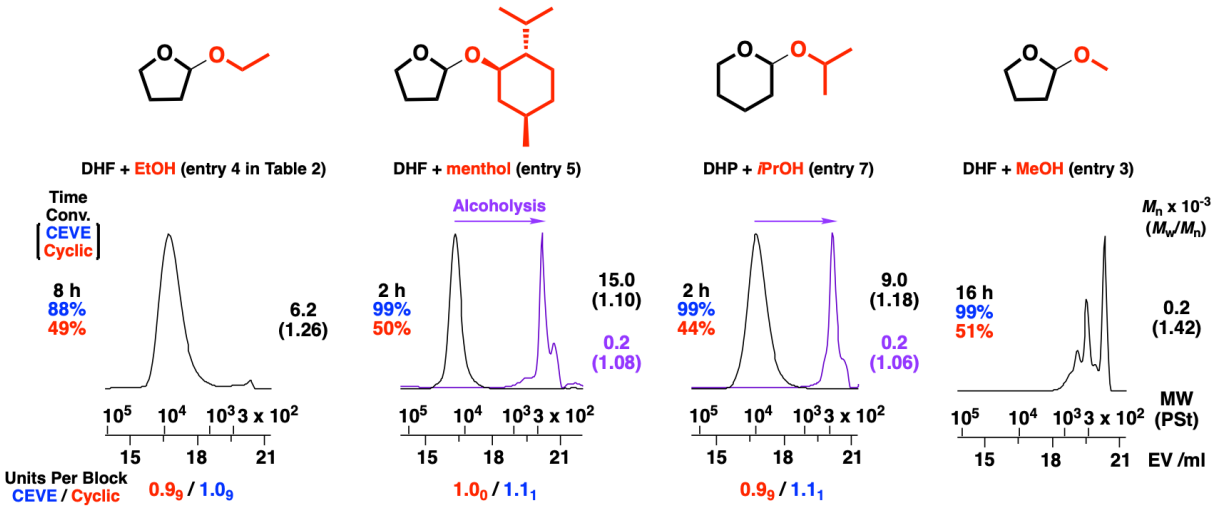

Figure 4. MWD curves of poly(CEVE-*co*-2-alkoxy cyclic ether)s (black) and alcoholysis products (purple). The data correspond to entries 3–5 and 7 in Table 2.

agent rather than a monomer (Figure S4). The reaction mechanism for generation of the abovementioned products is discussed in the following sections.

The exceptional copolymerizability of 2-alkoxy cyclic ethers in the copolymerization with CEVE is most likely attributed to the stability of the carbocation derived from 2-alkoxy cyclic ethers and the negligible homopolymerizability of 2-alkoxy cyclic ethers (Scheme 3). In the propagating reaction, the oxygen at the 1-position of a 2-alkoxy cyclic ether reacts with the CEVE-derived propagating species (Scheme 3a) to form an oxonium ion species, which is subsequently transformed into a carbocation via the ring-opening reaction (Scheme 3b). The alkoxy group-adjacent stable carbocation is structurally identical to the carbocation derived from a VE, which is responsible for the frequent crossover reaction from the cyclic monomer-derived carbocation to CEVE (Scheme 3c). The negligible homopolymerizability of 2-alkoxy cyclic ethers, which probably stems from the small change in the Gibbs free energy of the homopropagation reaction, under the adopted conditions (entry 9 in Table 2) also contributes to the exclusive crossover to CEVE (Scheme 3e). In general, the polymerization of THF derivatives with a substituent at the 2-position negligibly proceeds because of steric repulsion.[28–30] Similar effects were possibly exerted on the inertness of homopropagation of 2-alkoxy cyclic ethers. The preferential occurrence of the crossover reaction from CEVE to the cyclic ethers (Scheme 3a) over CEVE homopropagation (Scheme 3d) likely stems from the higher reactivity of cyclic ethers to the propagating carbocations than that of CEVE. In the preceding chapters, the use of various cyclic acetals was effective for crossover reactions with VEs. The higher basicity of 2-substituted cyclic ethers compared to cyclic acetals is also likely responsible for the frequent crossover reactions.[55] The initiation reaction most likely occurs via ring opening of the cyclic acetal with $ZrCl_4$ in a manner similar to the acetal-initiated living cationic polymerization of VEs.[31–33] The living cationic copolymerization proceeded via a dormant-active equilibrium consisting of the reversible activation of carbon-chlorine bonds at the VE-type propagating ends derived from both monomers in a similar manner to the living cationic polymerization of VEs (Scheme 3f and g; using $SnCl_4$ as a Lewis acid catalyst).[19]

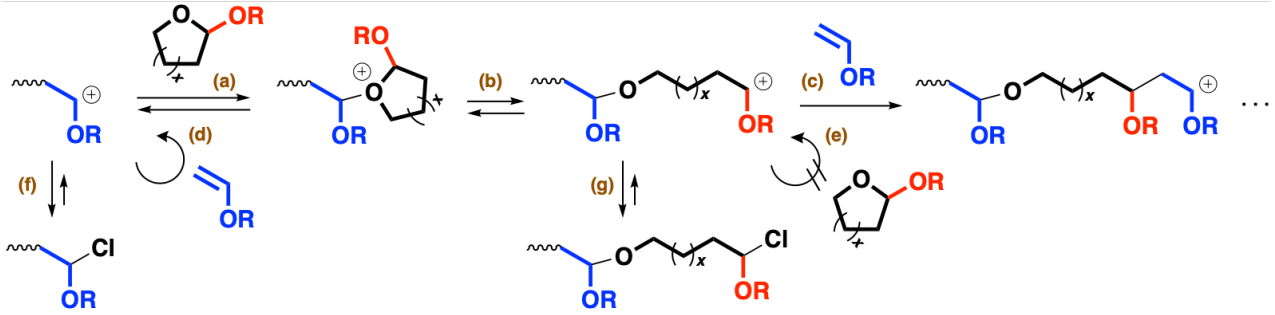

Scheme 3. Copolymerization Mechanisms

The sharp difference in the polymerization behavior between the methanol-derived cyclic ether and other cyclic ethers was likely derived from the selectivity in the reaction of cyclic ethers with the propagating species. During the propagating reaction, the reaction of the oxygen atom at the 1-position of the 2-alkoxy cyclic ethers leads to ring-opening and the subsequent crossover reaction with CEVE (Scheme 3), whereas the reaction of the alkoxy group at the 2-position of the cyclic ethers results in an acetal chain end and an oxygen atom-adjacent cyclic carbocation (Scheme 4). The subsequent addition of CEVE to the cyclic carbocation generates another chain with a THF structure at the α-end. The bulkiness of the alkoxy groups is likely related to the selective occurrence of crossover reactions. Methanol-derived cyclic ether, which has a less bulky alkoxy group compared to the other molecules, was not effective for the crossover reactions and rather underwent frequent chain transfer reactions. In addition, the methanol-derived cyclic ether potentially functioned as not only a chain transfer agent but also a cationogen via the abstraction of the methoxy group by a Lewis acid catalyst. Further investigation is required for better understanding.

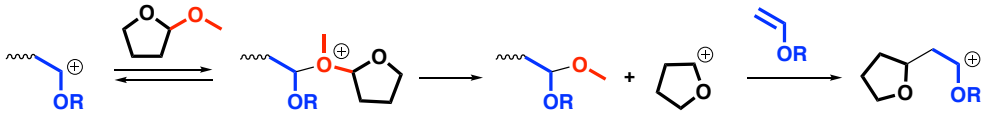

Scheme 4. Chain Transfer Reaction Using Methanol-Derived Cyclic Ether

Conclusion

The development of a successive process consisting of selective monomer generation and subsequent alternating copolymerization was demonstrated to generate well-defined copolymers from simple compounds using alcohols, cyclic enol ethers, and a vinyl ether. The use of a series of alcohols, cyclic enol ethers and acid catalysts was effective for the selective synthesis of 2-alkoxy cyclic ethers with corresponding structures. The subsequent copolymerization of the 2-alkoxy cyclic ethers with CEVE produced alternating copolymers with well-defined structures. In addition, the selective generation of 2-alkoxy cyclic ethers was crucial for the progress of the copolymerization reaction using alcohols as a starting material. The difference in the bulkiness of the alkoxy groups of 2-alkoxy cyclic ethers was possibly related to the preferential occurrence of the crossover reactions rather than the chain transfer reaction. The results obtained in this study will provide a facile strategy of sequence-controlled copolymers with various structures from diverse resources.

References

1. Lutz, J.-F.; Ouchi, M.; Liu, D. R.; Sawamoto, M. *Science* **2013**, *341*, No. 1238149.
2. Lutz, J.-F. *Macromol. Rapid Commun.* **2017**, *38*, No. 1700582.
3. Szymański, J. K.; Abul-Haija, Y. M.; Cronin, L. *Acc. Chem. Res.* **2018**, *51*, 649–658.
4. Meier, M. A. R.; Barner-Kowollik, C. *Adv. Mater.* **2019**, *31*, No. 1806027.
5. Rzaev, Z. M. O. *Prog. Polym. Sci.* **2000**, *25*, 163–217.
6. Ishido, Y.; Aburaki, R.; Kanaoka, S.; Aoshima, S. *Macromolecules* **2010**, *43*, 3141–3144.
7. Yuki, H.; Hatada, K.; Inoue, T. *J. Polym. Sci., Part A-1: Polym. Chem.*, **1968**, *6*, 3333–3343.
8. Yuki, H.; Okamoto, Y. *Polym. J.* **1970**, *1*, 13–18.
9. Yuki, H.; Okamoto, Y. *Bull. Chem. Soc. Jpn.* **1969**, *42,* 1644–1649.
10. Oh, D.; Furuya, Y.; Ouchi, M. *Macromolecules* **2019**, *52*, 8577–8586.
11. Elling, B. R.; Xia, Y. Living *J. Am. Chem. Soc.* **2015**, *137*, 9922–9926.
12. Cho, I.; Hwang, K. M. *J. Polym. Sci., Part A: Polym. Chem.* **1993**, *31*, 1079–1081.
13. Cho, I. *Prog. Polym. Sci.* **2000**, *25*, 1043−1087.
14. Zhang, J.; Matta, M. E.; Hillmyer, M. *ACS Macro Lett.* **2012**, *1*, 1383–1387.
15. Yokota, K. *Prog. Polym. Sci.* **1999**, *24*, 517−563.
16. Hibi, Y.; Ouchi, M.; Sawamoto, M. *Angew. Chem., Int. Ed*. **2011**, *50*, 7434−7437.
17. Kametani, Y.; Nakano, M.; Yamamoto, T.; Ouchi, M.; Sawamoto, M. *ACS Macro Lett.* **2017**, *6*, 754–757.
18. Gutekunst, W. R.; Hawker, C. J. *J. Am. Chem. Soc.* **2015**, *137*, 8038–8041.
19. Aoshima, S.; Kanaoka, S. *Chem. Rev.* **2009**, *109*, 5245–5287.
20. Hirao, A.; Goseki, R.; Ishizone, T. *Macromolecules* **2014**, *47*, 1883–1905.
21. Krompiec, S.; Penkala, M.; Szczubiałka, K.; Kowalska, E. *Coord. Chem. Rev.* **2012**, *256*, 2057–2095.
22. Meskens, F. A. J. *Synthesis* **1981**, *7*, 501-522.
23. Kumar, B.; Aga, M. A.; Rouf, A.; Shah, B. A.; Taneja, S. C. *RSC Adv* **2014**, *4*, 21121–21130.
24. Rezai, N.; Meybodi, F. A.; Salehi, P. *Synth. Commun.* **2000**, *30*, 1799–1805.
25. Gogoi, D.; Baruah, N.; Bez, G. *Synth. Commun.* **2007**, *37*, 593–597.
26. Maruyama, K.; Kanazawa, A.; Aoshima, S. *Polym. Chem.* **2019**, *10*, 5304–5314.
27. Maruyama, K.; Kanazawa, A.; Aoshima, S. *Macromolecules,* **2022**, *in press.*
28. Ishigaki, A.; Shono, T.; Hachihama, Y. *Makromol. Chem.* **1964**, *79*, 170–179.
29. Yamashita, Y.; Tsuda, T.; Okada, M.; Iwatsuki, S. *J. Polym. Sci. Part A1* **1966**, *4*, 2121–2135.
30. Okada, M.; Takikawa, N.; Iwatsuki, S.; Yamashita, Y.; Ishii, Y. *Makromol. Chem.* **1965**, *82*, 16–24.
31. Van Meirvenne, D.; Haucourt, N.; Goethals, E. J. *Polym. Bull.* **1990**, *23*, 185–190.
32. Haucourt, N. H.; Goethals, E. J.; Schappacher, M.; Deffieux, A. *Makromol. Chem. Rapid Commun.* **1992**, *13*, 329–336.
33. Satoh, K.; Kamigaito, M.; Sawamoto, M. *Macromolecules* **2000**, *33*, 748–753.

Supporting Information

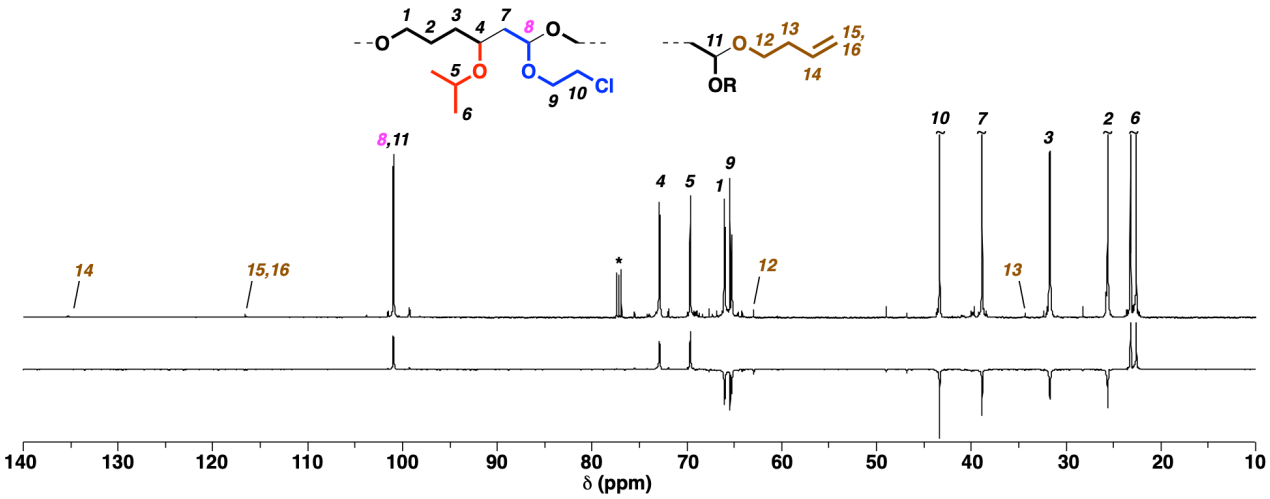

Figure S1. ^{13}C and DEPT 135 NMR spectra of *i*PrOH–DHF–CEVE copolymer. (in $CDCl_3$ at 30 ºC). * $CDCl_3$.

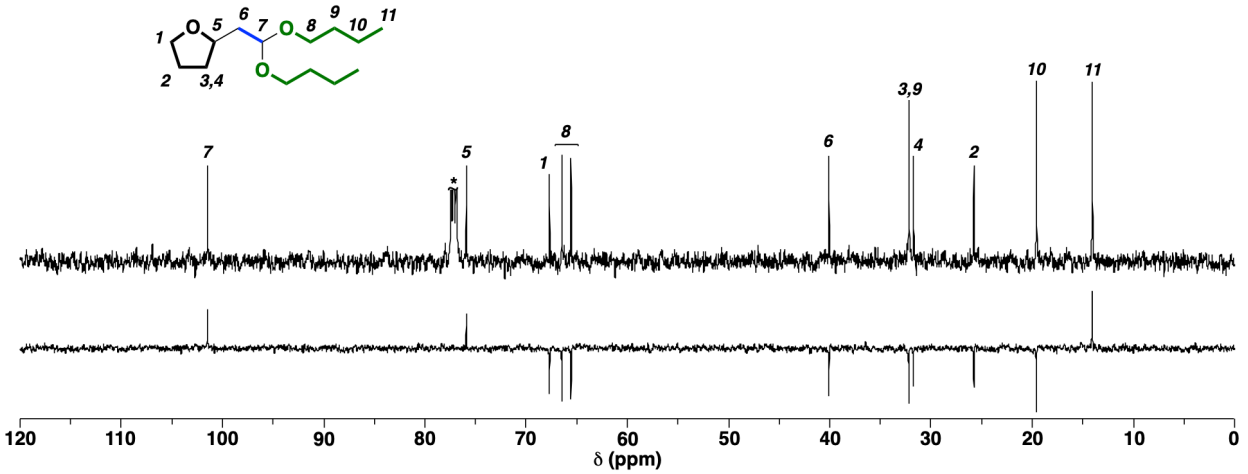

Figure S2. ^{13}C and DEPT 135 NMR spectra of alcoholysis products of *i*PrOH–DHF–CEVE copolymer. (in $CDCl_3$ at 30 ºC). * $CDCl_3$.

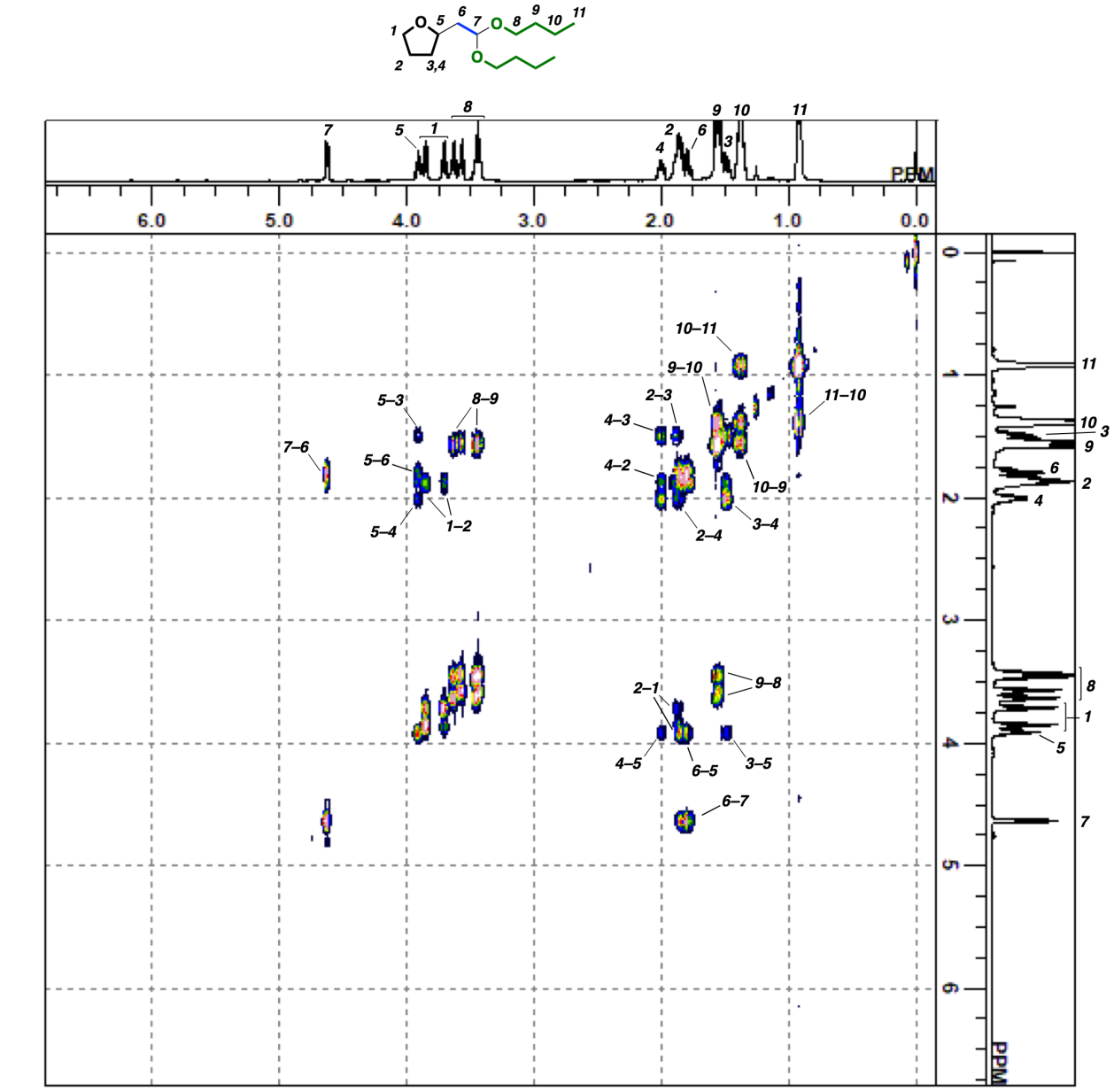

Figure S3. ^{1}H–^{1}H COSY NMR spectrum of alcoholysis products of *i*PrOH–DHF–CEVE copolymer. (in $CDCl_3$ at 30 ºC). * $CDCl_3$.

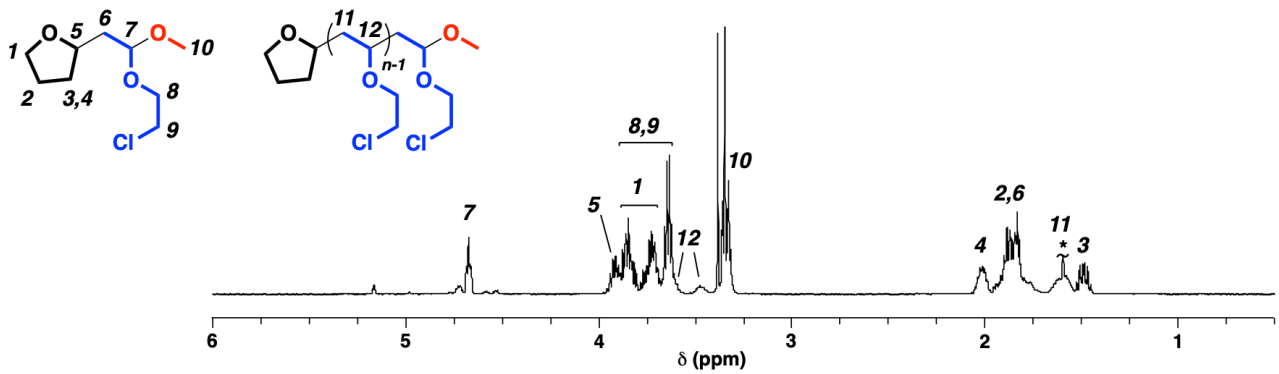

Figure S4. ^{1}H NMR spectrum of the copolymerization product of a cyclic ether from MeOH and DHF and CEVE. (in $CDCl_3$ at 30 ºC). * water

Chapter 6.

Summary

The development of the polymerization methods for controlling molecular weights, topologies, sequences, and microstructures of polymers have enabled the synthesis of polymeric materials with high functionality and encouraged to discover novel polymerization reactions. The significant progress in polymer chemistry have afforded well-defined homopolymers and copolymers from similar types of monomers via specific polymerization mechanism. In contrast, the copolymerization of different types of monomers potentially generates novel functional polymers with special primary structures. However, such copolymerization is difficult because of the sharp differences in the reactivity of different propagating species derived from the monomers. As a suitable candidate for the successful crossover reactions between different types of monomers such as vinyl and cyclic monomers, the author focused on cyclic acetals that generate active species structurally similar to those derived from vinyl ethers. This thesis addressed the comprehensive study of the relationship between the structures of active species and copolymerization behavior in concurrent vinyl-addition and ring-opening copolymerization. Moreover, the rationally designed process consisting of selective cyclic acetal formation from various compounds and subsequent copolymerization was developed as a facile approach for sequence-controlled polymers.

Part I described a systematic investigation of the effects of the structures of cyclic acetals and vinyl monomers on the copolymerization behavior via the concurrent vinyl-addition and ring-opening mechanism.

In Chapter 2, it was demonstrated that the number of substituents and ring-member of cyclic acetals significantly affected the frequency of crossover reactions between vinyl ethers and cyclic acetals and copolymerization rates. Methyl substituents at the 2-position of cyclic acetals largely influenced the stability of carbocations generated by the ring-opening reaction of the oxonium ion species. Specifically, cyclic acetals with no, one, or two methyl groups at the 2-position resulted in the generation of multiblock, random, or approximately alternating sequences, respectively. In addition, the ring-member of cyclic acetals was related with the degree of ring strain and the Lewis basicity, which affected the frequency of the crossover reactions and the polymerization rates.

Chapter 3 presented the electronic and steric effects of the substituents of cyclic acetals on the copolymerization mechanism. Cyclic acetals with various substituents, which were prepared from aldehydes, ketones, and diols, were subjected to the cationic copolymerization with vinyl monomers. Among the various structures, cyclic acetals with aryl substituents at the 2-position underwent the exclusive occurrence of the crossover reactions in the copolymerization with vinyl ethers. The high tendency for the crossover reactions was mainly derived from the resonance-stabilization of the active species by the aryl substituents adjacent to the carbocation. The characteristic stabilization of the 2-aryl cyclic acetals was effective for the copolymerization with a wide range of vinyl monomers, such as vinyl ethers with diverse reactivities and styrene derivatives.

Chapter 6

In Part II, the author developed novel strategies for the synthesis of sequence-controlled polymers in one-pot process. In this method, cyclic acetals selectively synthesized from starting materials were subjected to subsequent alternating copolymerization without any isolation or purification.

Chapter 4 dealt with the successive process consisting of cycloaddition reaction of oxiranes and carbonyl compounds and subsequent alternating copolymerization with vinyl monomers. The elaborate design of reaction conditions that enable both the quantitative synthesis of a sequence-programmed cyclic acetal and the controlled copolymerization of the cyclic acetal with a vinyl monomer afforded ABC-type periodic terpolymers with defined molecular weight, molecular weight distribution, chain ends, and monomer sequences.

In Chapter 5, the synthesis of sequence-controlled polymers from diverse and abundant resources was demonstrated using alcohol, cyclic enol ethers, and a vinyl ether as starting materials. 2-Alkoxy cyclic ethers, which are cyclic acetals with an exocyclic alkoxy group, were selectively synthesized via addition of a variety of alcohol to cyclic enol ethers. Living cationic copolymerization of the generated 2-alkoxy cyclic ethers and a vinyl ether effectively proceeded without any purification, yielding alternating copolymers with well-defined structures. The slight bulkiness of the alkoxy group derived from alcohols possibly affected the preferential occurrence of the crossover reactions between the cyclic ethers and a vinyl ether rather than the chain transfer reaction.

In conclusion, this thesis demonstrated the overall investigation into the concurrent vinyl-addition and ring-opening cationic copolymerization by using cyclic acetals as a key component for designing the propagating species. The results obtained in this study will provide the guidelines for cationic copolymerization of different types of monomers. The consecutive approaches consisting of selective organic reaction and subsequent polymerization opened the possibilities of transforming simple monomers into polymers with diverse structures and complexity. Therefore, the author believes that the studies in this thesis contribute to construction of polymers with unique properties from various types of monomers and to the development of novel technologies for highly designed polymers.

List of Publications

1. Kazuya Maruyama, Arihiro Kanazawa, Sadahito Aoshima
"Controlled Cationic Copolymerization of Vinyl Monomers and Cyclic Acetals via Concurrent Vinyl-Addition and Ring-Opening Mechanisms: the Systematic Study of Structural Effects on the Copolymerization Behavior"
Polym. Chem. **2019**, *10,* 5304–5314. (Corresponding to Chapter 2)

2. Kazuya Maruyama, Arihiro Kanazawa, Sadahito Aoshima
"Alternating Cationic Copolymerization of Vinyl Ethers and Cyclic Acetals with Resonance-Stabilized Substituents: Structural Investigation of Cyclic Acetals on the Copolymerizability"
to be submitted. (Corresponding to Chapter 3)

3. Kazuya Maruyama, Arihiro Kanazawa, Sadahito Aoshima
"ABC-Type Periodic Terpolymer Synthesis by a One-Pot Approach Consisting of Oxirane- and Carbonyl-Derived Cyclic Acetal Generation and Subsequent Living Cationic Alternating Copolymerization with a Vinyl Monomer"
Macromolecules **2022**, *in press.* (Corresponding to Chapter 4)

4. Kazuya Maruyama, Arihiro Kanazawa, Sadahito Aoshima
"Synthesis of Alternating Copolymers via Selective Generation of Alcohol-Derived 2-Alkoxy Cyclic Ethers and Subsequent Cationic Copolymerization with a Vinyl Ether in One-Pot Process"
to be submitted. (Corresponding to Chapter 5)

Related Publication

1. Jennifer Imbrogno, Kazuya Maruyama, Frederick Rivers, Jacob R. Baltzegar, Zidan Zhang, Paul W. Meyer, Venkat Ganesan, Sadahito Aoshima, Nathaniel A. Lynd
"Relationship between Ionic Conductivity, Glass Transition Temperature, and Dielectric Constant in Poly(vinyl ether) Lithium Electrolytes"
ACS Macro Lett. **2021**, *10*, 1002–1007.